

A STUDY OF RESIDUAL SHEAR STRENGTH OF NAMURIAN
SHALES IN RESPECT OF SLOPES IN NORTH DERBYSHIRE.

VOL II

THANON H. AL-DABBAGH

Thesis submitted in fulfilment of the requirements for the
Degree of PH.D.

Department of Geology
University of Sheffield

June 1985

CHAPTER 7

MORPHOLOGY AND MAIN FEATURES OF LANDSLIPS IN THE STUDY AREA

7.1 Introduction

The classification of landslides was discussed in Chapter 6 from which it may be deduced that characteristic landforms can provide diagnostic information. Typically, as shown in Fig. 7.1, the area near the upper end of the slide from which material has been removed is accompanied by an area of deposition near the lower end of the slip. Changes in geometry of the ground surface due to the transport of material provides evidence for past landslip activity and areas of potential instability may be identified from topographical studies. As described in Chapter 3 ten areas of instability were mapped using surface observations, existing topographic maps and stereo-paired aerial photographs. The chief objective of this work was to establish the dimensions of the landslips and their modes of movement. The nomenclature adopted follows that advocated by Varnes (1978), the main features of which are shown in fig. 7.2 and summarised below:

MAIN SCARP

A steep surface around the upper periphery of the slide produced by movement of slide material away from undisturbed ground. The projection of scarp surface under the displaced material represents the surface of rupture near the base of the main scarp.

MINOR SCARP

A steep surface of displaced material produced by differential movement within the slide mass and on the flanks of the landslip.

HEAD

The upper part of the slide material forming the contact between displaced material and the main scarp.

TOP

The highest point of contact between displaced



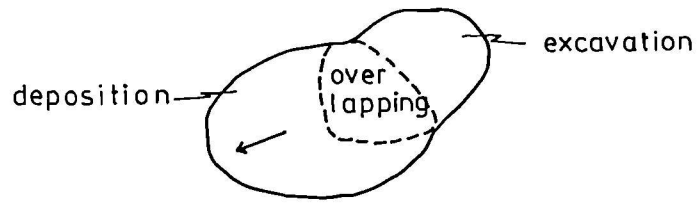


Fig. 7.1 Schematic plan view of a slide.

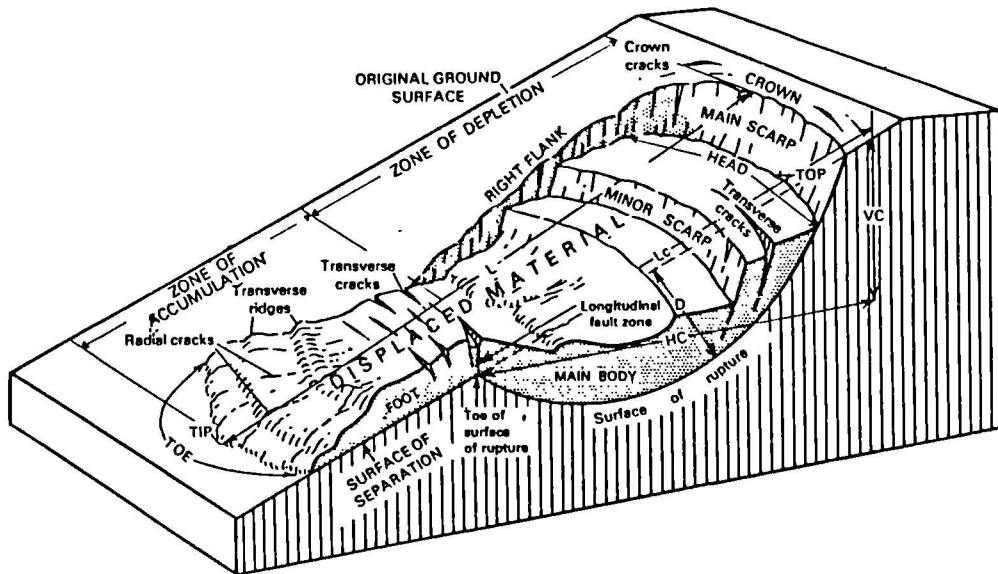


Fig. 7.2 Main features of rotational slide. (After Varnes, 1978).

material and the main scarp.

TOE OF SURFACE OF RUPTURE

The intersection (sometimes buried) between the lower part of surface of rupture and the original ground surface.

TOE

The margin of displaced material that lies down slope from the toe of surface of rupture.

MAIN BODY

That part of the displaced material that overlies the surface of rupture between the main scarp and the toe of the surface of rupture.

FLANK

The side of the landslide.

CROWN

The undisturbed ground adjacent to the highest part of the main scarp.

ORIGINAL GROUND SURFACE

The ground surface that existed before movement occurred.

DISPLACED MATERIAL

The material that has moved away from its original position on the slope, it may be an undeformed or deformed state.

ZONE OF DEPLETION

The area within which the displaced material lies below the original ground surface.

ZONE OF ACCUMULATION

The area within which the displaced material lies above the original ground surface.

SURFACE OF SEPARATION OR RUPTURE

The surface separating displaced material from stable material.

The various sources of data for the observations and measurements presented on the maps are summarized in Table 7.1. The method by which heights were obtained from aerial photographs is described in Appendix E and

Table 7.1 The observation and measurements data presented on the maps (Figs.7.6 to 7.15)

Data	Field observation	Topographic maps	Aerial photographs
Height of main scarp.			●
Lithology of outcrops.	●		
Geological structure.	●		
Steepness of slopes.	●	●	
Irregularity of slopes.	●		●
Location of marshy areas.	●	●	
Location of footpaths, Roads and rivers.	●	●	
Location of seepages.	●		
Extent of instability.			●



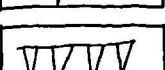
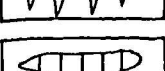
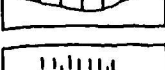
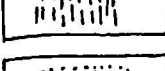

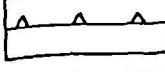
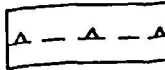
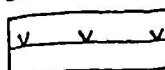
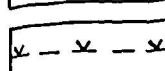

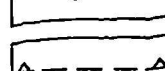
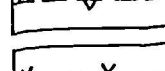
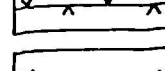
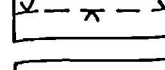

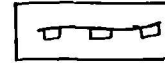
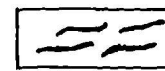
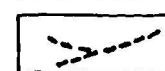
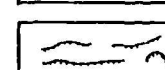
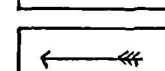
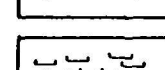
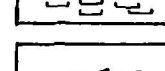
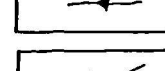
the various symbols used on the maps (Figs. 7.3 and 7.7 to 7.15) are illustrated in Table 7.2.

7.2 Mam Tor

The landslide at Mam Tor is of particular interest because of its continued instability which forced the closure of A625 Sheffield-Manchester Road in 1966 (Derbyshire County Council, 1966). According to Brown (1977), permanent closure occurred in 1977. Although the age of this landslide has not been established it would appear from Brown (1977) that in common with other North Derbyshire landslips, the initial instability occurred during the wetter climatic conditions of late Devensian times (10,000-20,000) years before present. In fact, instability prior to 1977 had caused Derbyshire County Council to undertake substantial road maintenance work dating back to 1906 when they assumed responsibility for its upkeep. The history of instability is summarized below according to Derbyshire County Council (1966) catalogues:-

<u>Year</u>	<u>Month</u>	<u>Style of Movement</u>	<u>Weather Observation</u>
1909	Dec.	Cracks appeared along side the road (made good in Sept. 1911)	
1912	Jan.	Severe cracking, twisting of the carriageway and subsidence	Wet, weather and snow.
1915	Jan.	Subsidence of whole road by 2.4-2.7m. (8-9ft.)	Excessive rainfall.
1919 and 1920	Jan. Jan.	Slight twisting of the road.	
1929	Feb. & Dec.	Cracks, subsidence in some places and uplift in others.	
1930	Jan.	Slipping	Heavy rainfall.

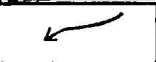
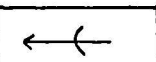
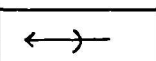
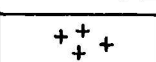
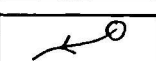
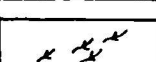

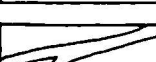

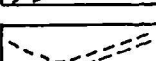
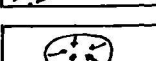

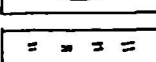

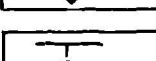
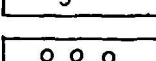
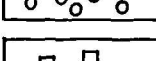
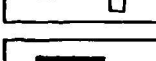
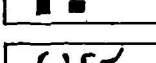
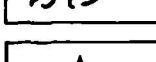
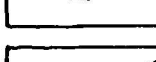
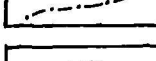
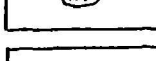
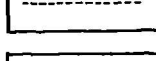
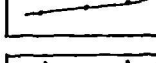
Table 7.2 symbols used for the interpretation of geomorphological maps

Symbol	Description
	Main scarp
	Minor scarp in bed rock
	Minor scarp in slipped material
	Minor scarp in river bank
	Scree material
	Artificial fill
	Sharp convex break in slope
	Round convex break in slope
	Sharp concave break in slope
	Round concave break in slope
	Sharp convex break in slope
	Round convex break in slope
	Sharp concave break in slope
	Round concave break in slope
	Vertical face of main scarp
	Other vertical face
	Linear ridges
	Small valley
	Peat filled channels formed by run off
	Direction of river flow
	Marsh
	Direction of water flow in marshy area
	Stream
	Drain
	Slope direction and amount

NOTE

Arrows are drawn on the side of the line having the steeper slope.

Darkest lines indicate more angular or rounder convexity or concavity of slope.

Symbol	Description
	Undulating slope
	Concave slope
	Convex slope
	Horizontal ground
	Spring
	Water flow from joints
	River
	Road
	Narrow road
	Foot path
	Depression
	Dome
	Talus
	Direction of slickenside
	Bar direction of strike. Tick direction of dip. Amount of dip in degrees.
	Ancient rock fall
	Fresh rock fall
	Farm buildings
	Outcrop of rock
	Location of samples (with sample number)
	Boundary of landslip
	Pond or lake
	Inflection (change in slope)
	Transverse crack
	Line of cross section

<u>Year</u>	<u>Month</u>	<u>Style of Movement</u>	<u>Weather Observation</u>
1931	Feb.	Serious, slipping along upper part of road.	
1937	Mar.	Slight movement	
1939	Jan.	Slight movement	
1942	Oct.	Slight movement, cracks on the road side.	
1946	Feb.	Extensive slipping.	Heavy rainfall
1946	Nov.	Slight movement	
1948	Apr.	Subsidence	
1950	Jan.	Slipping	Heavy rain
1952	Apr.	Large scale movements	
1966	Jan.	Very serious movement.	Unusually heavy rain.

Work to drain water and reduce percolation was carried out in September 1931, in April 1946 traffic was restricted to a single line and in December 1966 further movements forced closure of the road.

The records make frequent reference to periods of high rainfall and thawing of snow and it would appear that instability may be temporarily related to these. It is also significant that much of the instability occurs during winter months.

7.2.1 Morphology

The Mam Tor landslip, shown in map Fig. 7.3 and Plates 7.1 and 7.2, may be divided into two main parts. The main unit consists of a non-circular rotational slip stretching from the back scarp to near the lower loop of the road. A translational flow slide stretches from the toe of the main slide to the furthest edge of the instability. According to Skempton and Hutchinson's (1969) classification the slide is a complex type with a 500m. long by 300m. wide main unit, and a translational toe of 400m. length and 450m width.

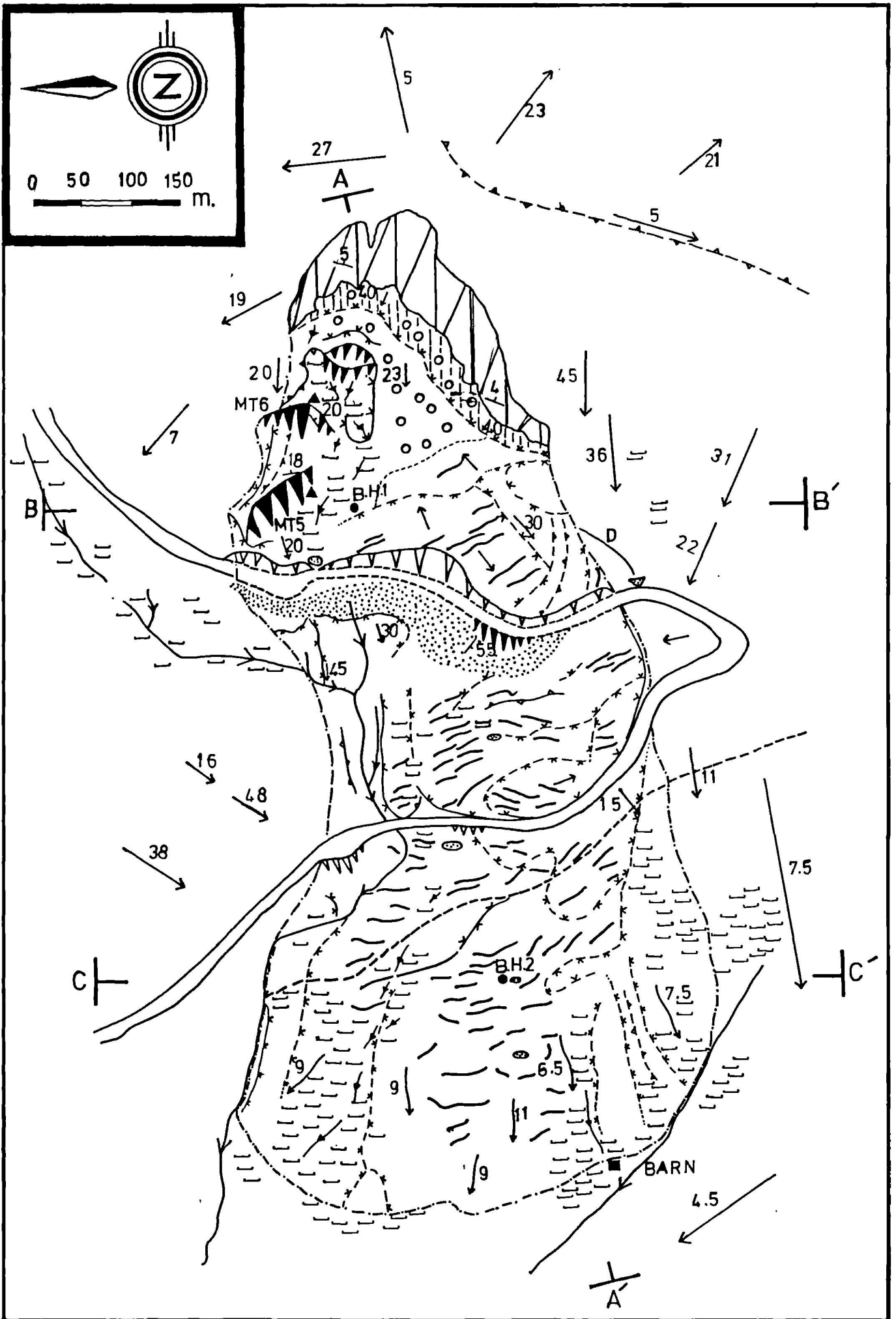


FIG. 7.3 GEOMORPHOLOGICAL MAP OF MAM TOR LANDSLIP.

Plate No. 7.1 Aerial photographs of Mam Tor landslip.
Scale: 1:6000





Plate 7.2 General view of Mam Tor landslip in a southerly direction. Note the contrast in the character of the ground surface between the toe and other parts of the landslip. August 1983.

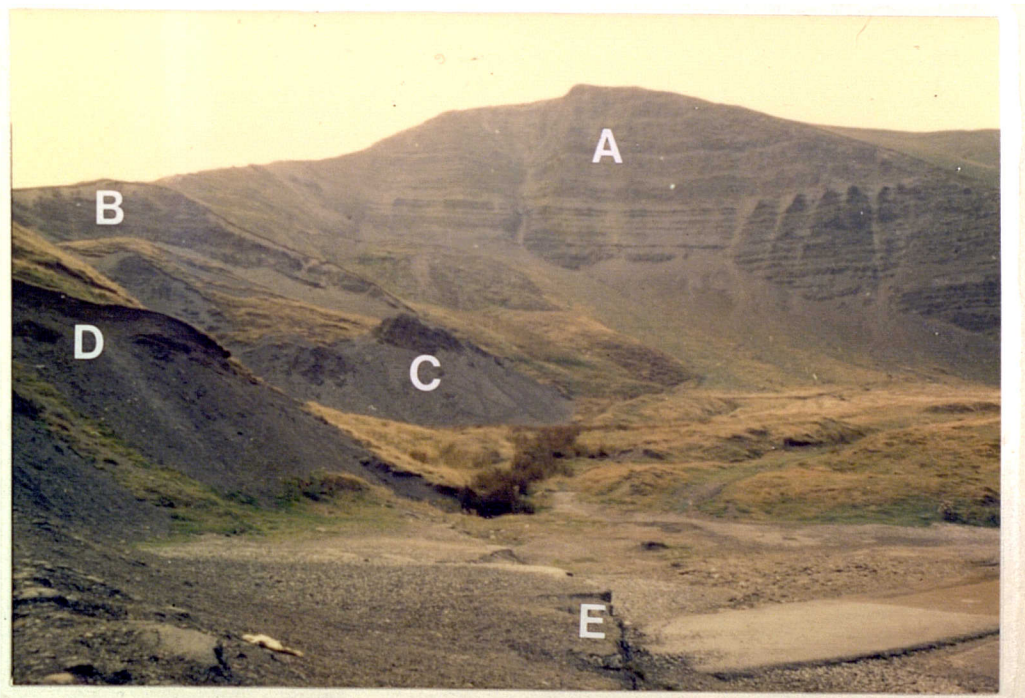


Plate No. 7.3 Landslip at Mam Tor. Main scarp 'A' viewed in a westerly direction with minor scarp B, C, and D on the southern flank of the landslip. Note downward movement of road surface 'E'.



Plate 7.4 Slickensided, back scarp surface at Mam Tor.



Plate No. 7.5 Damage at the upper road at Mam Tor. Note that successive layers of road surfacing material have been applied in an attempt to maintain the road. French drains on main unit of Mam Tor landslide 'F'.

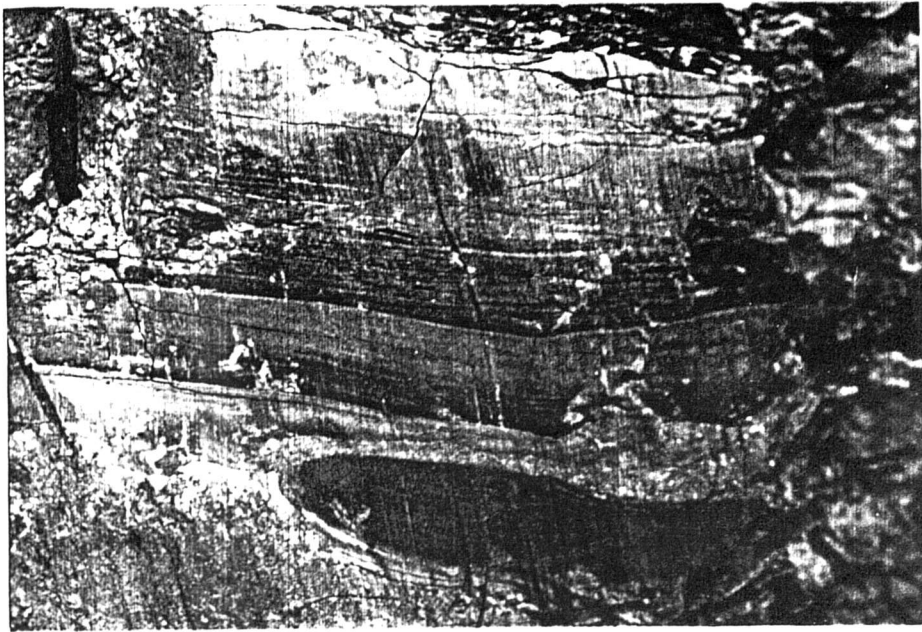


Plate 7.4 Slickensided, back scarp surface at Mam Tor.

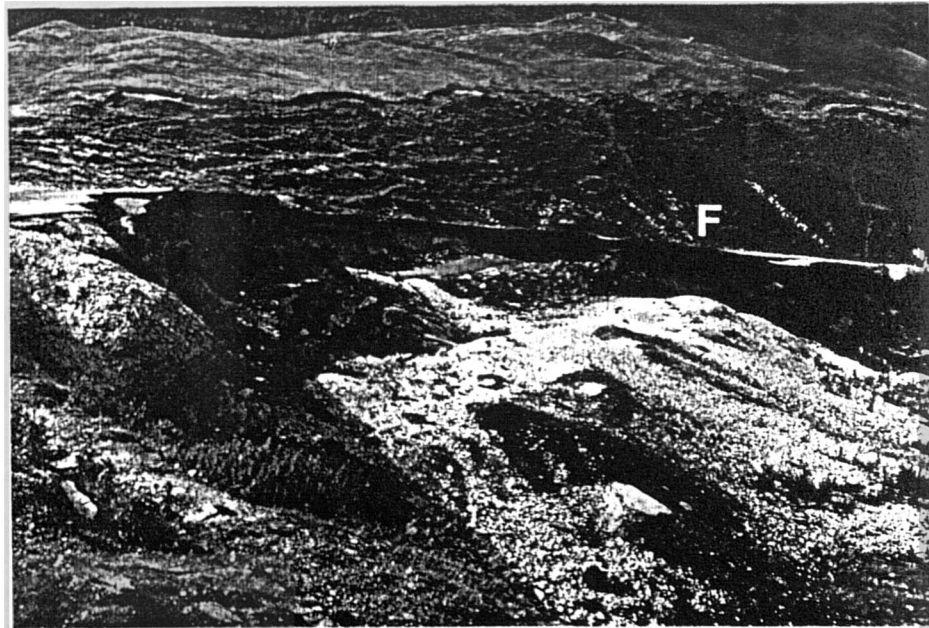


Plate No. 7.5 Damage at the upper road at Mam Tor. Note that successive layers of road surfacing material have been applied in an attempt to maintain the road. French drains on main unit of Mam Tor landslide 'F'.

The chief morphological features of the main unit of the landslip are as follows:

- i. The crown forms the highest point of a series of crests running in a NE-SW direction, vegetation covers most of the area.
- ii. The steep back scarp has a vertical height of 90m. and is composed of Mam Tor Sandstone, Plate 7.3.
- iii. The sandstones and interbedded shales comprising Mam Tor Sandstone exposed in the back scarp dip 5° in a NW direction (into the face). Rotation of the main unit of approximately 50° is apparent since outcrops in the part dip 55° in a NE direction (See map Fig. 7.3).
- iv. Beds, in particular sandstone in the main unit, have suffered distortion.
- v. The back scarp is a free face subject to not infrequent rock-fall instability which together with smaller talus flows contribute to the 40° scree slope shown in Plate 7.3. The slickensided failure surface photographed in Plate 7.4 is preserved beneath talus at the top of the scree slope. This surface which dips at an angle of about 85° becomes exposed when the rate of downward movement of scree exceeds the rate of scree debris accumulation.
- vi. Small scale instability of land along southern flank of the main unit produces the minor scarps illustrated in Plate 7.3. The SE-NW trending fault shown on geological map Fig. 2.2 accounts for the outcrop of Edale Shale in this part of the landslip.
- vii. At the base of one of these retrogressive slides a seepage occurs which Vear and Curtis (1981) interpret as flow from the fault crush zone (See geological map, Fig. 2.2).
- viii. Present day instability of the minor scarps along the southern flank of the landslip is evidenced by the lack of vegetative cover and surface disturbance in this area.

- ix. A well developed debris lobe extends from one of the main retrogressive slips of the southern flank. The downward facing convex front of this lobe has buried the vegetation which it overrides giving a clear indication of active movement. Also large angular blocks at the base of the lobe show signs of rotational within the surrounding turf.
- x. As shown on map Fig. 7.3. The surface of main unit above the upper part of the road is affected by a conspicuous intersecting pattern of linear ridges and hollows trending WNW-ESE. This feature may be the result of internal displacement along bedding planes in the Mam Tor Sandstone of the main unit or it may be due to slope processes which pre-date the main instability.
- xi. As indicated in Plates 7.5 and 7.6 the upper part of the road has been seriously damaged by the instability and in some places several metres of vertical and horizontal movement prevent the passage of wheeled traffic. The upper road is mainly damaged at the edge of unstable area, where downward movement shown in Plate 7.5 is evident.
- xii. A series of minor scarps shown in Plate 7.7 also affect the upper road for most of its transverse across the displaced ground.
- xiii. The foot of the main unit is characterized by hummocky ground with a system of linear ridges and hollows running in SE-NW and NNE-SSW, directions. These are illustrated in Plate 7.8.
- xiv. Examination of the aerial photograph, Plate 7.1 indicates that in most places, the edge of the landslide is well-defined. In fact, the location map, Fig. 2.1, (1:25000 Geological map) shows a northward extension of the area of instability, but it would appear that this part is now stable.
- xv. The lower road has also been damaged by the movement with the upward movement shown in Plate 7.9 and Fig. 7.4 at the northern margin while at the southern margin the horizontal translation and vertical movement shown in Plate 7.8 are evident.



Plate No. 7.6 Damage of the upper road at Mam Tor. Note that the recent instability has caused a downward movement with lateral displacement.



Plate No. 7.7 Minor scarp at little Mam Tor 'A'.



Plate No. 7.8 Hummocky ground at the foot of main unit. Recent downward movement of lower southern edge of the road in January 1983.



Plate No. 7.9 Heave movement at northern part, Lower road.

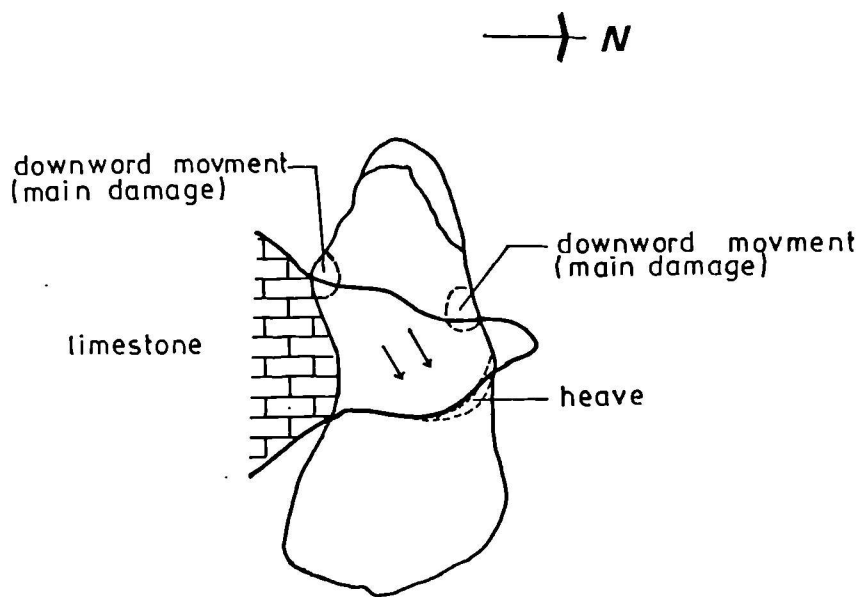


Fig. 7.4 Mam Tor landslip showing the main damage and the heave area.

The toe of the landslip is characterized by:

- i. Various seepages which occur in the locations indicated in map Fig. 7.3. Although these wet areas are marshy in part, they are also the sites of iron oxide precipitation which forms a hard crusty deposit.
- ii. The aerial photograph, Plate 7.1 indicates a system of linear ridges and hallows in this area.
- iii. As indicated by Plates 7.10 and 7.11 the toe of the slide is convex in profile and rises to height of average of 10m. above the original ground surface (See Fig. 8.5).
- iv. The toe of the slide is very active as evidenced by the destruction of Blacketlay barn in March 1983. Plate 7.10 shows the barn before its destruction whereas in Plate 7.11 it has been pushed over by advancing movement.

7.2.2 Movement at Mam Tor

According to the EDM survey described in Chapter 3, at Mam Tor movements can be characterised into three areas in which the main unit, the foot of the main unit and the leading edge of the toe undergo different styles. The magnitude and the direction of the movement of the 21 survey stations located on map Fig. 3.5 are given in Fig. 7.5 and Table 7.3.

Movements which have occurred between October 1981 and May 1983 may be summarized as follows:

Main unit	30cm in a NE direc.	Oct 1981-May 1983
Upper main scarp	75cm in a NE direc.	Oct 1981-May 1983
Upper road	34cm in a NE direc.	Oct 1982-May 1983
Minor scarp upper road	46cm in a NE direc.	Oct 1981-Oct. 1982
Foot of main unit	101cm in a ENE "	Oct 1981-May 1983
Lower road	60cm in a ENE "	Oct 1981-May 1983
Upper part of toe	92cm in a ENE "	Oct 1981-May 1983
Middle & lower part of toe	43cm in a NE "	Oct 1981-May 1983



Plate No. 7.10 Blacketlay Barn before March 1983.



Plate No. 7.11 Destruction of Blacketlay Barn. March 1983. Note convex character of toe.

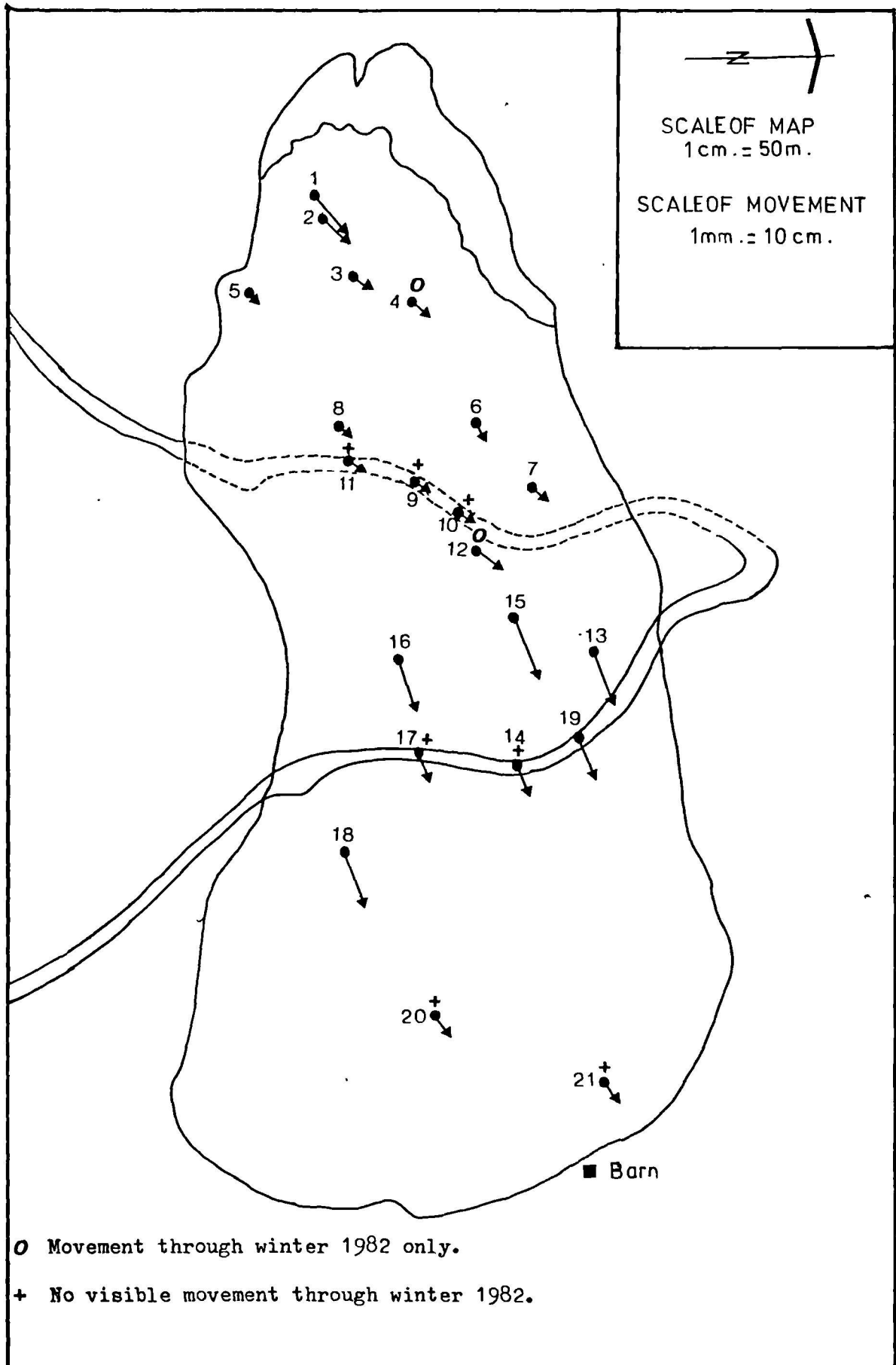


Fig. 7.5 Results of surveying at Mam Tor.

Table 7.3 Results of EDM survey at Mam Tor.

Location	Movement cm Oct,1981-Oct,1982	Movement cm Oct,1982-May,1983	Total cm
1	40	46	86
2	27	47	64
3	9	22	31
4	28	---	28
5	3	13	16
6	8	19	27
7	17	20	37
8	5	20	25
9	-	24	24
10	-	23	23
11	-	39	39
12	46	---	46
13	40	58	98
14	-	53	53
15	52	63	115
16	11	81	92
17	-	51	51
18	42	50	92
19	14	63	77
20	-	45	45
21	-	40	40

- indiscernable movement

--- survey point lost

The diversion in the direction of the movement at the foot of the main unit and the lower road may be due to the resistance offered by the stable area on the southern flank which also causes the heave in the northern part of the toe shown in Plate 7.9 and Fig. 7.4.

Table 7.4 shows the average rates of movement for a various parts of the landslide. The main unit has moved in an average rate of 4.1 cm./month, while the foot part shows the higher rate of movement of 10.4 cm./month. The toe of the landslide has moved at a rate of 8.2 cm./month, during the period of October 1981 to May 1983.

From the consideration of the road maintenance records and weather observations, it may be concluded that large movements of the landslide may be correlated with instances of high rainfall. It would be interesting to consider the results of the surveying at Mam Tor over the period October 1981 - May 1983 with respect to rainfall, but due to the absence of suitable climatic records, only tentative conclusion can be drawn.

Rainfall records obtained by the Meteorological Office (Bracknell, Berkshire) for Edale Mill and Hope Valley Cement Works. (See map Fig. 2.1 for location of the measuring stations). For the years 1981-1983 are presented in Fig. 7.6 on a month by month basis. These records may be compared with the recorded movements of various parts of the Mam Tor landslide listed in Table 7.3. It can be seen that comparatively low rainfall during the winter of 1981-1982 was followed by relatively small movements of the landslide. A relatively dry year in 1982 in which rainfall amounts varied between monthly low of about 15mm and height of about 190mm was followed in January 1983 in which 250mm was measured. This high rainfall may account for the relatively rapid movement observed to have occurred between October 1982 and May 1983. It is also significant that the accelerated damage shown in Plate 7.8 which effected the southern part of the lower road was observed at the end of January 1983.

Table 7.4 Average rates of movement at Mam Tor landslip between October 1981 and May 1983.

Mam Tor	Movement 1982 Oct 1981-Oct1982	Movement 1983 Oct1982-May1983	Total movement Oct1981-May1983
Main unit	0.9 cm/month	3.2 cm/month	4.1 cm/month
Foot	1.7 cm/month	8.7 cm/month	10.4 cm/month
Translation Toe	1.1 cm/month	7.0 cm/month	8.1 cm/month

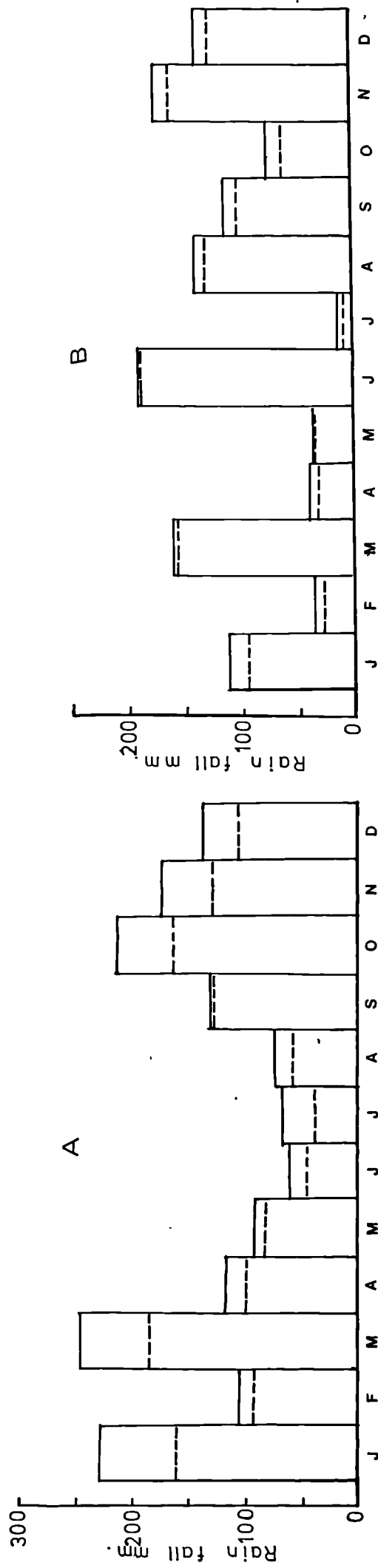
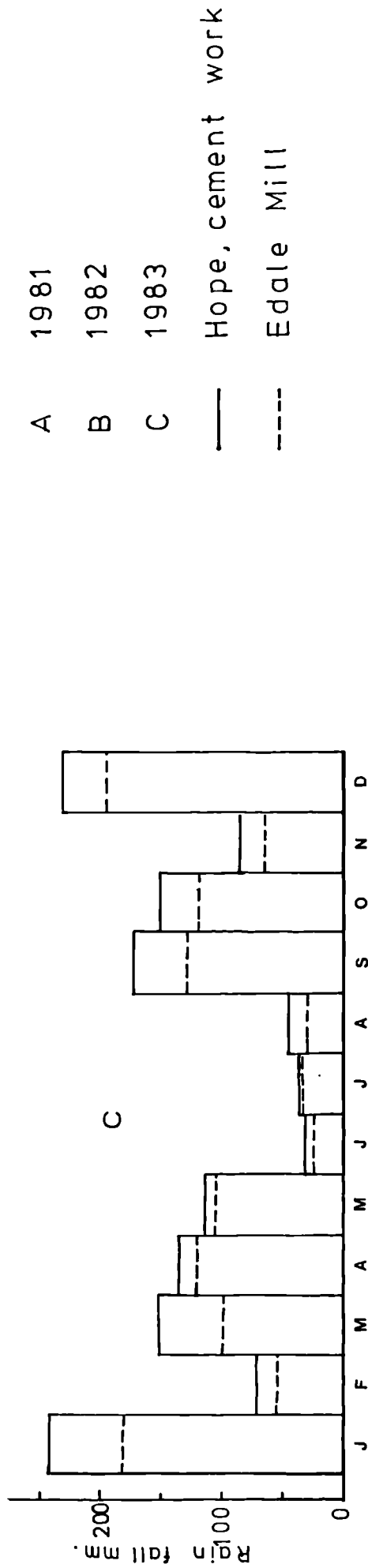


Fig. 7.6 Histogram of monthly rainfall of Edale Mill
 and Hope Cement Works. Years - 1981, 1982 and
 1983.

7.3 Rushup Edge

The landslide at Rushup Edge, near Mam-Nick is one of the most well-known landslips developed in the Millstone Grit Series rocks. As indicated in map Fig. 7.7 and Plate 7.12, in common with landslide at Mam Tor, it can be divided into two main parts. The upper part is characterized by a non-circular rotational slide with a translational slide or flowage forming the toe. According to Skempton and Hutchinson's (1969) classification the landslide is a complex type in which the rotational part measures 500m. long by 750m. wide while the translational part covers an area 600 m. long by 600m. wide.

The main features of the Rushup Edge landslide are as follows:-

- i. The crown of the landslide forms an E-W trending crest with a system of transverse cracks affecting the western part. Most of this area is vegetated.
- ii. A well-developed main scarp of maximum height 52m. marks the top of the unstable area. Since as shown in Plate 7.13, for the most part this is vegetated so it would appear that it is stable.
- iii. The Minor scarp seen in Plate 7.13 form a series of NE-SW trending steps near to and below the head of the landslide. These are an indication of the rotational failure of the main unit.
- iv. Few outcrops occur in the Rushup Edge area but near the top of the landslide, where a minor road cuts through the crest of Rushup Edge, undisturbed beds of Mam Tor Sandstone dip 10° towards the NE. Inward rotation of approximately 4° is indicated since dip of about 6° to the NE within the main unit. Generally speaking, the main unit of the landslide is characterized by well developed hummocky ground shown in Plate 7.13.
- v. Hollows within the landslide area, and particularly between the crest and the back scarp contain, accumulations of peat.

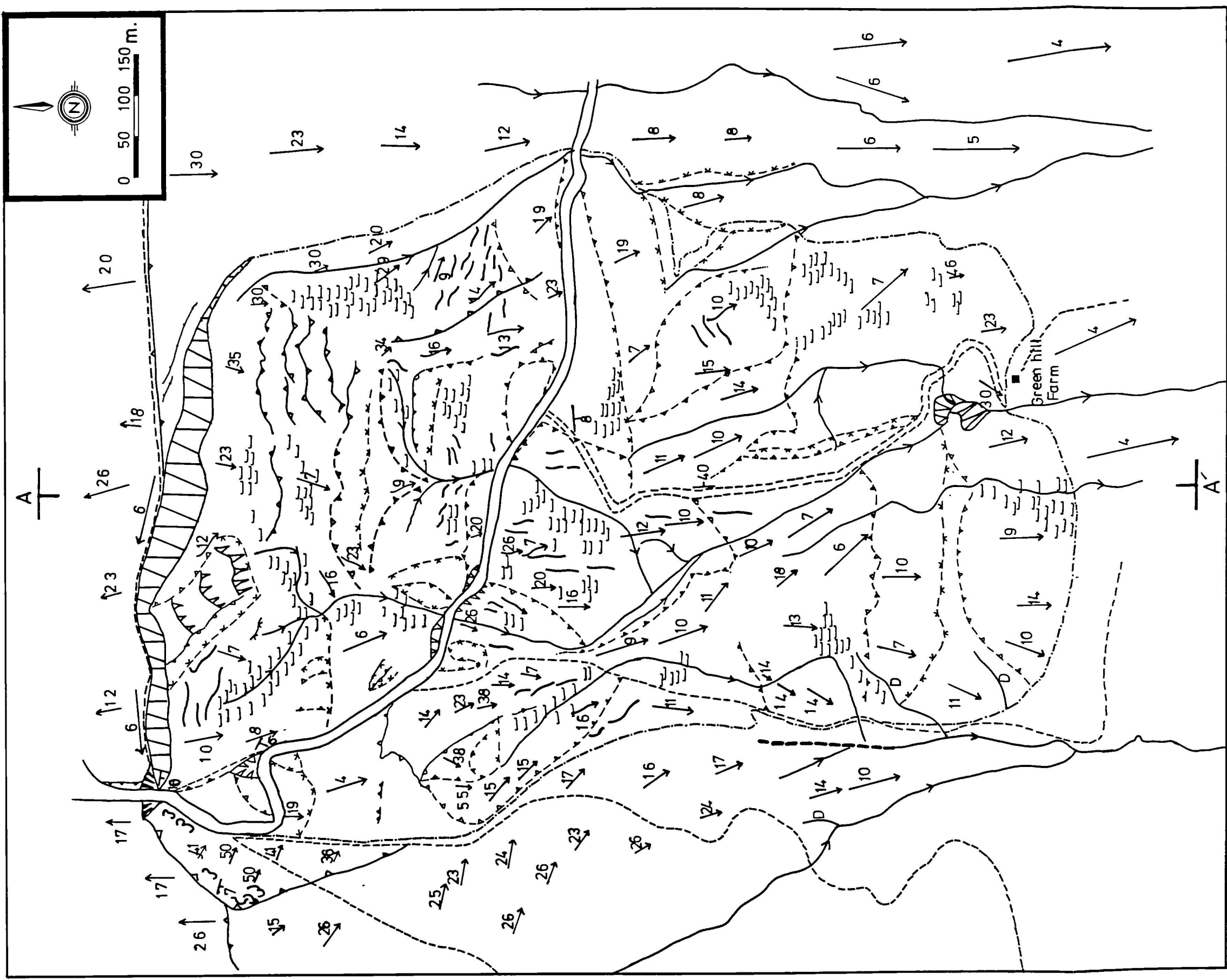


FIG. 7.7 GEOMORPHOLOGICAL MAP OF RUSHUP EDGE LANDSLIP.

Plate No. 7.12 Aerial photograph of Rushup Edge landslip.
Scale: 1:6000





Plate No. 7.13 Main scarp and main unit landslip
at Rushup Edge.



Plate No. 7.14 Toe of landslip at Rushup Edge.
Note the present of marshy areas.

- vi. The translational toe (See Plate 7.14) is also characterized by hummocky ground but of a less intense nature than that of the upper part.
- vii. The flanks of the landslip are clearly defined as in Plate 7.12.
- viii. The toe of the landslip rises to a height which averages 8m. above the valley floor (see Fig. 8.6). It is well defined, as shown in Plate 7.14. The toe displays a convex profile shown in Plate 7.15 and a tongue like shape shown in Plate 7.14.
- ix. The general trend of the movement is towards the NNW.
- x. The lack of evidence of recent activity of this landslide is demonstrated by Plate 7.13. The road is undeformed both within the slide area and where it crosses the slide margins. Furthermore, a wall presumed to be quite old shows no sign of displacement and both the fence at the toe of the landslip shown in Plate 7.15 and Greenhill Farm buildings are not affected by movements. Although Fig. 7.15 shows lean and slight curvature of some trees at the toe of the convex these features do not apply to all trees in area, also the fence in this area has not been disturbed.

The presence of water seepage over the whole landslip area (See Fig. 7.7) indicates a high water table. The well formed system of surface drainage also indicates comparative stability.

7.4 Cold Side

A large area of instability at Cold Side affects Millstone Grit Series rocks which occur on the southern side of Edale Valley (See Map Fig. 2.1). This landslip is a rotational type 575m long by 650m wide where movement has occurred generally in a North western direction. The main characteristics of this landslip are illustrated



Plate No. 7.15 The convex margin of the toe of the landslide at Rushup Edge.

in map Fig. 7.8 and Plates 7.16 and 7.17. Attention is drawn to the following features:-

- i. The crown forms a 26° NE-SW trending slope on the valley side. Much of this area is vegetated although a small tension crack on the eastern margin of the main scarp provides evidence of recent instability.
- ii. A well developed main scarp marks the upper margin of the instability. In fact this feature consists of two linear portions, one trending EW, and the other NE-SW where, the maximum height of 43m. decreases respectively towards the west and north east until it merges with the original ground slope. The rock exposed in the scarp are Mam Tor Sandstone.
- iii. As indicated by Plate 7.18, for the most part, the main scarp is vegetated. This area is not subject to rockfalls.
- iv. Seepage water emanates from the main scarp and forms a stream which flows to the toe of the landslip.
- v. Several minor scarps are well developed within the landslip area. These are shown in Plates 7.16 and 7.19, since most are vegetated, they are probably stable.
- vi. Rather few outcrop occur in the landslip area. Beds of sandstone in the main unit scarp dip to the SE at angles of $5-7^{\circ}$ whilst beds within the main body of the landslip dip $12-16^{\circ}$ NE thus implying an outwards rotation of $7-9^{\circ}$. The beds which occur within the main body of the landslip, have apparently suffered little distortion in consequence of this rotation.
- vii. The rock which outcrops in the foot and toe areas is probably Edale Shale.
- viii. The foot of the slip is marked by a minor scarp with a steep slopes which become rather irregular towards the eastern part.
- ix. At a number of locations, especially in the eastern sector, hollows contain accumulation of peat.
- x. The toe of the landslip shown in Plate 7.20 consists of a smooth 8° slope formed of landslip debris.

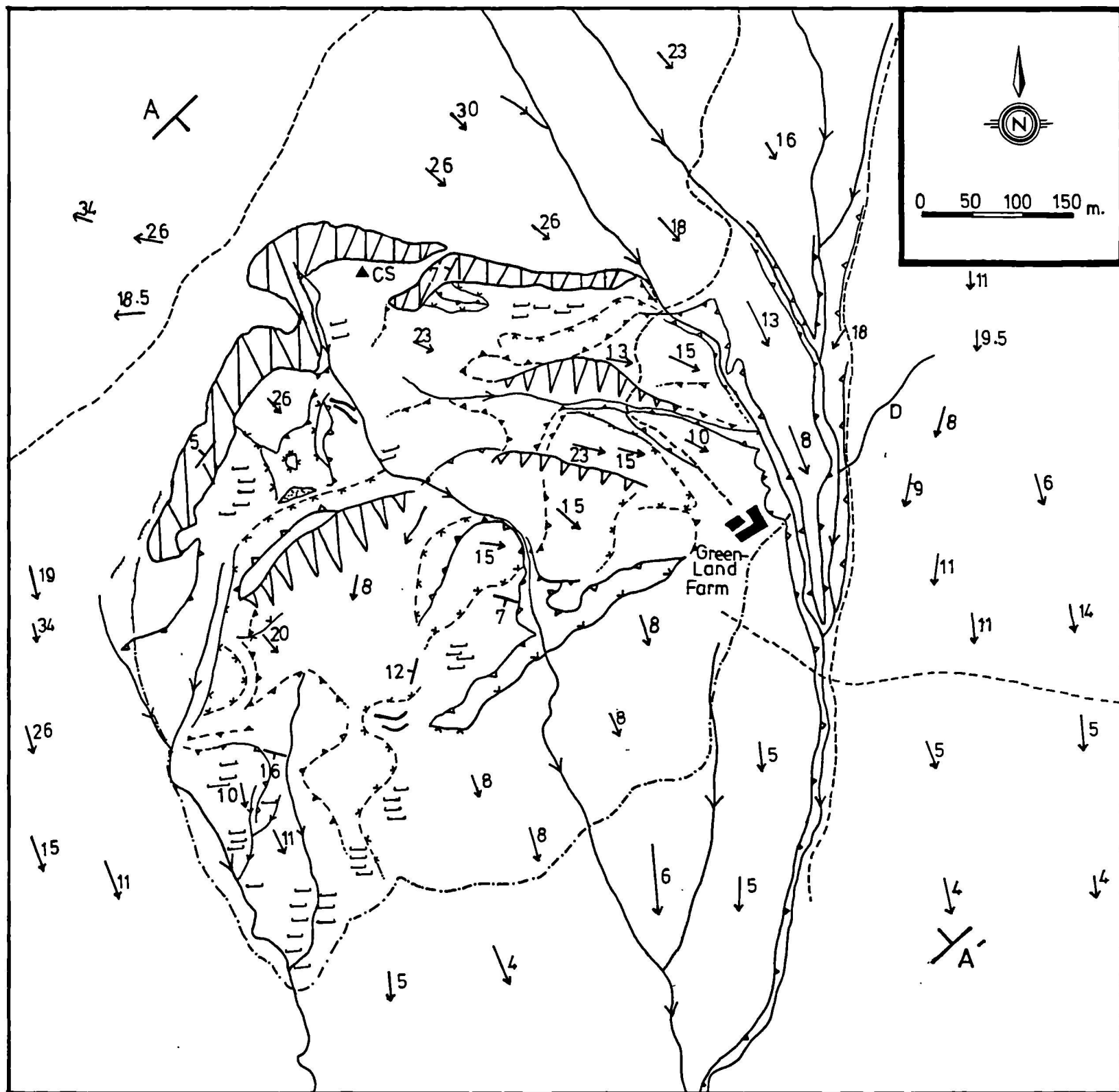


FIG. 7.8 GEOMORPHOLOGICAL MAP OF COLD SIDE LANDSLIP.

Plate No. 7.16 Aerial photograph of Cold Side landslip.
Scale: 1:13000





Plate No. 7.17 General view of Cold Side landslip.
Note the vegetated character and
change in direction of the minor
scarp.



Plate No. 7.18 East-west part of the main scarp of the landslide at Cold Side.



Plate No. 7.19 Minor scarps in the landslide at Cold Side, note that there are mostly grass covered.



Plate No. 7.20 The toe of Cold Side landslide. Note the presence of marshy areas.

- xi. The limit of landslip is well defined as shown in Plate 7.16.
- xii. The tension crack already mentioned is the only trace of recent activity. Field boundary walls, trees, the footpath as well as the buildings of Greenland farm show no sign of displacement. Furthermore, since the surface drainage is moderately well developed and the landslip is almost entirely covered with vegetation, it seems likely that only in the most unfavourable groundwater condition does the factor of safety approach unity.

7.5 Back Tor

As shown in Fig. 2.1 the Back-Tor landslip extends from the crest to the base of the hill separating Edale and Castleton valleys. Movement has occurred in a NNW direction and the landslip is 950 m. long by 720 m. wide. According to Skempton and Hutchinson's (1969) classification it is a rotational failure. The geological map Fig. 2.2 indicates that the landslip has occurred in Millstone Grit Series rocks.

The main features of this landslip described below are illustrated in map Fig. 7.9 and Plates 7.21 and 7.22:

- i. The crown slopes 30° to the north-west and forms part of the crest of the hill slope between the two valleys, this area is covered with vegetation.
- ii. The main scarp is curved and may be divided into three parts. The eastern part includes a large exposure of undisturbed bedrock which consists of alternating thick beds of well jointed sandstone and highly fissile shale belonging to the Shale Grit and Mam Tor Sandstone. The near vertical face shown in Plate 7.23 reaches a maximum height 49m. The middle part is much less steep with average slopes of 26° and it is covered with vegetation. The western part shown in Plate 7.24 slopes at angle of up to 50° and it is vegetated.

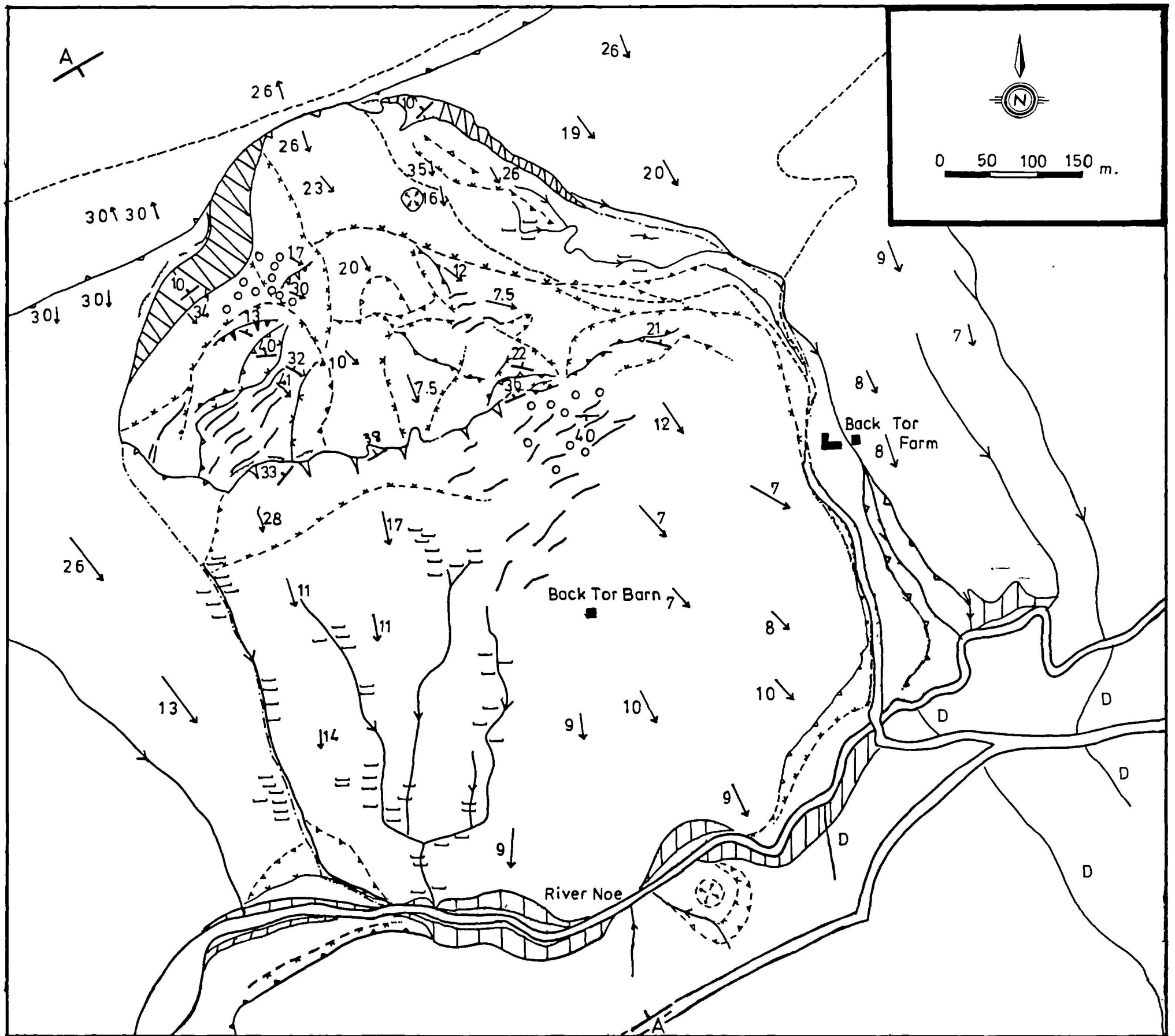


FIG. 7.9 GEOMORPHOLOGICAL MAP OF BACK TOR LANDSLIP.

Plate No. 7.21 Aerial photograph of Back Tor landslip.
Scale: 1:13000





Plate No. 7.22 General view of Back Tor landslip.
Note the steep exposure of Shale
Grit and Mam Tor beds in the back
scarp.



Plate No. 7.23 Eastern side of the main scarp of the landslip at Back Tor.



Plate No. 7.24 Western side of the main scarp of Back Tor landslip. Part of the main unit shows the hummocky ground with sandstone blocks below the main scarp.

- iii. Movements in the eastern part are much greater than those of the western or middle parts. A well developed minor scarp occurs in the eastern part of the main unit of the landslip. This feature can be seen in Plate 7.23 and 7.21 and map Fig. 7.9, which also show the hummocky ground that comprises a series of generally NE-SW trending hollows and ridges in this area.
- iv. The eastern part of the main scarp is subject to rock fall instability, the debris of which forms the scree slope shown in Plate 7.23 and 7.24.
- v. According to the geological map and field observations, the main unit of the landslip occurs in Mam Tor Sandstone while the foot and toe are situated on Edale Shale.
- vi. At the foot of the landslip a minor scarp in Plate 7.25 gives rise to an E-W trending steep slope which becomes less severe in a westerly direction.
- vii. The sandstone beds exposed in the main scarp dip SE at 10° while the bed at foot of the landslip dip 38° SE which gives an outward rotation of 28° .
- viii. The field observations shown in map Fig. 7.9 indicate variations in the attitude of beds at the foot of the landslip which suggests that the beds have suffered distortion during movement.
- ix. As shown by Plate 7.21 and map Fig. 7.9 in the middle part of the landslip there is a series of NE-SW trending hollows and ridges which gradually die out towards the top which forms the smooth slope of $7-8^{\circ}$ shown on Plate 7.26. These features may be the result of internal displacement along the bedding planes within the Mam Tor Sandstone.
- x. Surface drainage consists of a ditch on the western side of the main unit which carries water from near the western flank of the landslip to the River Noe. The eastern side of foot and toe have a well developed system of surface drainage.



Plate No. 7.25 Minor scarp at foot of the main unit of Back Tor landslip.



Plate No. 7.26 Part of the foot and toe of the landslip at Back Tor. Note the gentle slope of toe.

- xi. The toe of the landslip forms a steep slope at the bank of the River Noe as shown in map Fig. 7.9. The great steepness of this slope is probably due to undercutting by the river.
- xii. The boundary and the flank of the landslip are well defined as seen in Plate 7.21.
- xiii. The condition of the field boundary walls, foot path, trees and Back Tor farm buildings suggest that the landslip is now stable. Also the vegetation and surface drainage is moderately well developed.

7.6 Burr Tor

The landslip at Burr Tor located on map Fig. 7.10, is a rotational landslip affecting Millstone Grit Series rocks. It is situated near the village of Little Hucklow (See map Fig. 2.1). The generally westerly movement affects an area of maximum length 500m. and width 760m. The features illustrated in map Fig. 7.10 and Plate 7.27, 7.28 and 7.29 may be summarized as follows:

- i. The crowns forms a flat grass covered area.
- ii. The main scarp illustrated in Plates 7.28 and 7.29 comprises a steep cliff of vertical height 20m which is for the most part vegetated. This scarp consists of sandstone units belonging to the Shale Grit Series (See geological map Fig. 2.2).
- iii. The head of the landslip is densely vegetated with bushes and trees which occupy a depression along the edge of the main scarp.
- iv. The sandstone bed in the main scarp dips SE at an angle of 10° , while in the main unit of the landslip the dip is 34° SE. Thus an outward rotation of about 24° is indicated. No distortion of the ground surface consequential upon instability was noted during field observations.
- v. The main unit of the landslip can be divided into northern and southern parts, the latter of which is characterized by hummocky ground with rock

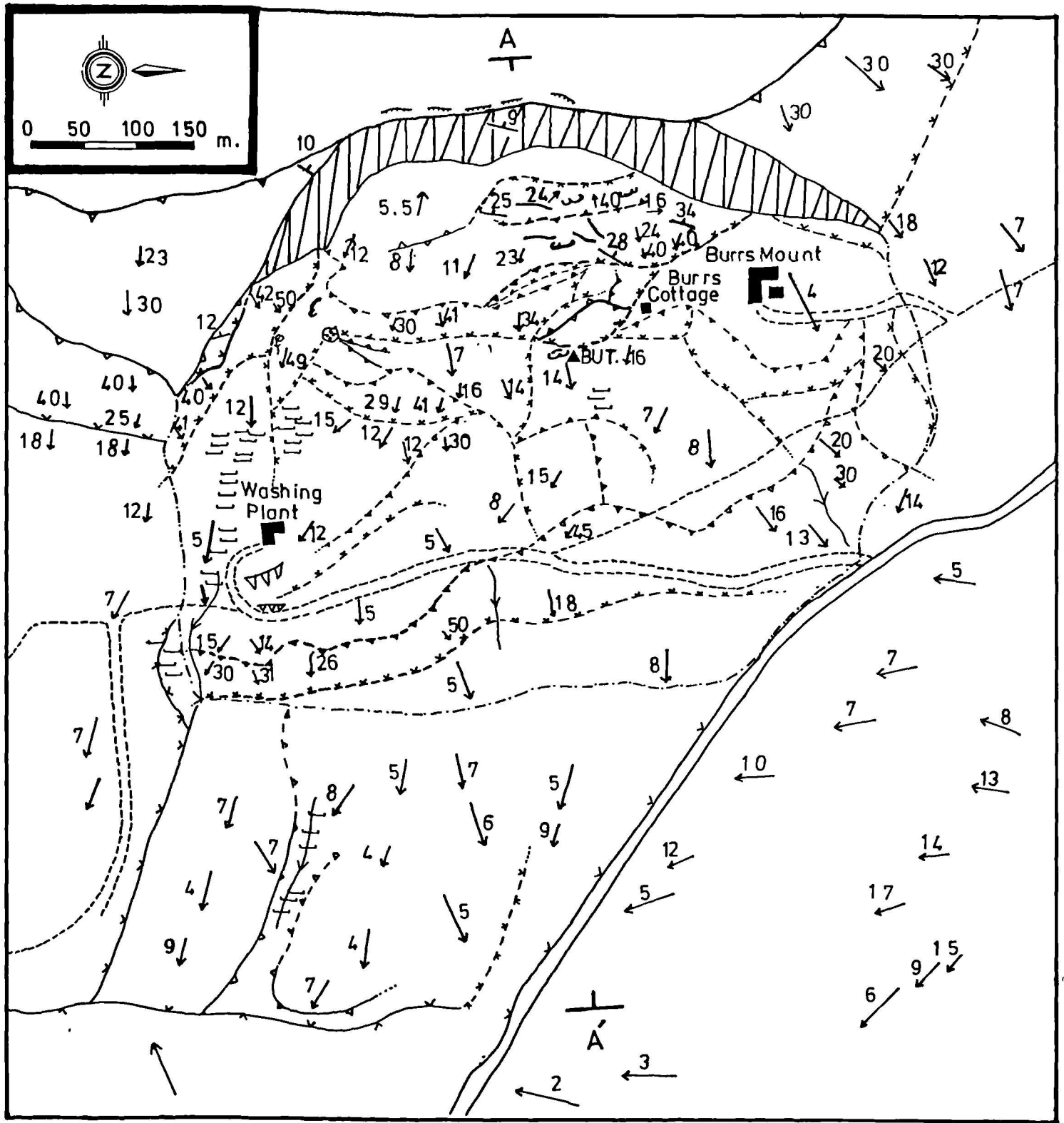


FIG. 7.10 GEOMORPHOLOGICAL MAP OF BURR TOR LANDSLIP.

Plate No. 7.27 Aerial photograph of Burr Tor landslip
Scale: 1:4000





Plate No. 7.28 General view of landslip at Burr-Tor. Note the main scarp behind the belt of trees.



Plate No. 7.29 Main scarp of the landslip at Burr Tor. Note the steep exposure of sandstone of Shale Grit, and hummocky ground at the main unit.

exposure and a conspicuous pattern of N-S trending ridges and hollows. These features do not occur in the northern area which consists of smooth vegetated slope.

- vi. Seepage water and springs occur near the northern flank of the landslip.
- vii. The foot is characterized by a smooth 5-8° slopes with W and NW trend in the southern part, and a SW trend in the northern part. This gentle slope is broken across the whole width of the foot by a steep slope which ranges between 26° and 50° in the northern part and about 13° in the south.
- viii. The northern part of the toe of the landslip shown in Plate 7.29 is characterized by a convex slope. To the south of the toe the slope gradually decreases until it merges with the undisturbed ground.
- ix. The geological map Fig. 2.2 and field observation show that the main unit and toe occur on shale of Millstone Grit Series.
- x. The limits of the landslip are well defined as indicated by Plate 7.27.
- xi. There is no evidence of recent activity of the landslip at Burr Tor since neither Burrs Mount nor Burrs Cottage Farms have been affected and also the large well established trees in the upper part of the landslip show no sign of movement.

7.7 Bretton Clough

At Bretton Clough (See map Fig. 2.1) an elongated landslip with a maximum width of 2200m. occurs. It is convenient to separate the area of instability shown in map Fig. 7.11 into western and eastern landslip by taking an intervening narrow neck as the dividing line as shown in Fig. 7.11A. In fact, this narrow area of width 130m. has also been affected by movement. The landslip at Bretton Clough occurs in Millstone Grit Series rocks as shown in geological map Fig. 2.2. Analysis of map Fig. 7.11 and Plate 7.30 indicates that according to Skempton

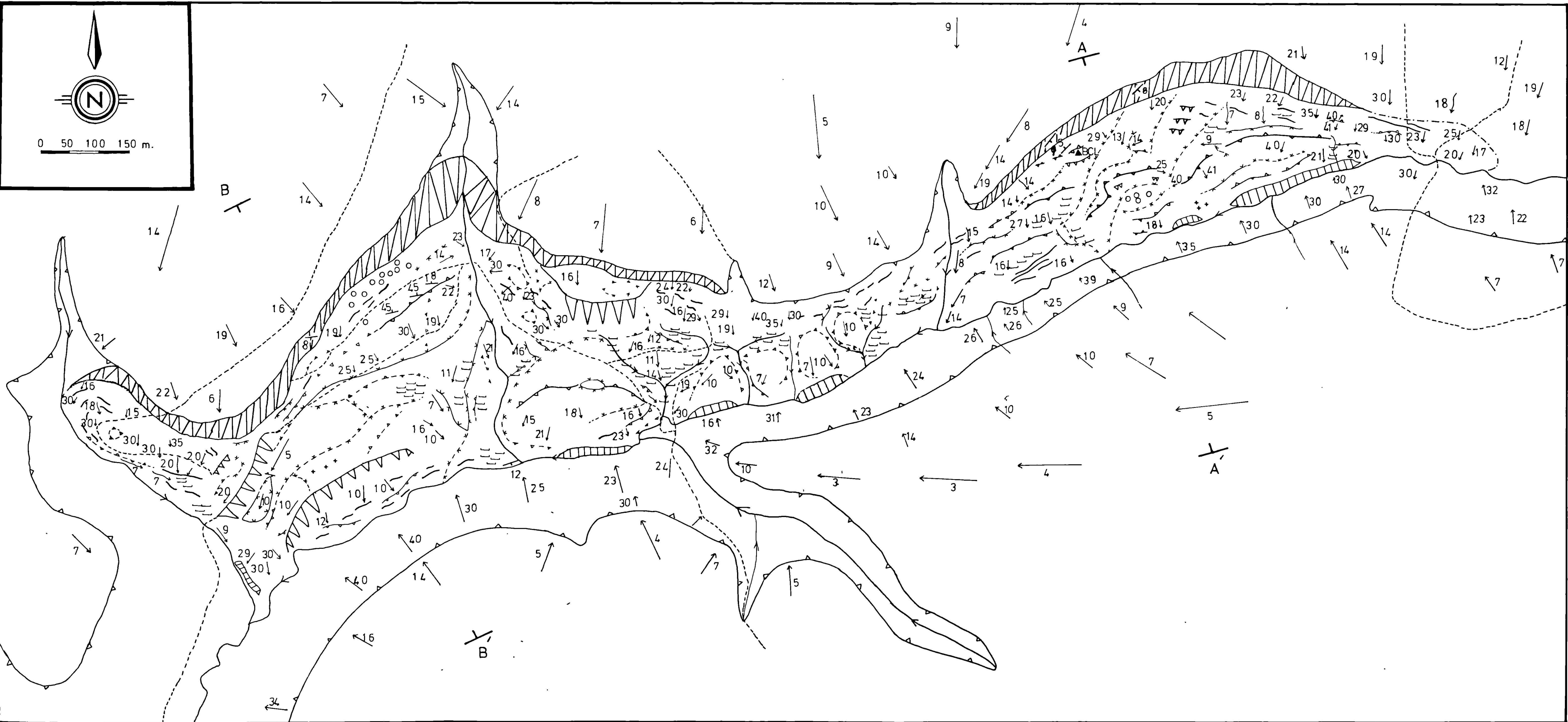


FIG. 7.11 GEOMORPHOLOGICAL MAP OF BRETTON CLOUGH LANDSLIP.

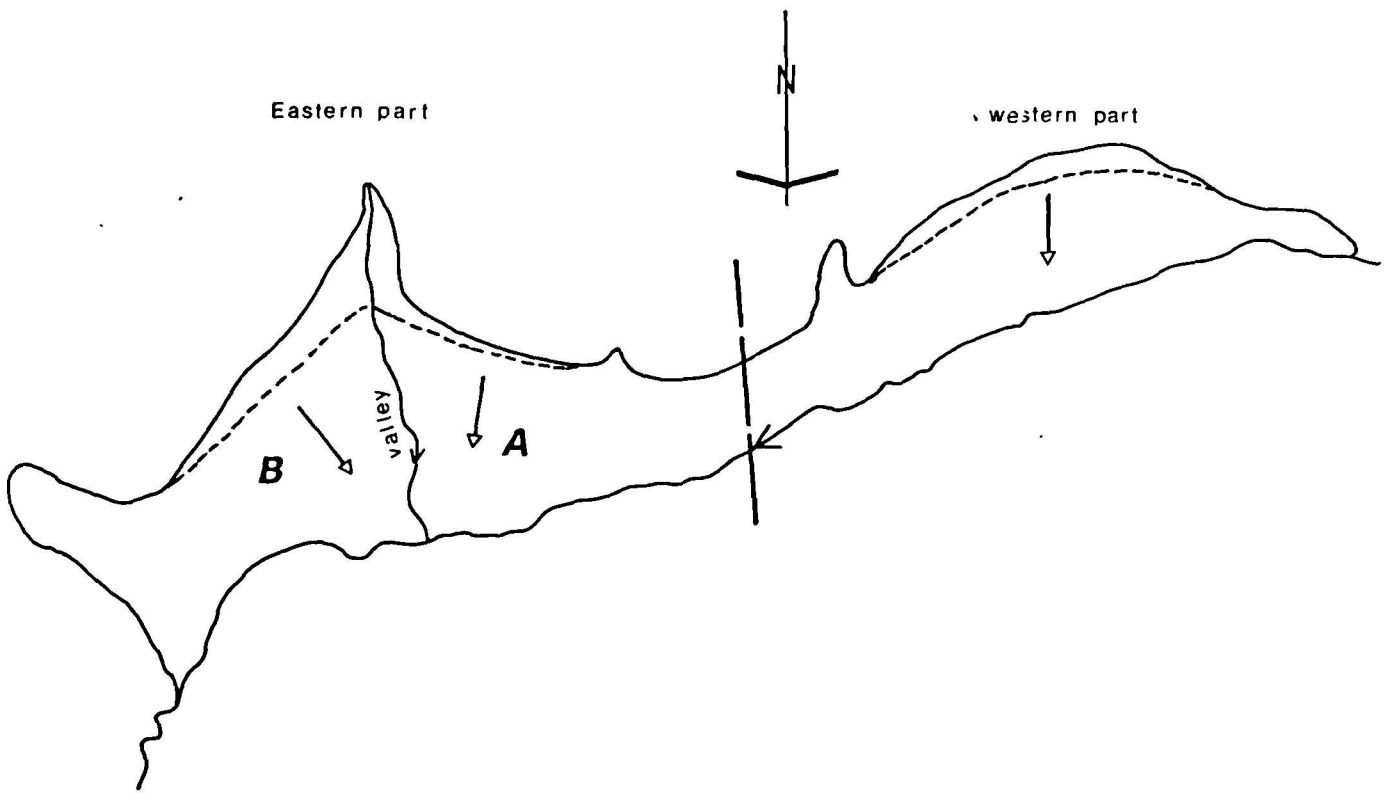


Fig. 7.11 A Sketch showing regional subdivisions of Bretton Clough landslip to which reference is made in the text.

Plate No. 7.30 Aerial photograph of Bretton Clough land-
slip.

Scale: 1:12000



and Hutchinson's (1969) classification these landslips are rotational, non-circular types. Owing to their rather different character, the main features of the western and eastern parts will be considered separately.

Western part .

- i. The crown forms part of gentle E-W trending slope of hilly vegetated ground.
- ii. The well developed curved main scarp shown in map Fig. 7.11 and Plates 7.30 and 7.31 has a near vertical face of maximum height 25m. A large exposure of undisturbed bedrock consists of alternating beds of well jointed sandstone and shale from the Shale Grit Formation. The height of the main scarp reduces towards the eastern end where a small N-S trending valley has been formed.
- iii. Small minor scarps form a series of SE-NW trending steps below the head of the landslide area. These are an indication of rotational failure (See map Fig. 7.11). The main unit of this landslide has a series of 10-15m. high ridges running generally WSW-ENE with steep slopes formed on the northern side. As indicated in Plate 7.31 the intensity of these ridges diminished towards the foot zone. The foot is characterized by hummocky ground.
- iv. The toe of the landslide in Plate 7.31 is not well developed since it is subjected to river erosion where the slide has raised by several metres the level of Bretton Clough. Erosion produces a steep slope towards the river in some places. The main unit and the toe overlie shale from Millstone Grit Series as indicated by map Fig. 2.2.
- v. Marshy areas occur in the hollows between the ridges.
- vi. The dip sandstone beds in the main scarp is 9° NW while the dip within the main unit is 5° SE. This implies an outward rotation of 14° . It is also observed that sandstone beds within the main unit have suffered some distortion due to movement.



Plate No. 7.31 Western part of the landslip at Bretton Clough. Note ridged ground.



Plate No. 7.32 Eastern landslip at Bretton Clough - general view.

- vii. The general direction of movement of the slipped material is NNE and the limit of the landslide is well defined, as shown in Plates 7.30 and 7.31.
- viii. Apart from erosion by the stream, no evidence of recent mass movement was noticed in this part of the landslide. The well established trees and the ground surface have not been disturbed and furthermore marshy areas are moderately well disturbed over the area.

Eastern part.

The eastern part is shown in Plate 7.32 Fig. 7.11 and Plate 7.30. the further subdivision adopted for this part of the landslide is indicated in Fig. 7.11A where a deep highly vegetated S-N trending valley separates two points labelled A and B. The main characteristic features are as follows:

Part A.

- i. The crown consists of a 7° NE slope which is practically entirely vegetated.
- ii. The main scarp is well defined with a maximum height of 10.5m as shown in Plates 7.30 and 7.32. This area is mostly vegetated but small outcrops of sandstone with some thin shale beds belonging to the Shale Grit Formation occur in this area.
- iii. A minor scarp which runs from the head of the landslide has a northward slope.
- iv. The main unit is characterized by hummocky ground. The whole of the foot consists of a curved ridge about 15m. high. The surface drainage in this area is well developed.
- v. The toe of this part of the landslide is not as well developed as that in the western part and it slopes gently towards the river as shown in Plate 7.33.
- vi. The general direction of movement is towards the NE.

Part B.

- i. The Crown consist of a vegetated area sloping 14° - 16° in a south westerly direction.



Plate No. 7.33 Part of the toe in the eastern part of landslide at Bretton Clough - Note the gentle slope towards the river.



Plate No. 7.34 Minor scarp on the eastern side of Bretton Clough with evidence of recent instability

- ii. The main scarp shown in Plates 7.30 and 7.32 is well defined with a maximum height of 21.5m. This area is mostly vegetated.
- iii. A SW-NE trending ridge occurs at the top of the main unit of the landslip. An exposure of sandstone beds in the main unit dips 45° SE while the dip of the sandstone beds in the main scarp is 8° NE. Thus an outward rotation of 53° has occurred.
- iv. At the eastern end, that is at the extreme flank of the landslip, as shown in map Fig. 7.11, a minor scarp forms a series of NE-SW trending steps from the main unit to near the toe of the landslip. The minor scarp nearest to the toe shows recent instability since in Plate 7.34 trees have become bent towards the river.
- v. The toe in this area is not as well developed as the one in Part A.
- vi. Apart from the instability noted in the foot, there is no evidence of movements within the remaining area.

7.8 Alport Castles

Alport Castles, located in Fig. 2.1, is an area of landslip which is one of the most interesting cases of instability in the area studied. It is a complex type of failure with a maximum length 800m. and width 1500m. developed in Millstone Grit Series rocks. Many aspects of the landslip are illustrated on map Fig. 7.12 and Plates 7.35 and 7.36. The main features may be described as follows:

- i. As shown in map Fig. 7.12, the crown of the landslip slopes in the opposite direction to the main scarp. It is mostly vegetated and along the upper edge of the main scarp there are a number of 60-70 cm. deep trenches containing peat as shown in Plate 7.37.
- ii. A well developed main scarp up to 32m. high shown in Plate 7.38 exposes jointed sandstone in thick

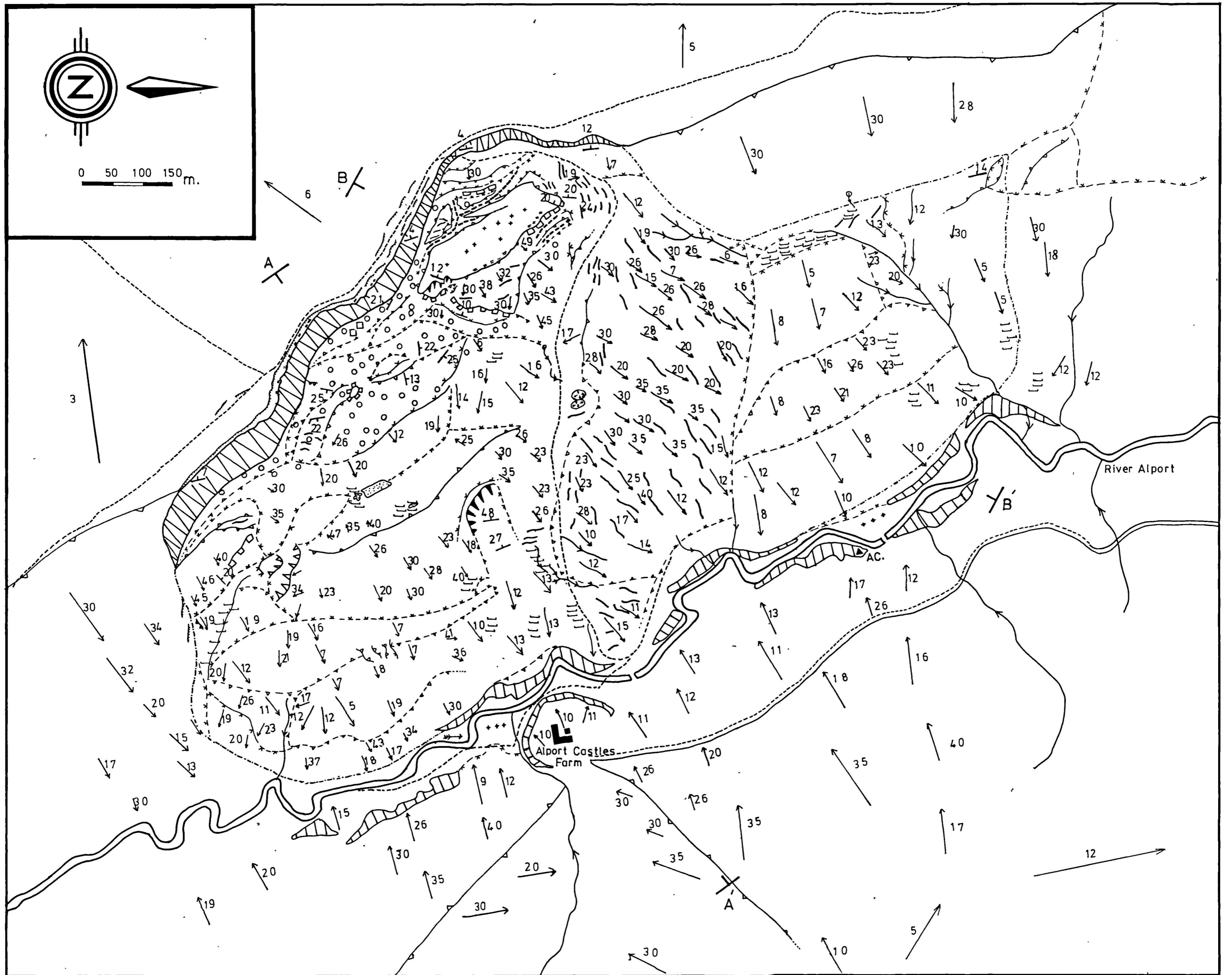


FIG. 7.12 GEOMORPHOLOGICAL MAP OF ALPORT CASTLES LANDSLIP.

Plate No. 7.35 Aerial photograph of Alport Castles
landslip.
Scale: 1:13000





Plate No. 7.36 General view of the landslip at Alport Castles.



Plate No. 7.37 The crown of Alport Castles landslip. Note the trenches contain peat.



Plate No. 7.38 Main scarp of landslide at Alport Castles showing a recent rockfall. Note the detached of block of the main unit.



Plate No. 7.39 The main scarp at the southern side of Alport Castles landslide. Note the hummocky ground of the main unit.

- beds. The slope of the main scarp decreases in a southerly direction into a vegetated 30° slope seen in Plate 7.39.
- iii. Instability in the form of rock falls shown in Plates 7.38 and 7.40 affects the main scarp where sandstone blocks form a scree slope.
 - iv. It is very noticeable in map Fig. 7.12 and Plate 7.35 that the toe of the landslip is affected by river erosion which has produced minor scarps up to 5m. high as shown in Plate 7.43.
 - v. From field observations and the geological map of Fig. 2.2, the main scarp and main unit consists of sandstone and shale beds of the Shale Grit and Mam Tor Sandstone Formations, while the toe of the landslip occurs on Edale Shale.
 - vi. The dip of the beds in the main scarp face vary between 4° ESE in the southern part and up to 7° ESE in the northern part. This compares with dips in the main unit of the landslip which vary from place to place in both magnitude and direction due to distortion during movement. The maximum dip of 25° to the SW implies a rotation of the main unit of up to 32° while in middle part of area as shown in Fig. 7.12 dips of 48° towards the ESE imply a rotation of up to 44°.

In view of the rotation which appears to have occurred and the presence of the major secondary movement, in terms of Skempton and Hutchinson's (1969) classification, the landslip is a complex type.

It is convenient to divide the landslip into the three areas "A", "B" and "C" shown in fig. 7.12 A.

The morphology of part A is as follows:

- i. This area is dominated as a large block 250m. long by 75m. wide shown in Plate 7.35 and 7.41 which appears to have become detached from the large area of ground involved in the initial instability. As shown in Fig. 7.12 A and Plate 7.38, further detached





Plate No. 7.40 Scree formed by distribution of sandstone blocks in the main unit of landslip at Alport Castles with a detached block due to secondary movement. Note Back scarp of sandstone and shale beds of Shale Grit formation.



Plate No. 7.41 Part of the main unit of the landslip shows a block of 250 m. by 75 m. wide at Alport Castles landslip.



Plate No. 7.42 Northern side of the main unit of the landslip at Alport Castles. Note the ponding of water.



Plate No. 7.43 Part of the toe at landslip of Alport Castles forming minor scarp along flank of river Alport.

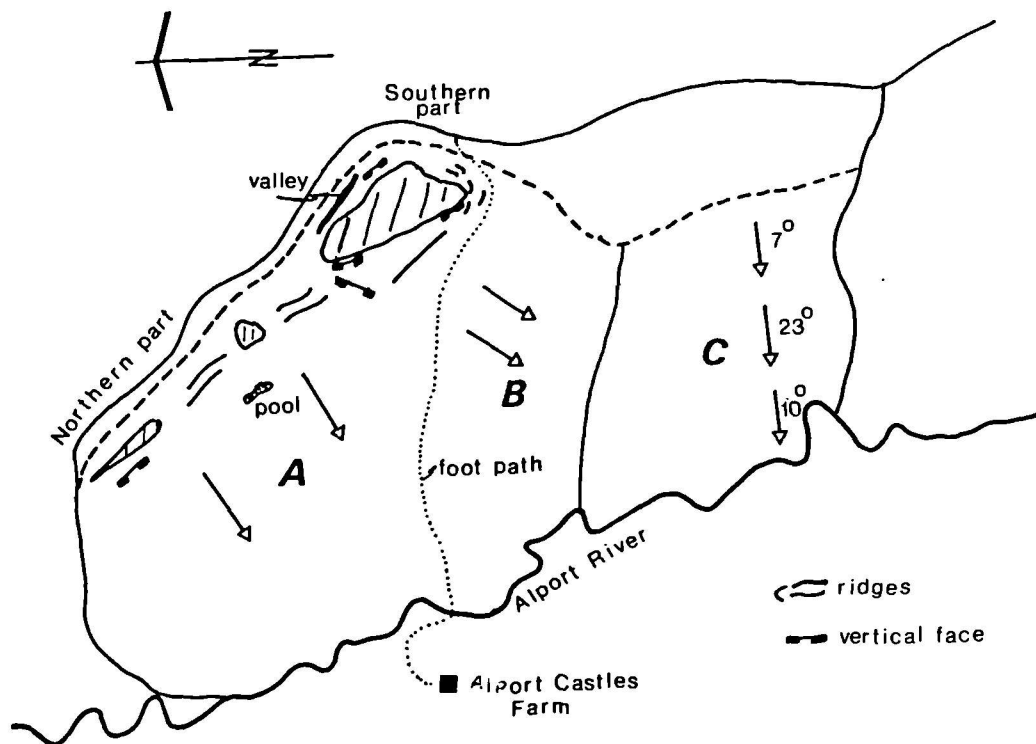


Fig. 7.12 A Sketch showing regional subdivisions of Alport Castles landslide to which reference is made in the text.

blocks lie to the north. The smaller block of sandstone is surrounded by a system of NW-SE minor ridges shown in Fig. 7.12. These ridges continue to the northern end of the landslide.

- ii. As shown in Plate 7.42 the main unit is characterized by a series of ridges running NW-SE. In the hollows at the base of the ridges see pages of water give rise to marshy areas and ponds.
- iii. Minor scarps in the main unit and foot occur as located in map Fig. 7.12.
- iv. The morphology of the ground between the large detached block and the main scarp in the southern part consist of NW-SE running ridges and hollows which include a vertical face of bedrock sandstone and deep valleys. In addition the ground is hummocky with small ridges and hollows running in a NE-SW direction. The toe of the landslide is characterized as shown in map Fig. 7.12 by a gently undulating area.
- v. The northern flank of the landslide is well defined as indicated by map Fig. 7.12.
- vi. The general trend of movement of part A of the landslide is towards a south westerly direction.

The morphology of area "B" is as follows:

As shown in map Fig. 7.12 and Plate 7.39 the area to the south of the foot path is an irregular slope with a hummocky ground surface. Since the predominant slope direction is towards the southwest, it would appear that this part of the landslide has been twisted during secondary movement. If this is so, then the near vertical NW-SE face of the block would be at the head of this part of the slope.

The morphology of area "C" is as follows:

- i. The main scarp forms a slope of 30° which is for the most part, vegetated.
- ii. The general trend of the movement is in a south westerly direction and unlike areas A and B, it would

appear that this took place in a single episode of instability.

- iii. The main unit and the toe consist of a sloping, undulating piece of ground which slopes at an average of 7°, 23° and 10° over the landslide area.
- iv. As shown in Plate 7.35, because of the effects of the neighbouring landslip at Rowlee Pasture the southern flank of the landslip is not well defined.

Present instability appears to be confined to minor falls along the river banks and rock falls from the main scarp. Plate 7.44 shows the result of one rock fall which occurred during the winter of 1982. No other evidence of activity is apparent and also the surface drainage system is well developed over the landslip area

7.9 Rowlee Pasture

The landslip at Rowlee Pasture is one of the largest landslip in North Derbyshire. The location of this landslip which is developed in Millstone Grit Series rocks is shown in map Fig. 2.1. According to Skempton and Hutchinson's (1969) classification, this landslip, which has a maximum length 600m and maximum width 3250m., is a rotational non-circular type. The main features of this landslip are illustrated by map Fig. 7.13 and Plate 7.45. Briefly, the crown consists of a flat plateau in some places while in others it slopes towards the back scarp. Most of this area is covered with vegetation. It is convenient to consider the morphology of this landslip in three parts as shown in Fig. 7.13 A.

Area A

- i. In some places, as shown in map Fig. 7.13, the main scarp forms a vertical face consisting of sandstone beds which are subjected to rock fall instability.
- ii. The main unit of this landslip is characterized by smooth changes in slope as shown in map Fig. 7.13.



Plate No. 7.44 Recent rockfall in the main scarp
at Alport Castles. August 1982
Scale 1cm. = 0.5m.

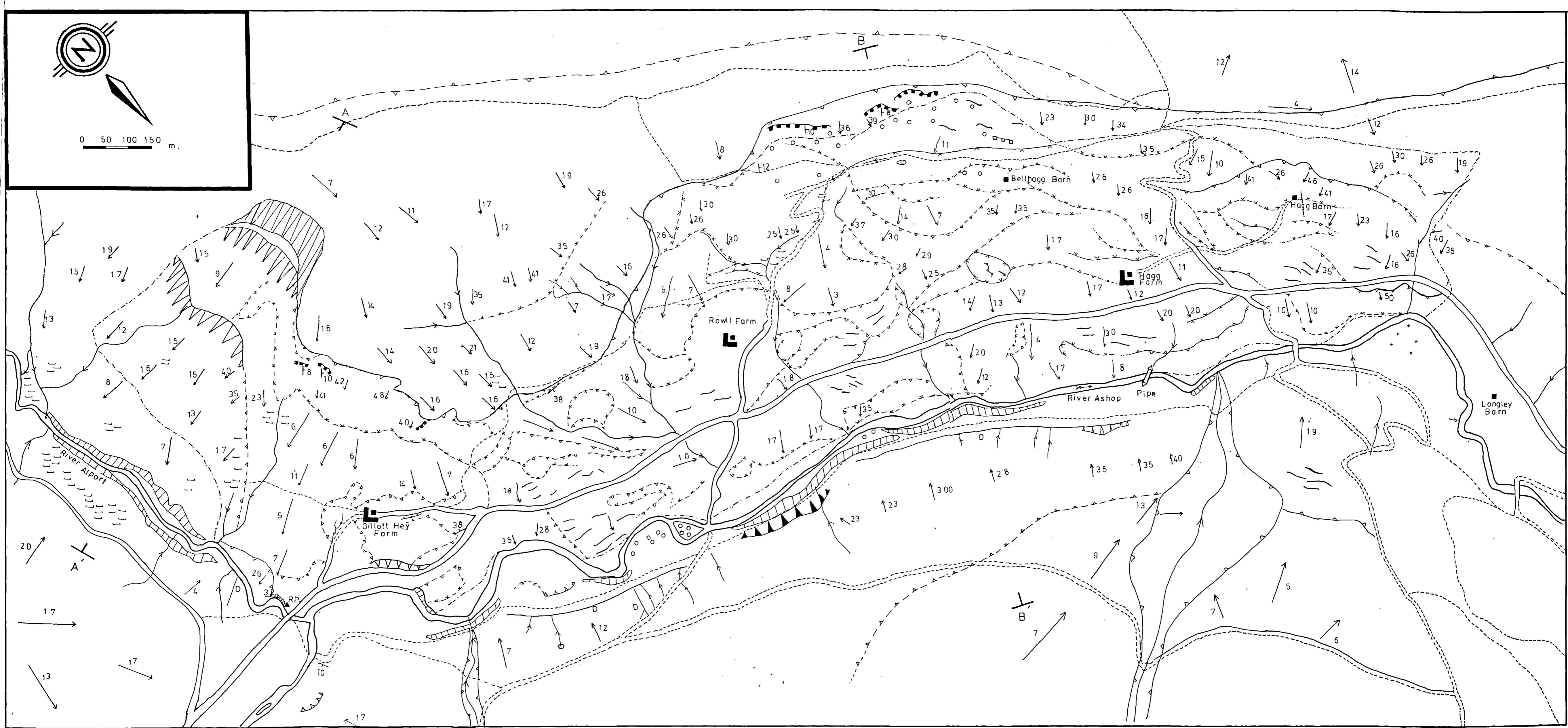


FIG. 7.13 GEOMORPHOLOGICAL MAP OF ROWLEE PASTURE LANDSLIP.

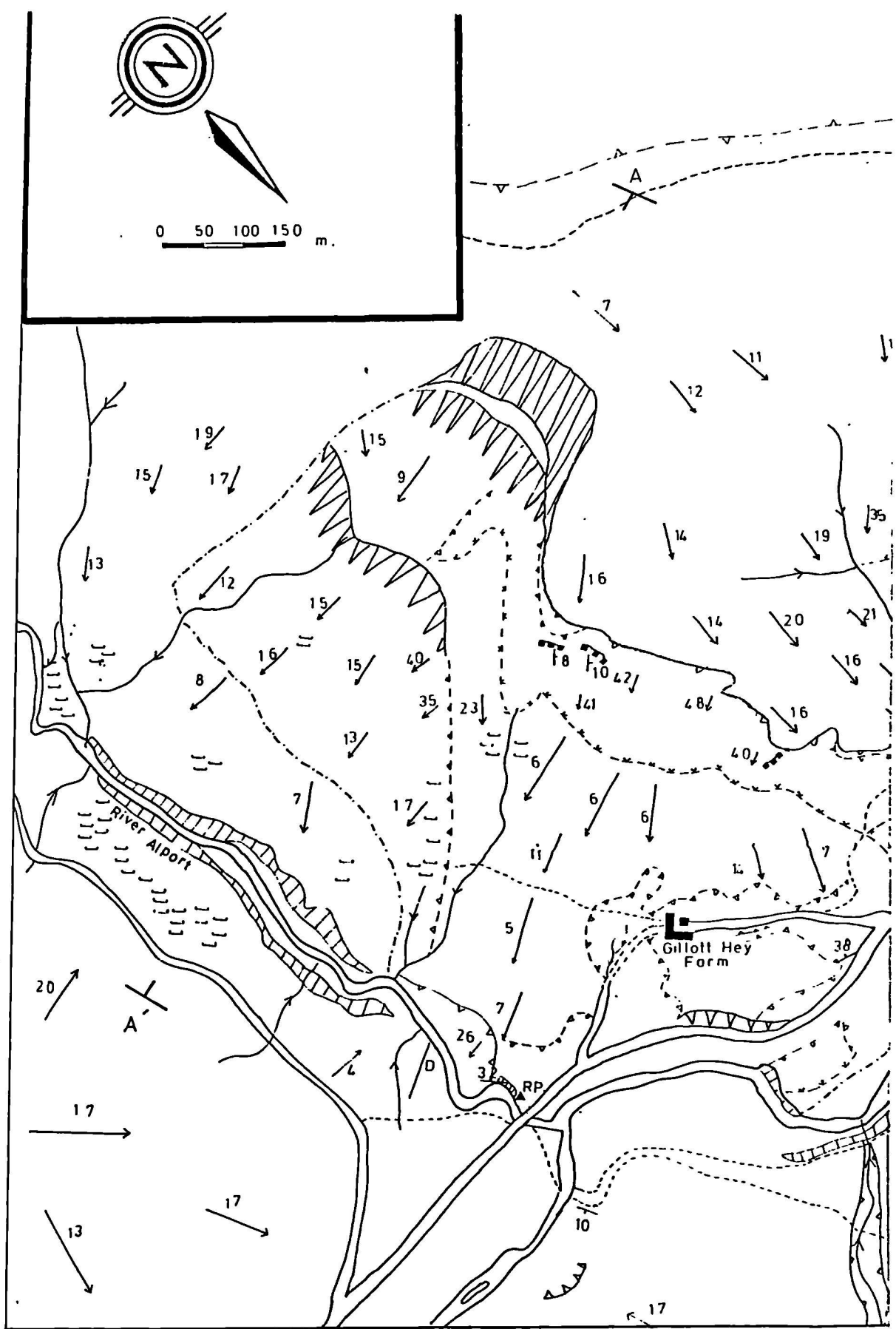
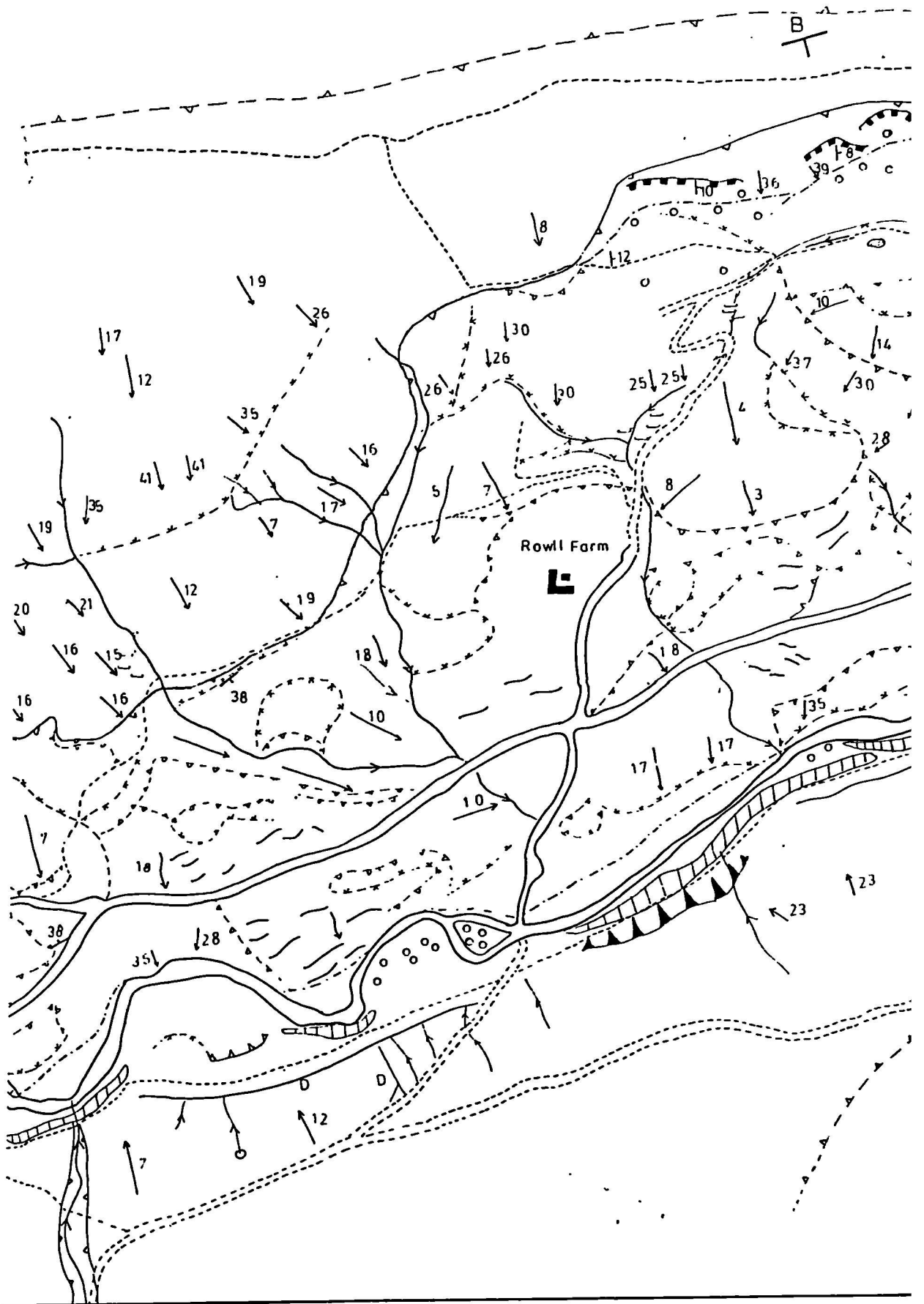


FIG. 7.13 GEOMORPHOLOGICAL M



ICAL MAP OF ROWLF PASTURE LANDSLIP.

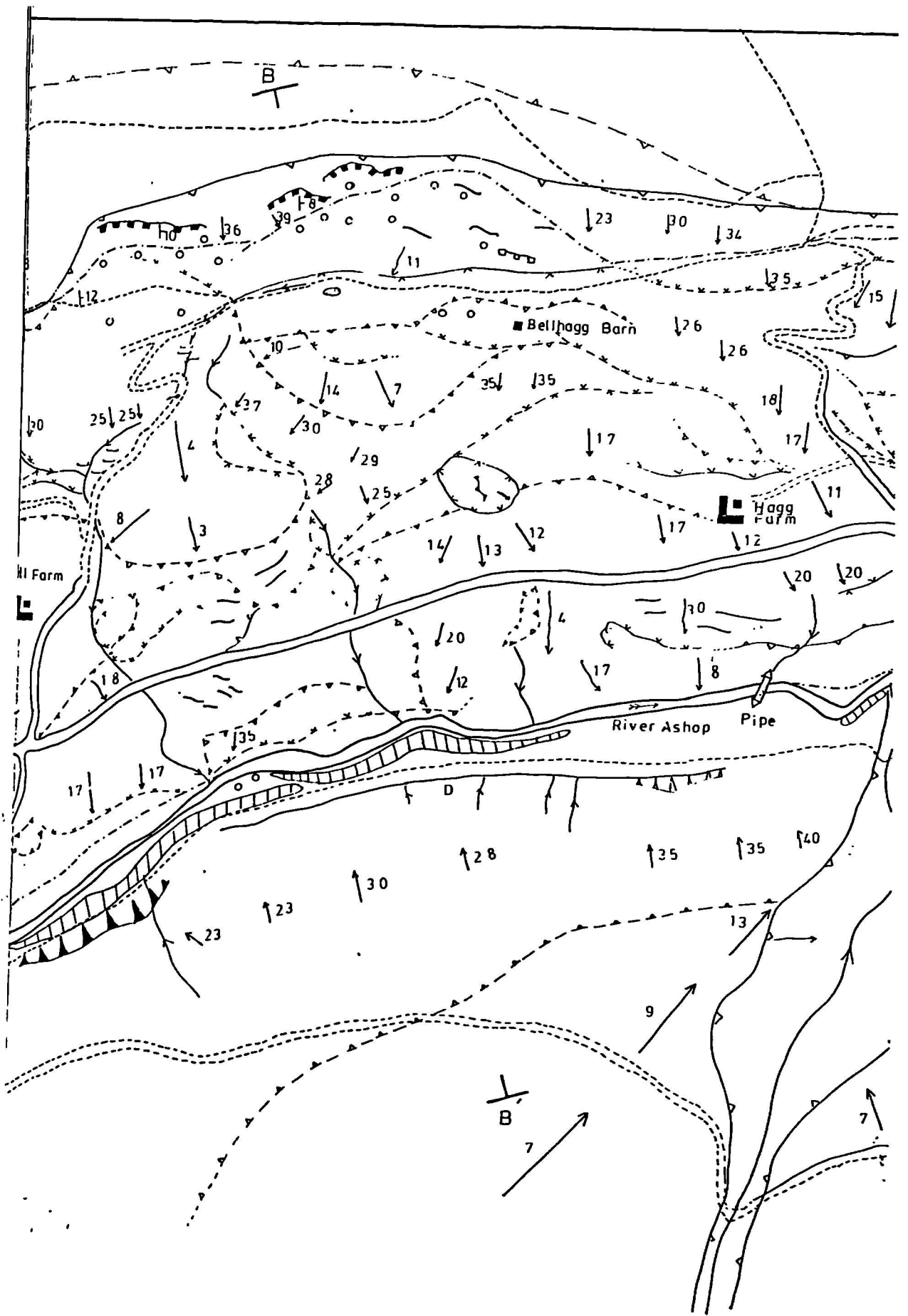
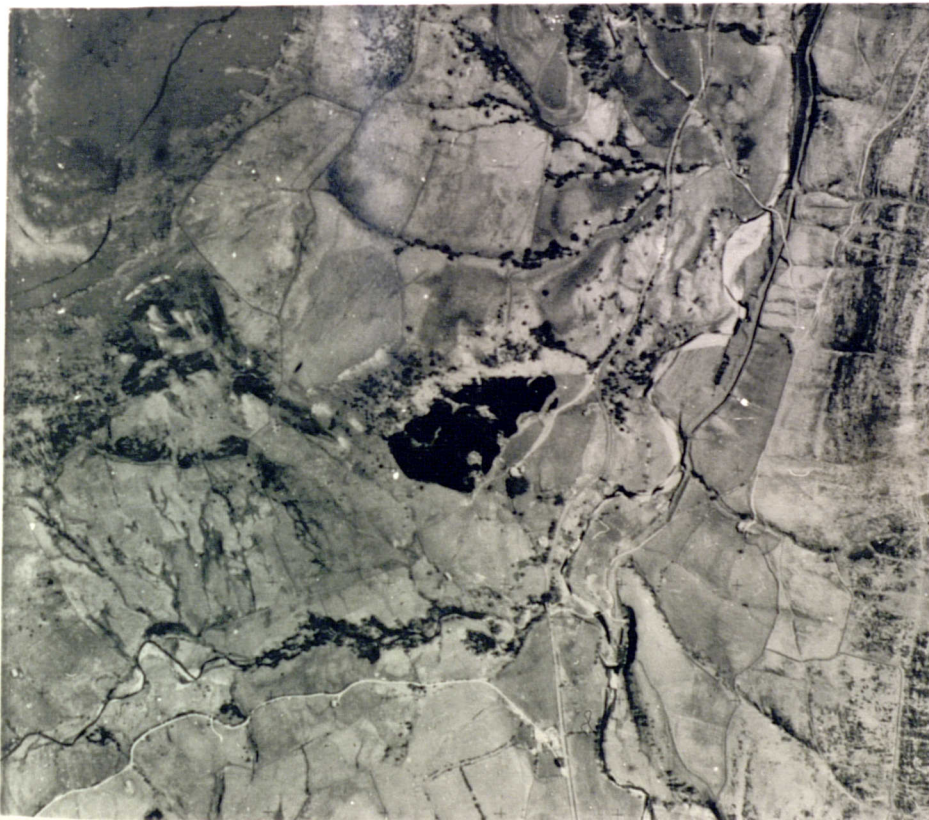
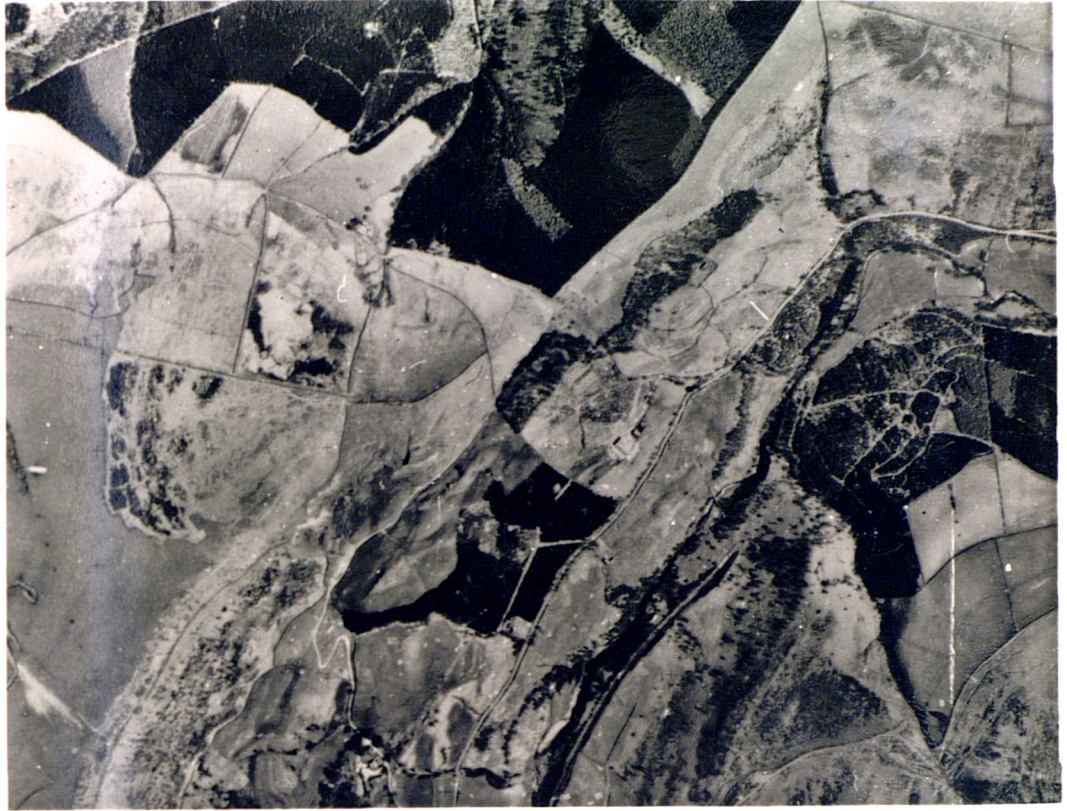


Plate No. 7.45 Aerial photograph of Rowlee Pasture
landslip.
Scale: 1:17300



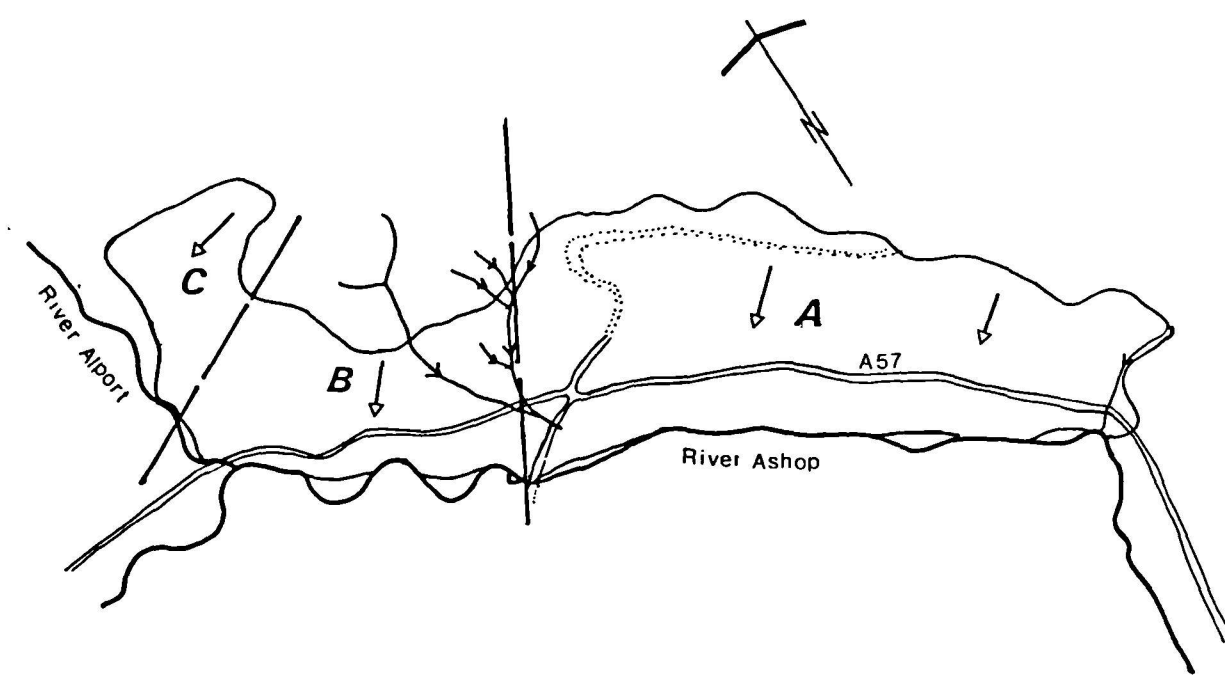


Fig. 7.13 A Sketch showing regional subdivisions of Rowlee Pasture landslip to which reference is made in the text.

The highly vegetated nature of both the main unit and the foot areas are illustrated in Plate 7.46.

- iii. Few outcrops of rock occur in the main unit, those at the head of the landslide have a dip of 12° SE. The dip of sandstone beds in the main scarp is 8° - 10° SE, thus implying an inward rotation of between 2° and 4° .
- iv. The general direction of movement is SW.
- v. Seasonal springs occur along the track which runs NE-SW.
- vi. The toe is an area of undulating slopes in some places where an Edale Shale exposure forms a minor scarp adjacent to the River Ashop.
- vii. The eastern flanks of the landslide are marked by a stream which flows south to join the River Ashop.

Area B.

- i. In main scarp this part of the landslide an exposure of sandstone dips 8° - 10° SE which compares with dips of 32° - 38° NE for the minor scarp in the river bank. An outward rotation, averaging 22° to 30° is implied by these values. The beds have suffered distortion due to movement.
- ii. The eastern side of this area is characterized by undulating ground in which a series of small E-W ridges occur in the foot area. The western side of the area forms a smooth 5° - 7° slope.
- iii. Shale outcrops in a minor scarp in the western part of the toe.
- iv. No marshes or other forms of surface drainage occur in this part of the landslide.
- v. The general direction of movement is southwesterly.

Area C.

- i. The main scarp forms a very steep or nearly vertical slope where sandstone beds of the Shale Grit formation are well exposed.
- ii. Two highly vegetated minor scarps give slopes of up to 35° .

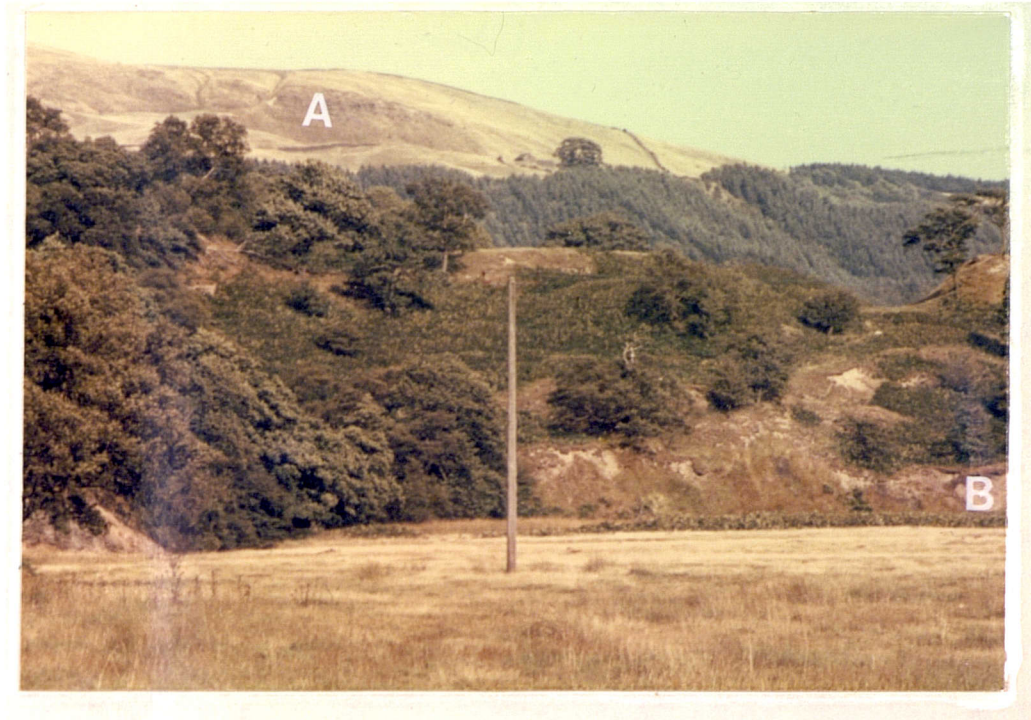


Plate No. 7.46 Part of the main scarp (A) of landslide at Rowlee Pasture. Main unit and foot are highly vegetated. Note part of the toe forming minor scarp (B).



Plate No. 7.47 Repairs to the A57 road due to movements of the landslide at Rowlee Pasture.

- iii. As shown in map Fig. 7.13 the foot and the toe produce a smooth slope. The toe is not well developed, it forms a smooth slope of 13° - 16° .
- iv. A number of marshy area occur around the River Ashop.
- v. The western flank is well defined as shown in Plate 7.13.

According to the field observation and geological map, Fig. 2.2, the main unit and foot are situated in a sandstone unit of the Shale Grit and Mam Tor Sandstone formation, while the toe is in Edale Shale.

Recent activity of this landslip is indicated along the A57 road and particularly in the area of the toe where fences and traffic signs have been displaced. The edge of the road shown in Plate 7.47 and 7.48 is subjected to fracturing and measures to prevent erosion of the toe of the landslip by the River Ashop include the construction of gabions and concrete walls, shown respectively in Plates 7.48 and 7.49. However, as indicated in Plate 7.50, these defences have not entirely prevented movement. No landslide activity was noticed in the remainder of area C.

7.10 Cowms Moor

The landslip at Cowms Moor is developed in Millstone Grit Series rocks at a location shown in Fig. 2.1. A false impression of the landsliding activity is liable to be gained from a cursory examination since as shown in map Fig. 7.14 and Plate 7.51 it appears that there is a stable area in the centre of the landslip. An alternative explanation derived by intensive field observation, aerial photography and topographical maps is that this area has been affected by two separate movements along different slip surfaces.

The main features of the landslip area are as follows:

- i. The crown of the upper slip forms a gently sloping portion of mostly wet, vegetated ground. A series



Plate No. 7.48 Gabbion wall to protect the toe of the landslip at Rowlee Pasture.



Plate No. 7.49 Concrete wall to protect the toe of the landslip at Rowlee Pasture.

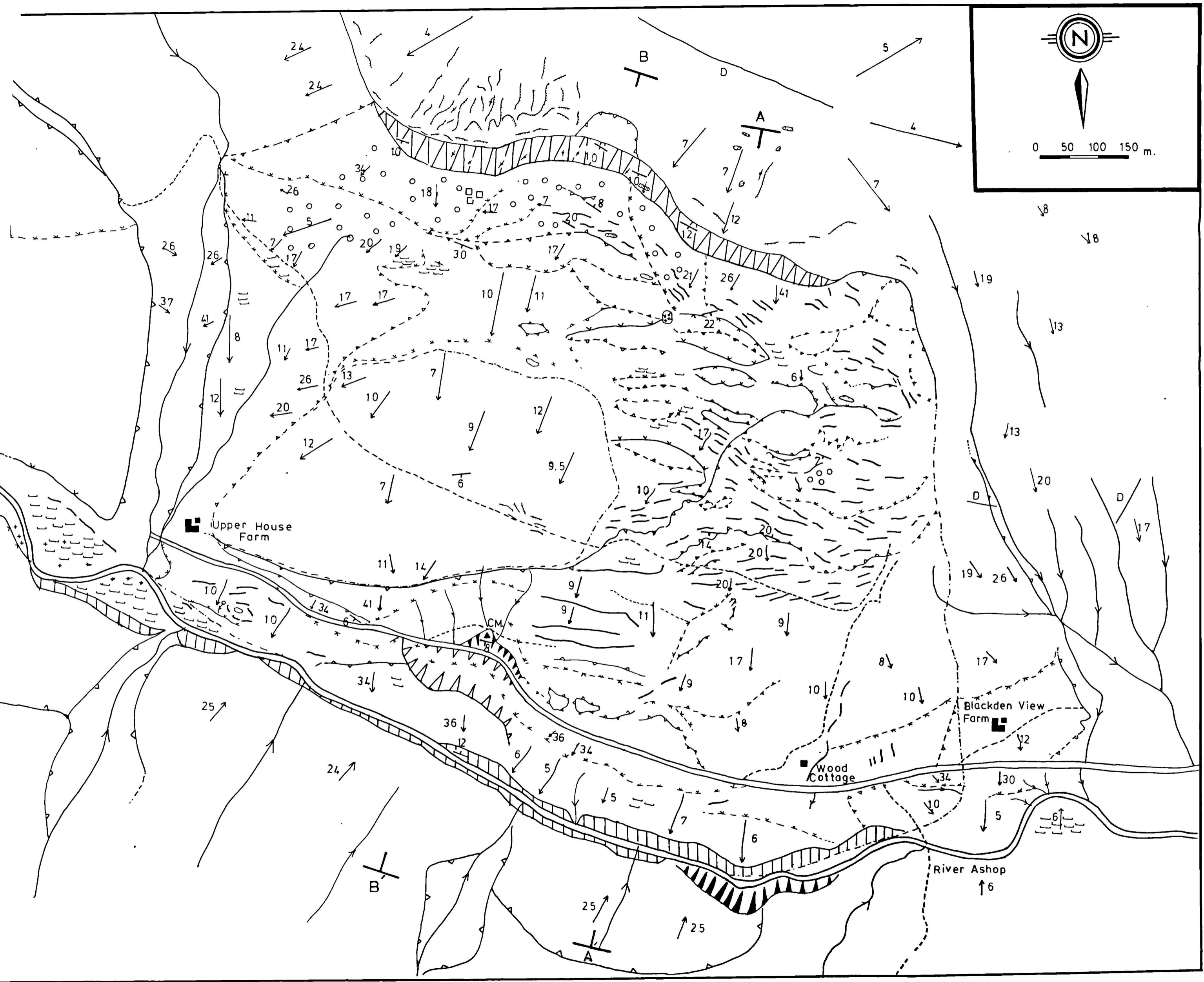


FIG. 7.14 GEOMORPHOLOGICAL MAP OF COWMS MOOR LANDSLIP.



Plate No. 7.50 The gabbion protection has not entirely prevented movement of toe of the Rowlee Pasture landslide.

Plate No. 7.51 Aerial photograph of Cowms Moor landslips.
Scale: 1:13000



of channels containing peat deposits have been eroded. The surface drainage includes ponds and several streams, which decrease in number towards the east and there are also a number of small hollows or sheep scars along the edge of the crown at the western limit of the landslide area.

- ii. A well developed main scarp that attains a maximum height of 39 m. and which decreases in steepness in a westerly direction as illustrated in Plate 7.52, consists of sandstone beds. Water seepages from joints in this area supply the streams flowing across the main unit.
- iii. A slikensided sandstone surface occurs in the main scarp.
- iv. Since the dip of the beds in the main unit of the landslide varies in both magnitude and direction, it is concluded that it has suffered distortion during movement. The sandstone beds in the main scarp dip 10° SW, while the maximum dip of the sandstone bed within the main unit is up to 20° NE, thus implying an outward rotation of 30° .
- v. A number of fallen sandstone blocks are distributed over the main unit (See Plate 7.52).
- vi. Minor scarps clearly mark the eastern flank of the landslide as in map Fig. 7.14 but the western flank is less prominent. Plate 7.53 is a typical view of the hummocky ground of the main unit.
- vii. A number of marshes occur within the landslide area, particularly in the hollow between ridges, and a spring occurs in the western part of the area as indicated in map Fig. 7.14.
- viii. A sudden change in slope takes place along a NE-SW line which turns to an S-W direction in the western part. It is believed that this represents the scarp of the lower slip surface. The hummocky ground is cut by this lower movement, but it does not form a well developed scarp especially in the east where it becomes obscured by landslide debris from the upper movement.



Plate No. 7.52 Main scarp and main unit of landslip at Cowms Moor. Note the exposure of sandstone of Shale Grit formation in the main scarp at 'A' and the fallen sandstone block in the main unit at 'B'.



Plate No. 7.53 Hummocky ground in the main unit of landslide at Cowms Moor.



Plate No. 54 The main unit of the lower slip at Cowms Moor. Note the NW-SE ridges and hollows.

- ix. The eastern side of the main unit of the lower movement is characterized by differentiated NW-SE ridges and hollows as shown in Plate 5.54. Towards the west, and also in the middle part of the main unit, the ridges become less intensive.
- x. A minor scarp near an exposure of Mam Tor sandstone in a road cutting is developed in the middle part of the landslip between the River Ashop and the A57 road.
- xi. The geological map Fig. 2.2 and field observations indicate that the landslip occurs in sandstone and very thin shale beds belonging to the Shale Grit and Mam Tor Sandstone formations.
- xii. The surface drainage is well distributed over the whole area with some marshes concentrated in the western toe of the landslip.
- xiii. Hollows and sheep scars occur along the eastern flank of the landslip, while in the west a more or less smooth slope merges into the valley side. The general trend of movement of both the upper and lower landslips is towards the south.
- xiv. Recent instability appears to be confined to rock falls from the upper main scarp and river bank erosion. The buildings of Wood Cottage, Upper House Farm and Blackden View Farm, show no evidence of any movement.
- xv. According to Skempton and Hutchinson's (1969) classification the landslips at Cowms Moor are rotational non-circular types.

7.11 Kinder Scout

The landslips at Kinder Scout are located on map Fig. 2.1 and shown in Fig. 7.15 and Plate 7.55. There are in fact nine individual areas of instability indicated in Fig. 7.16 which together effect an area of about two square kilometres. These landslips occur in Millstone Grit Series rocks as shown in geological map Fig. 2.2. The main feature of these slips are indicated in Fig. 7.15 and may be listed as follows:

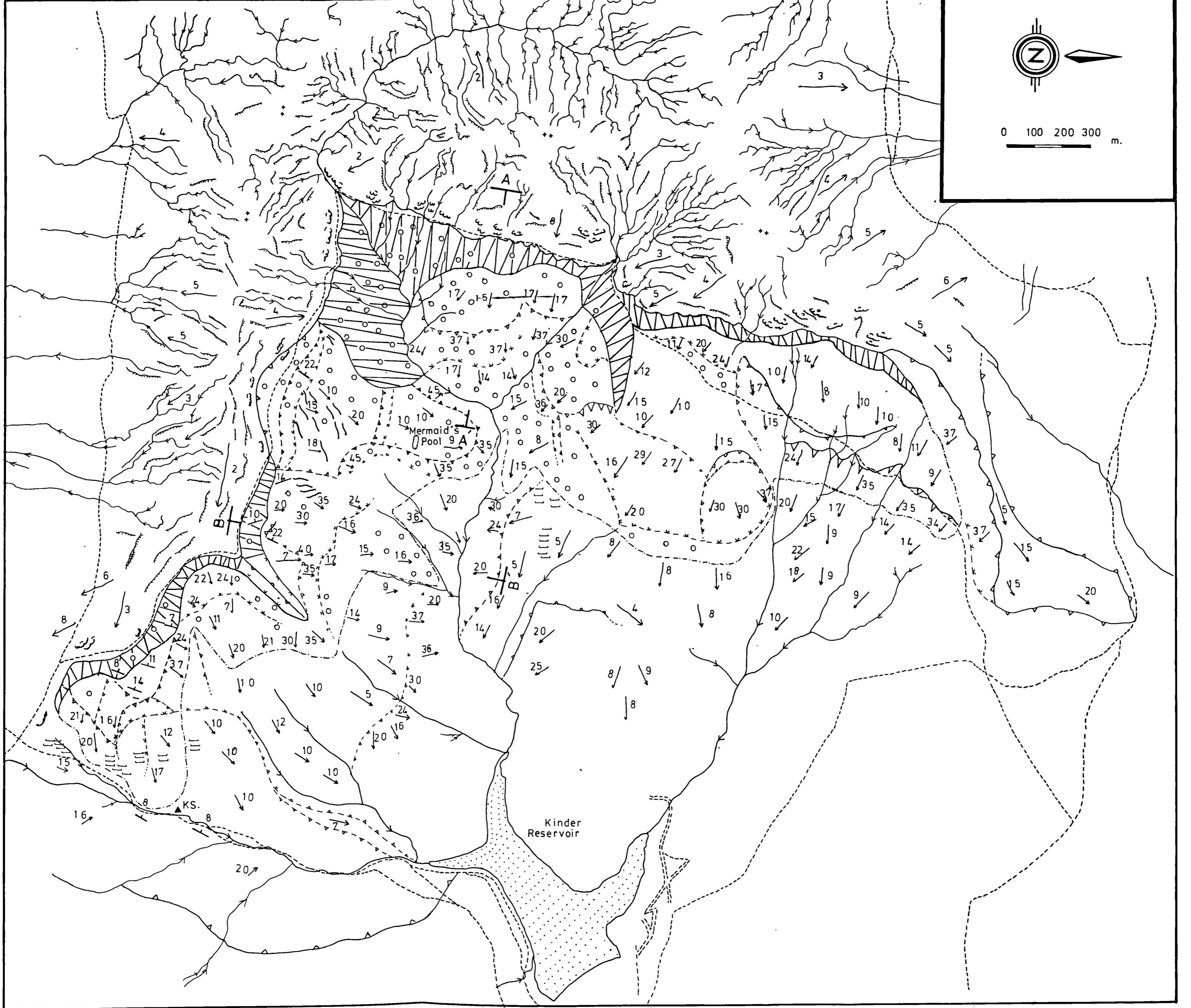


FIG. 7.15 GEOMORPHOLOGICAL MAP OF KINDER SCOUT LANDSLIPS.

Plate No. 7.55 Aerial photograph of Kinder Scout landslips.
Scale: 1:26000



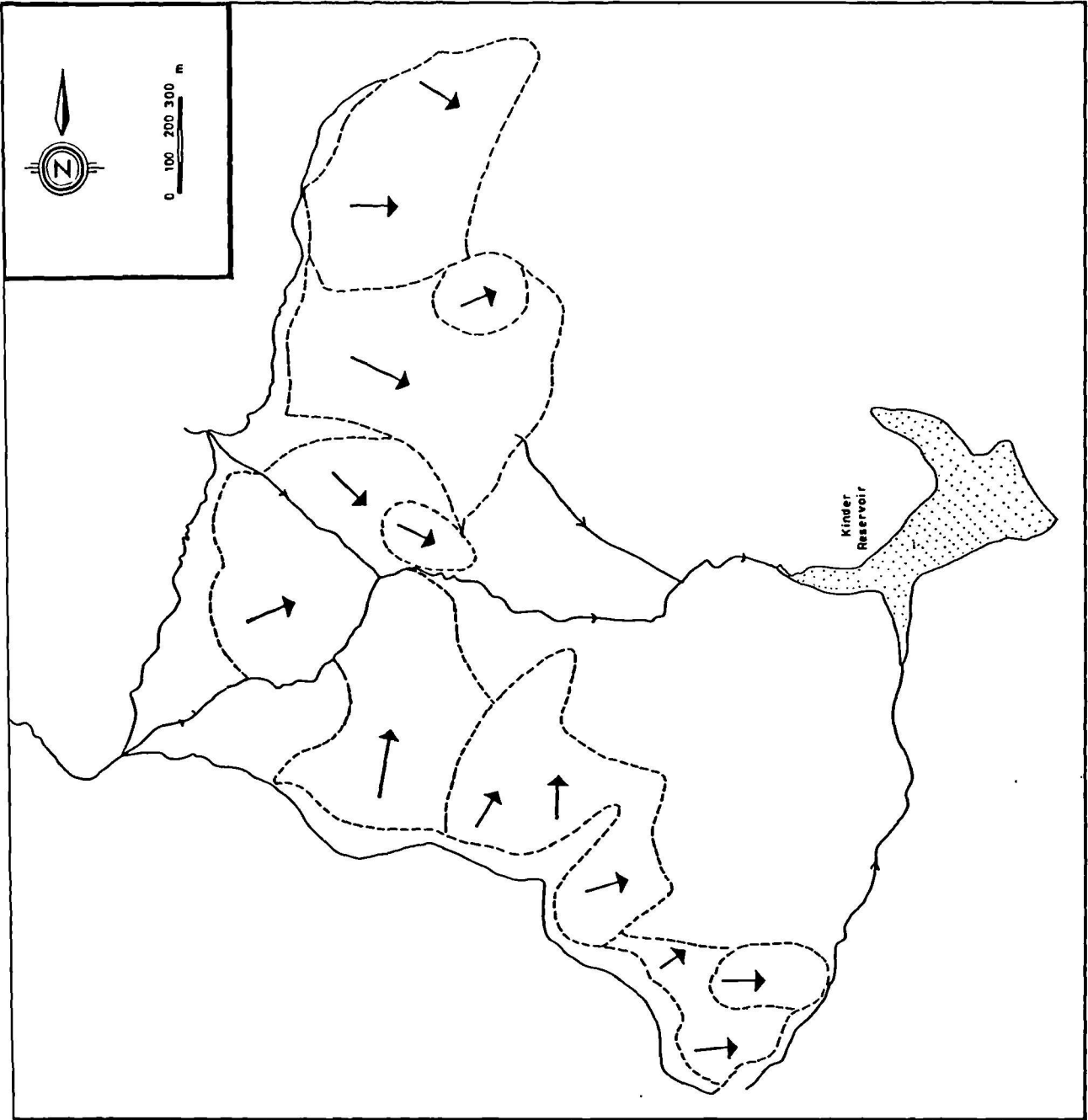


FIG. 7.16 AREAS OF INSTABILITY AND THE POSSIBLE DIRECTION OF MOVEMENT AT KINDER SCOUT.

- i. The crowns of the landslips are very nearly flat with some exposures of coarse feldspathic sandstone in thick exfoliating beds which are illustrated in Plate 7.56. Although the surface water drainage system shown in map Fig. 7.15 and Plate 7.57 is well developed over the whole of the crown with streams and ditches, the area is very wet with marshes in some places.

The landslide area can be divided into two main parts in which NW part is separated from the SW one by Kinder Downfall, a deep stream valley and water fall which runs in a south westerly direction.

- ii. The main scarp of the landslide consists of two faces at right angles to each other with Kinder Downfall stream at the intersection. Plate 7.56 show NW area and the SW part is shown in Plate 7.58. The vertical back scar face occurs in Kinderscout Grit Sandstone and is shown in Plate 7.59.
- iii. The main units of the landslide exhibit different slopes as indicated in map Fig. 7.15. Plates 7.56 and 7.58. A number of fallen blocks of sandstone are distributed over the main unit which is mostly vegetated except for certain areas represented on map Fig. 7.15 by dip and strike readings.
- iv. The surface drainage system is well developed along the whole area, and conveys water to Kinder Scout Reservoir.
- v. Field observations and geological map, Fig. 2.2 indicate that the main unit and toe are situated on shale beds belonging to the Grindslow Shales formations.
- vi. Beds of sandstone in the main scarp dip ESE at 8°-10° while the dip of the sandstone beds in the main unit ranges between 14° and 22°. Hence an outward rotation of 6° - 12° has taken place.
- vii. The toe forms a smooth slope over the stable ground.
- viii. The actual direction of movement of individual landslips is indicated in Fig. 7.16. These direction

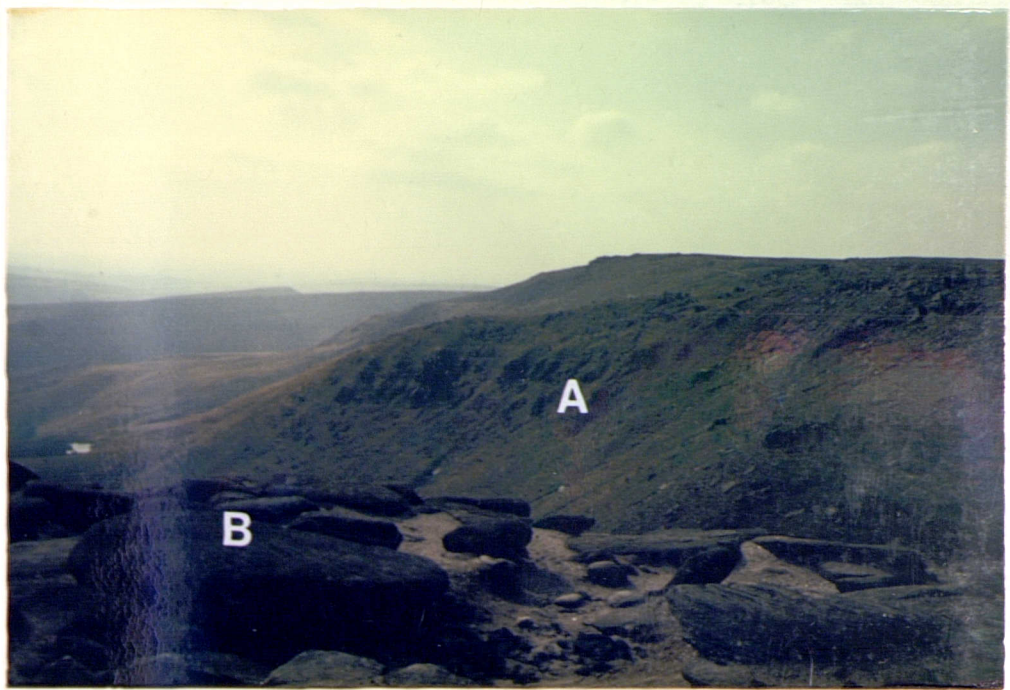


Plate No. 7.56 Main scarps in the NW part of landslip at Kinder Scout ('A') and exposure of coarse feldspathic sandstone at the crown ('B').



Plate No. 7.57 Crown of landslips at Kinder Scout showing the surface drainage.



Plate No. 7.58 The landslide in the SW part of Kinder Scout. Note. Exposure of sandstone at the crown and the ponding water.



Plate No. 7.59 Kinder Scout sandstone cliff forming part of NW Main scarp.

vary between SW in the NW part and WNW along the SW part of the landslip area.

- ix. No sign of recent activity was noticed in footpaths, walls and streams.
- x. According to Skempton and Hutchinson's (1969) classification, these landslips are of rotation non-circular type.

7.12 Conclusion

The North Derbyshire landslips generally involve the slipping of thick and competent sandstone beds overlying weaker shale. This may well be due to the withdrawal of ice support from slopes over-steep end by glaciation (See Higginbotton and Fookes, 1971).

Thick beds of jointed sandstones of the Mam Tor Sandstone and also the Shale Grit Formation overlying relatively weak beds of shale. High load causes cambering of the sandstone beds over the shale which results in opening of joints as shown in fig. 7.17 A and B. The shale beneath the sandstone beds becomes deformed as shown in Fig. 7.17 C.

The thawing of ice inclusions will cause a sudden rise in the moisture content which may induce excess hydrostatic pressures leading to instability along the bedding planes and joints. Under these conditions Shale undergoes softening and the consequent reduction in shear strength could cause failure to occur.

The main units are rotational and generally non-circular as might be expected with nonhomogeneous bedrocks. Also, the shale is an isotropic with beds of sandstone or ironstone and the bedding planes, which control the behaviour as shown in Fig. 7.17 C.

The rotation in some cases inwards while elsewhere it is outwards. This feature depends on the attitude of the beds before failure.

The toe of the landslips tend to be translational slides due to the movement of colluvium over the original ground surface.

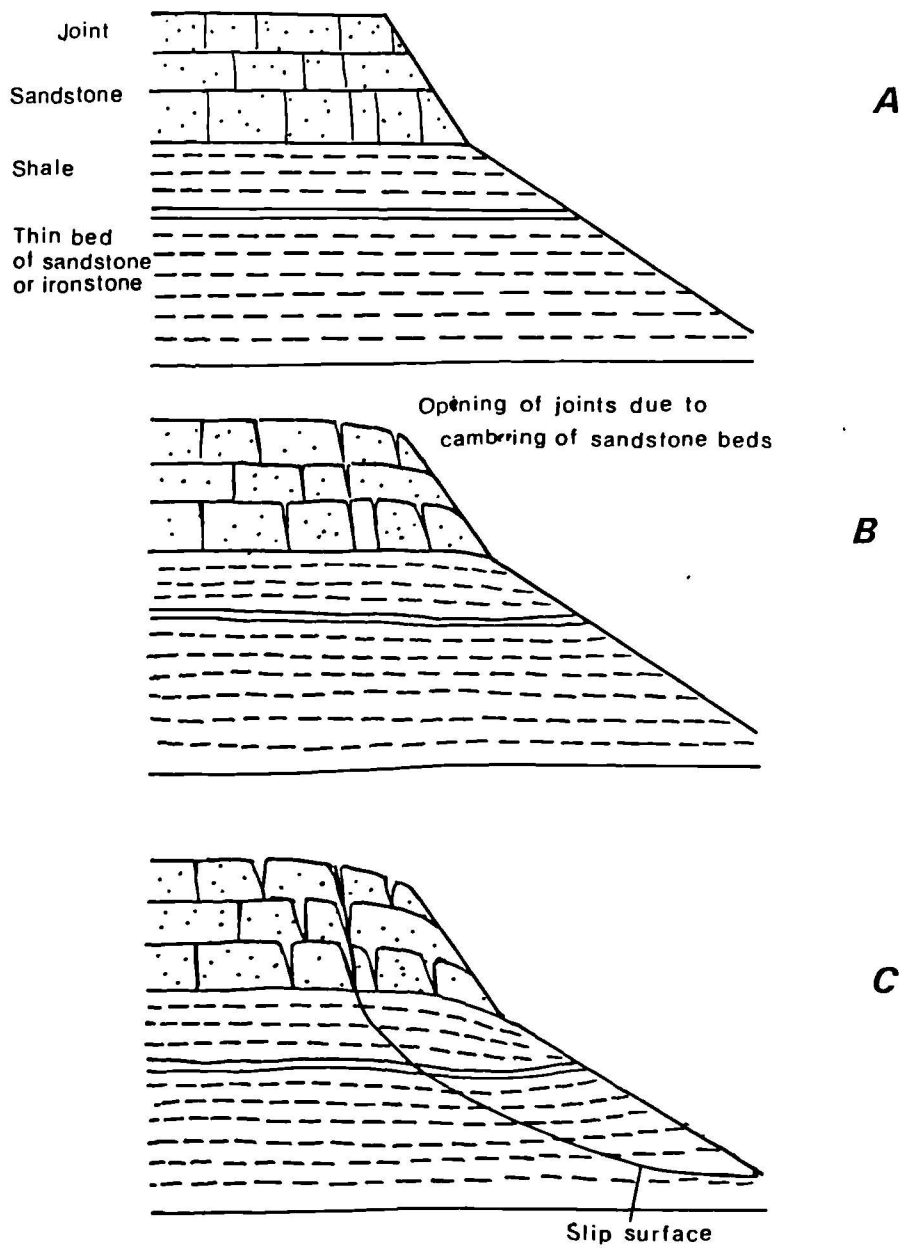


Fig. 7.17 Possible evolution of landslips.

The morphological technique used in establishing the dimensions of the landslips and their modes of movements are very important. Changes in the geometry of the ground surface after failure provides evidence for post landslip activity and thus the instability can be identified. In addition to defining the geometry of the slips studied, it has also been possible to draw conclusions regarding their present stability condition and the likely groundwater conditions. Further details are included in Chapter 8.

CHAPTER 8

STABILITY ANALYSIS FOR LANDSLIPS STUDIED

8.1 Introduction

The objective of this chapter is to examine the causes and conditions of instability of landslips in North Derbyshire. The general characteristics of the landslips are given in Table 8.1, and each of these areas of instability is located on map 2.1. Morphological observations are described in Chapter 7 are discussed in this Chapter with regard to features affecting the analysis of stability. Of particular importance to these analyses are the positions of the slip surfaces, the groundwater table and both the pre-slip and the post-slip topography. The analysis of each landslide is carried out in terms of its stability against both first time sliding and also post-failure movements.

8.2 Information Required for the Analysis of Stability

A knowledge of the position of the slip surface forms an essential part of analysis for both first-time and subsequent-instability. In practice, the most likely position was deemed to be the one which minimized the factor of safety for the worst probable groundwater conditions. This was found by trial and error from an initial position chosen on the basis of the various factors listed below and considered in detail in the subsequent text.

- i. Present geometry of slope
- ii. Geological cross section
- iii. Original geometry of slope
- iv. Position of the water table
- v. Shear strength parameters.

- i. Present geometry of slope

A topographic section of each landslide was drawn from the relevant Ordnance Survey 1:10000 scale

Table 8.1 Summary of Instability in North Derbyshire.

Landslip	Location (GR of Centre)	Type of instability
Mam Tor	xy 135837	<p>Main unit: Non-circular rotational slide cutting through Mam Tor sandstone and underlying Edale Shale.</p> <p>Toe: Translational slide of colluvium lying on Edale Shale and valley floor deposits.</p>
Rushup Edge	xy 122841	<p>Main unit: Non-circular rotational slide cutting through Mam Tor sandstone and underlying Edale Shale.</p> <p>Toe: Translational slide of colluvium lying on Edale Shale and valley floor deposits.</p>
Cold Side	xy 128845	<p>Main unit: Non-circular rotational slide cutting through Mam Tor sandstone and underlying Edale Shale.</p> <p>Toe: Convex to the original slope form, part of main unit movement.</p>
Back Tor	xy 143853	<p>Main unit: Non-circular rotational slide cutting through Mam Tor sandstone and underlying Edale Shale.</p> <p>Toe: Translational slide of colluvium lying on Edale Shale and valley floor deposits.</p>
Burr Tor	xy 178785	<p>Main unit: Non-circular rotational slide cutting through Shale Grit Sandstone and underlying shale.</p> <p>Toe: Convex to the original slope form, part of main unit movement.</p>

Table 8.1 cont'd.

Bretton Clough	xy 199788	<p>Main unit: Non-circular rotational slide cutting through Shale Grit sandstone and underlying shale .</p> <p>Toe: An accumulation of landslide debris raising valley floor, eroded by river.</p>
Alport Castles	xy 141912	<p>Main unit: Non-circular rotational slide cutting through Shale Grit sandstone, Mam Tor sandstone and underlying shale.</p> <p>Toe: Translational slide of colluvium lying on shale and valley floor deposits.</p>
Rowlee Pasture	xy 155893	<p>Main unit: Non-circular rotational slide cutting through Shale Grit sandstone, Mam Tor sandstone and underlying shale.</p> <p>Toe: Flow slide of landslide debris, part of the main unit. Convex to the original ground slope.</p>
Cowms Moor	xy 155893	<p>Upper part</p> <p>Main unit: Non-circular rotational slide cutting through Shale Grit sandstone, Mam Tor sandstone and underlying shale.</p> <p>Toe: Debris slide of landslide debris of the main unit.</p> <p>Lower part</p> <p>Main unit: Non-circular rotational slide cutting through Mam Tor sandstone and underlying shale.</p>

Table 8.1 cont'd.

		Toe:	Debris slide of landslide debris, of the main unit raising the valley floor, eroded by river.
Kinder Scout	xy 078886	Main unit:	Non-circular rotation in cutting through Grindslow shale.
		Toe:	Debris slide of landslide debris from the main unit. Convex to original slope of ground surface.

contoured maps. These maps were found to be very suitable for this purpose since they have a 5m. or 10m. contour interval. The maps were enlarged photographically to a scale of 1:5000 in order to simplify the task of section drawing and the sections themselves were similarly enlarged to a scale of 1:2500 for the purpose of analysis.

ii. Geological cross section

The geological cross section was prepared from geological maps published by the Institute of Geological Sciences (British Geological Survey) which were enlarged in the same way as the topographic maps. Where it was difficult to measure the dip and strike of the beds in the field the attitude of beds was deduced from geological maps. In a few cases due to the lack of suitable exposures or suitable bedding plane contour intersections, a suitable structure was assumed to be similar to that of the nearby scarp sandstone.

iii. Original geometry of slope

The stability conditions for the initial failure were analysed according to the pre-failure slope profile which was derived by extrapolation across the landslip of contour lines from either side of the unstable area. Analysis of post-initial failure was carried out using the present day topography.

iv. Position of the water table

The position of the water table is one of the main potential errors in calculating the factor of safety. Since for first-time sliding the slope geometry has been estimated before slippage, the location of the water table at the time of failure is not known. In order to carry out the stability analysis this position has been estimated. Due to the prevailing climatic conditions (See Section 7.12), it may be assumed that it would be relatively high. In the lower, and more gentle parts of the slopes, that is near the toes, it seems reasonable to assume that the water table was at or very near to the

ground surface. At the top of the slopes it has been assumed that the ground water table lies a small distance below the ground surface. Then the analysis was performed for a number of water table positions. Initially a water table which rises on a gentle curve which slopes a few degrees less than the original ground surface has been adopted. This follows the shape of the ground surface in a subdued manner. The general slope of the water table has then been changed in order to find by trial and error a position which gives a reasonable factor of safety.

Finding a suitable position for the water table in the case of the post-failure analyses is much easier than for first-time sliding. At Mam Tor, the piezometers readings are available (See Fig. 8.4). However, since the cross section chosen for determination the stability of Mam Tor landslip does not pass through the measuring positions, the water table was extrapolated on a tranverse sections (See Map Fig. 7.3), again using a shape which reflects in a subdued manner the ground surface. For the other landslips for which no measurements of the elevation of water table are available, the elevation of water table has been estimated after considering the location of marshes and seepages. These were observed during geomorphological maps work. Again different heights of water table were tested by trial and error analyses, and the most satisfactory one was adopted.

v. Shear strength parameters

Most analyses required a knowledge of the strength of both shale and sandstone.

a. Shear strength of shale.

The shear strength parameters for samples of shale were determined using the ring shear method as described in Chapter 5.

The shear strength may be expressed in terms of a peak (c_p' , ϕ_p'), fully softened or remoulded. (c_s' , ϕ_s') or residual values (c_r' , ϕ_r') for existing shear surfaces. The first time failures were analysed on the basis of the remoulded peak values while the remoulded residual parameters were used for the post initial calculations.

According to Skempton (1970) the stability of first-time slides in over-consolidated clay is controlled by the fully softened or remoulded strength and residual is appropriate to the analysis of over-consolidated clay with pre-existing failure planes. It is argued with reference to Fig. 8.1 that whatever the original condition of a clay, drained shear is accompanied by dilation in the case of over-consolidated clays and contraction in under-consolidated clays so that ultimately a condition of normal consolidation is attained during shearing. Roscoe et al (1958) define a critical condition after which further increments of shear distortion cause no change in water content, this is an equivalent condition to normal consolidation. Although Schofield and Wroth (1968) concluded that the peak strength of a normally-consolidated remoulded clay occurs just before the critical state is reached and he suggest a value of $\phi_c' = 22.5^\circ$ for London Clay compared with the remoulded peak strength of 20° found by Skempton (1970) for practical purpose, the critical condition strength is taken as being equal to the fully softened strength of an over-consolidated clay or the peak strength of remoulded normal consolidated sample.

b. Shear strength of sandstone.

Attempts were made to determine the shear strength parameters for sandstone using the 60mm square shear box.

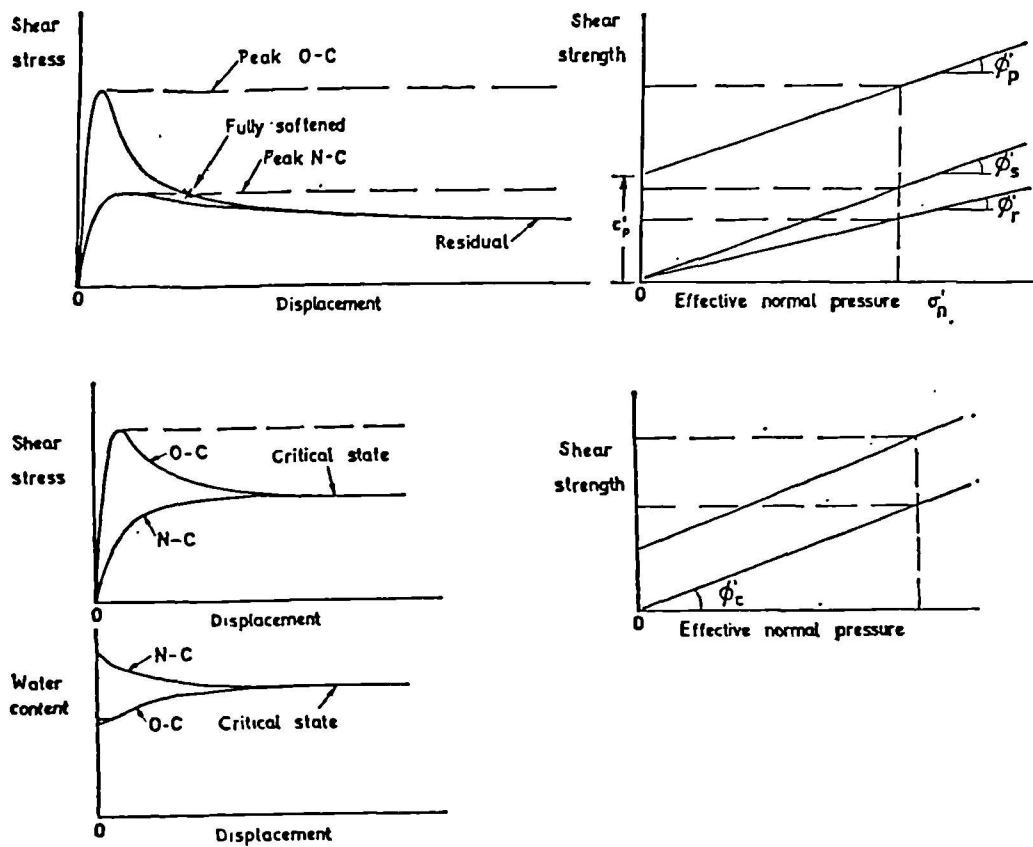


Fig. 8.1 Critical state for drained shear tests on ideal clay (After Skempton, 1970).

Samples for this determination was chosen from the Mam Tor Beds. They were a grey fine to medium grained laminated sandstone which consists of moderately to well-sorted quartz with a little feldspar (See also Allen, 1960). In order to measure the approximate strength mobilized along joint surfaces in this material an artificial discontinuity was formed in the sample by cutting rectangular block and breaking it with a wedge sample splitter. The two halves of the sample were then trimmed to fit in the shear box so that the induced discontinuity surface coincided with the joint between the two halves. Any spaces between the sample and the edges of the box were filled with plaster of Paris to ensure that the sample was held firmly in place. Unfortunately, probably due to the irregularity of the surfaces, during shearing, the joint between the two halves of the shear box opened and anomalously high values of shear resistance were obtained. The gap increased with continuous shearing and three attempts to overcome this problem were unsuccessful.

According to Bell (1981) the angle of friction (ϕ) of sandstones is generally between 32° and 42° depending on the type of rock. Data published by Wilum and Starzewski (1975) in Table 8.2 indicate that a ϕ'_p value of 35° to 37° would be appropriate. With respect to residual properties, Table 8.3 present Barton's (1973) compilation from a number of sources. Hence a ϕ'_r value between 30 and 32° was used in the analysis of post-initial failure.

8.3 Stability Analysis for Rotational Movement

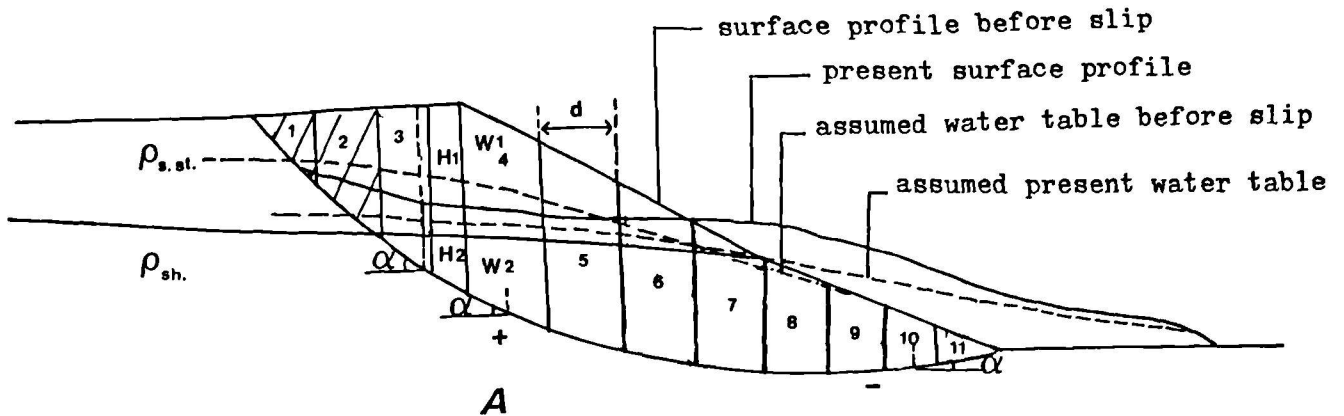
The stability was considered in terms of a typical vertical cross section drawn for the length of the landslide, generally along the centre line. As is normal practice, the potentially unstable area was divided up into a series of strips as indicated in Fig. 8.2. Jumikis (1965) recommends using a strip width of 10% of the radius of slip surface.

Table 8.2 Typical value of strength parameter ϕ' (after Polish code PN-591B-03026, 1959).

Type of soil	Density			
		Dense	Medium	Loose
sands coarse - medium	ϕ'	40 - 38°	38 - 35°	35 - 32°
sands fine & silty	ϕ'	37 - 35°	35 - 32°	32 - 28°
sands & organic	ϕ'	30 - 25°	25 - 22°	22 - 18°

Table 8.3 Residual friction angle of sandstone (after Barton, 1973)

Moisture	σ_n' KN/m ²	ϕ_r'	Reference
dry	0 - 490	26 - 35°	Patton (1966)
Wet	0 - 490	25 - 33°	"
wet	0 - 294	29°	Ripley and Lee (1962)
dry	294 - 2942	31 - 33°	Krsmanovic (1967)
dry	98 - 6864	32 - 34°	Coulson (1972)
wet	98 - 7158	31 - 34°	"



NOTE THAT: slices 1 - 8 the weight causes instability (+) whereas in slices 9 - 11 it contribute to stability (-).

slice no.	α	H1	H2	a	d	$\frac{W1}{d \cdot H1 \cdot \rho_{sst}}$	$\frac{W2}{d \cdot H2 \cdot \rho_{sh}}$	$W1+W2$	$\frac{W1+W2}{d} \cdot \sin \alpha$	$\frac{W1+W2}{d} \cdot \cos \alpha$	$\frac{U}{a \cdot d \cdot \rho_w}$	$\frac{W1+W2}{d} \cdot \cos \alpha - U$	L	c'
1														
2														
3														
⋮														
									$\sum_{\text{slice 1-11}}$			$\sum_{\text{slice 1 \& 2 sst.}}$ $\sum_{\text{slice 3-11 sh.}}$		$\sum_{\text{slice 3-11}}$

Where :

α = slope angle of slip surface at base of slice.

H1 = height of slice in sandstone beds.

H2 = height of slice in shale beds.

a = height of water table from slip surface.

d = width of slice.

L = base length of slice.

$W1, W2$ = weight of slice.

ρ_{sst} = density of sandstone.

ρ_{sh} = density of shale.

ρ_w = density of water.

c' = effective cohesion of shale.

Fig. 8.2 Method of calculating stability.

The calculations were carried out by a desk calculator method using the format in Fig. 8.2. It was considered that no advantage would be gained from using the computer for this operation, in view of the difficulty of finding the position of non-circular slip surfaces and water tables. Variations in shear strength are easier to accommodate in the manual method which also affords a greater 'feel' for the situation being modelled.

In order to carry out the analysis it was necessary to make the assumptions outlined below regarding the form of the slip surface.

- i. The shape of slip surface cuts more or less directly across the bedding of sandstone curves slightly when approaching shale. It takes a curved path through shale.
- ii. Where more than one lithology is present, the situation has been characterized by the properties of the major constituent.
- iii. The effective cohesion of sandstone is zero.
- iv. The density of shale is 2.3 Mg/m^3 and density of sandstone is 2.59 Mg/m^3 .
- v. Shear strength is uniformly mobilized on shear surface.
- vi. The interslice forces cancel out each other and have no overall effect (See Section 6.4.2).

Applying these assumptions to equation (6.22) gives the following working expression (See Fig. 8.2).

$$\text{Factor of safety against failure} = \frac{\sum (W \cos \alpha - u) \tan \phi'_{\text{sst}} + \sum c'_{\text{sh}} + \sum (W \cos \alpha - u) \tan \phi'_{\text{sh}}}{\sum W \sin \alpha}$$

Sandstone (sst) based slices Shale (sh) based slices

where:

W_1 = weight of slice

c'_{sh} = effective cohesion of shale

ϕ_{sh}' = effective internal friction of shale

ϕ_{sst}' = effective internal friction of sandstone.

α = slope angle of slip surface at the base of slice

l = base length of slice

8.4 Stability Analysis for Translational Movement

The stability of translational parts of the landslips were analysed using the infinite slope method outlined in Chapter 6. For this the assumptions listed below were necessary:

- i. The slip surface lies at the level of the original ground surface (See Fig. 8.3). Since most slides are terminated by a convex slope at their lower end, it seems likely that the landslip material over-rides the original ground surface.
- ii. The water table creates a hydrostatic component of pressure on the slip surface with flow out of the slope (See Haefeli 1948). This is supported by reference to seepages of water and the permanent high water table measured in borehole 2 at Mam Tor (See Fig. 8.4 B).
- iii. A second groundwater condition in which the water table is the below ground surface was also considered (See formula 6.13). This is likely to be more representative of the situation during dry seasons. Fig. 8.4 shows that the seasonal variation of water table for boreholes 1 and 2 at Mam Tor is approximately of 0.8 metre for Borehole 1 and 0.5 metre for Borehole 2.

8.5 Volumetric Changes

Longitudinal cross-sections for each landslip in Figs. 8.5 to 8.14 indicate that the land movements have

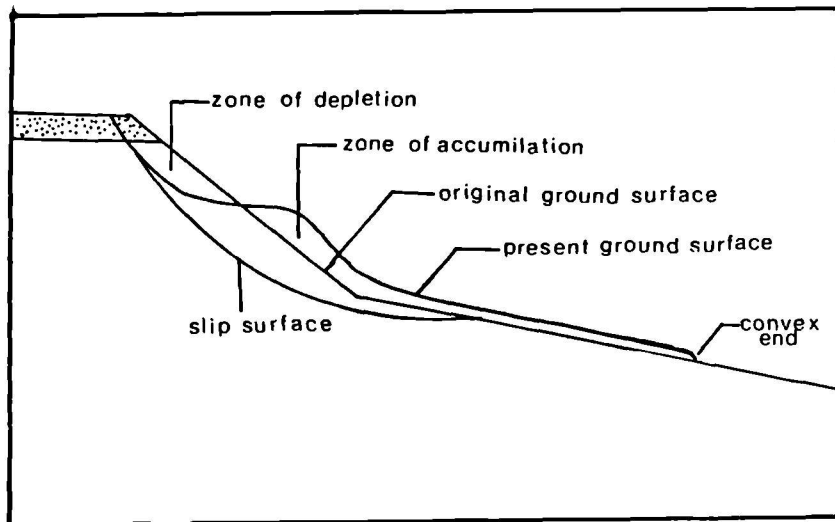


Fig. 8.3 Sketch of typical features of landslide.

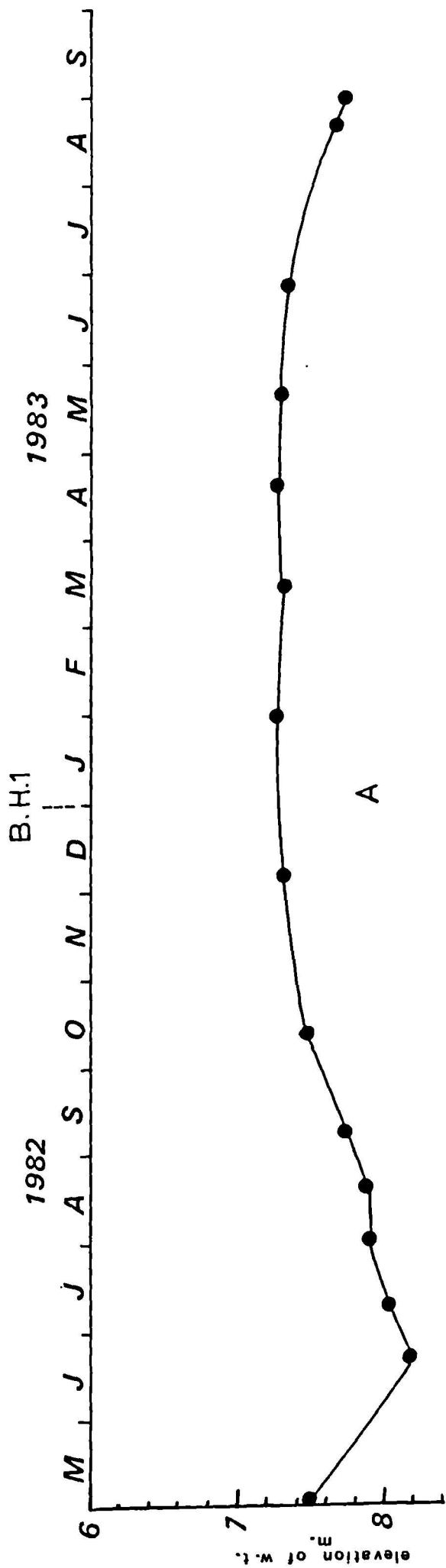


Fig. 8.4 Piezometers reading at Bore holes 1 and 2 (Mam Tor).

had the effect of creating zones of depletion and accumulation with respect to the previous land profile. Clearly the postulated movement has implications to the equality between these amounts which were found by measuring the area on the cross sections with a planimeter. Errors may be introduced since the zone of depletion consists of rock in a more dense condition than in the zone of accumulation. Also the cross section chosen may not have been truly representative, inaccuracies may have arisen in the estimation of previous profile and losses of material from-or gains of - material in landslide area may be due to erosion or other causes.

Table 8.4 shows that as would be expected, the volumes of accumulation zone material are more than the depletion material in all landslips except for Cowms Moor Upper landslide and Kinder Scout landslide section A - A' where the two volumes are nearly equal. This effect may be due to the interference between the upper and lower landslide.

8.6 Sources of Error

Apart from difficulties already considered, possible sources of error may arise from due to the choice of 'typical' cross section and also since stability is influenced by the assumptions regarding the position of geological boundaries. To some extent these problems were overcome by determining the sensitivity of the factor of safety to changes in various parameters. Hence for certain landslips more than one section was analysed. In addition several slip surfaces and water tables were considered for each landslide.

8.7 Results of Stability Analyses

The stability analysis for the ten landslips were carried out using the relevant shear strengths indicated in Table 8.5. In the cases of Mam Tor, Rushup Edge, Cold

Table 8.4 Volumetric changes for zones of depletion and accumulation of the landslips studied.

Landslip	Zone of Depletion (m ³)	Zone of accumulation (m ³)
Mam Tor	1,158,187	1,784,412
Rushup Edge	1,087,500	3,268,125
Cold Side	1,223,750	2,716,875
Back Tor	2,691,875	7,698,500
Burr Tor	512,500	3,750,000
Bretton Clough A - A'	710,937	1,638,000
Bretton Clough B - B'	1,365,625	2,625,000
Alport Castle	8,279,687	20,040,500
Cowms Moor upper slip	3,196,875	3,122,031
Cowms Moor lower slip	3,789,362	5,502,656
Kinder Scout A - A'	1,375,625	1,363,820
Kinder Scout B - B'	687,375	1,568,925
Rowlee Pasture A - A'	1,393,437	5,187,500
Rowlee Pasture B - B'	8,409,375	18,735,937

Table 8.5 Shear strengths used in the analysis.

SAMPLE	LANDSLIP
Mam Tor Borehole (MTBH)	Mam Tor Rushup Edge Cold Side Back Tor
Burr Tor (BUT)	Burr Tor Bretton Clough
Alport Castles (AC)	Alport Castles Cowms Moor
Rowlee Pastures (RP)	Rowlee Pasture Cowms Moor
Kinder Scout (KS)	Kinder Scout

Side and Back Tor slips, the underlying material is Edale Shale so it was assumed that the result of the shear tests on material from Borehole 1 at Mam Tor was representative. The Bretton Clough and Burr Tor landslips are reasonably near to each other and so the analysis is carried out using shear strength results for the Burr Tor sample. The shear strength parameter for material from Rowlee Pasture and Alport Castles have used in the analysis of the Cowms Moor landslip for the same reason.

By considering carefully the situation relating to each landslip (See Section 8.2), the most probable slip surface was postulated and used for analysis, other slip surfaces were tried and by a process of trial and error the most critical one to give a reasonable account of all the evidence was found. In addition, for first time sliding two other slip surfaces were also used in order to test the sensitivity of the factor of safety to this position. In the case of post-initial failure, calculation was based on the conditions for the most critical slip surface. In addition the residual shear strength measured by ring shear is assumed. The sensitivity of the factor of safety to the shear strength of sandstone and shale and to the elevation of water table are also considered. In addition the following sections include discussions of each postulated slip surface.

i. Mam Tor

a. Main unit, (rotational part).

The analysis is based on the most probable slip surface which is slip surface '2' in Fig. 8.5 A which yields a factor of safety of 0.92. Slip surface '1' gives a figure of 0.97 while slip surface '3' gives a figure of 0.96. Changes in the shear strength of the sandstone were found to produce little change in the factor of safety where an increase in ϕ' of 2° (from $35-37^\circ$) increased the factor of safety by 0.01 (from 0.92 to 0.93 for slip surface '2'). By lowering or raising the position of the water table by 5m. safety factors of 0.96 and 0.88 respectively were found. This is a change of only ± 0.04 .

Main unit, Noncircular rotational analysis

slip surface	factor of safety	ϕ_{rr} sh. deg.	c_{rr} sh. kn/m ²	ϕ'_{r} sst. deg.
1A	0.97	13.5	16.6	35
1A	0.98	13.5	16.6	37
2A	0.92	13.5	16.6	35
2A	0.93	13.5	16.6	37
3A	0.96	13.5	16.6	35
3A	0.97	13.5	16.6	37
2A-5m.	0.96	13.5	16.6	35
2A+5m.	0.88	13.5	16.6	35

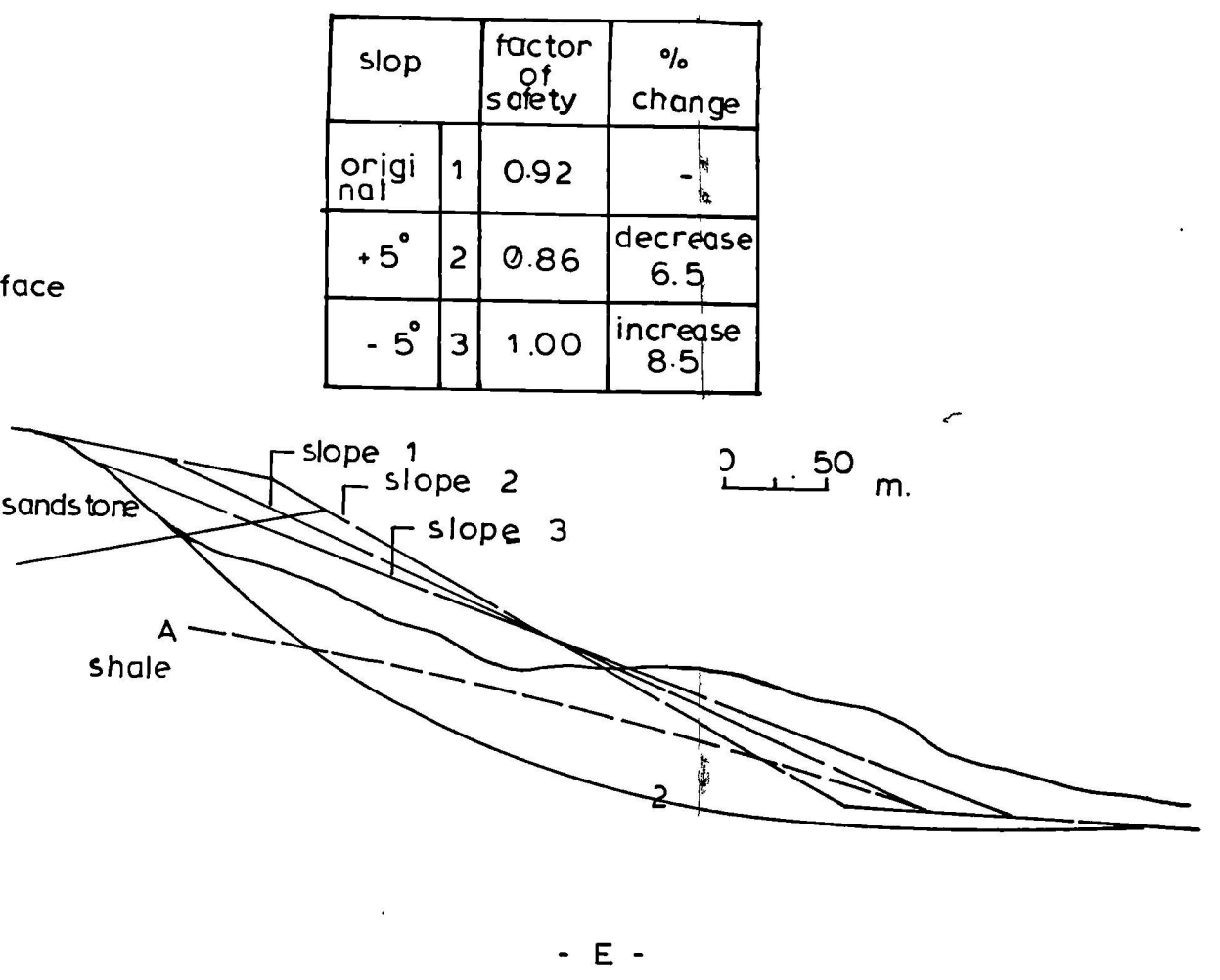
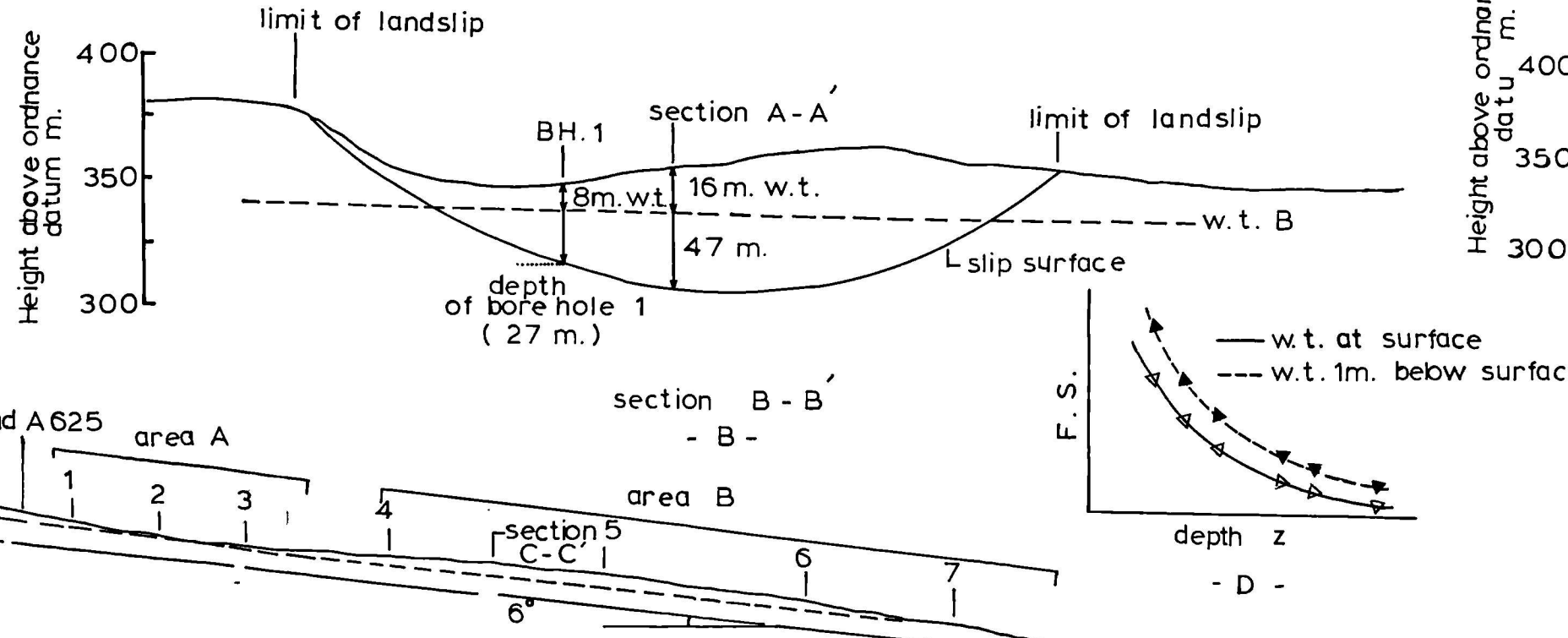
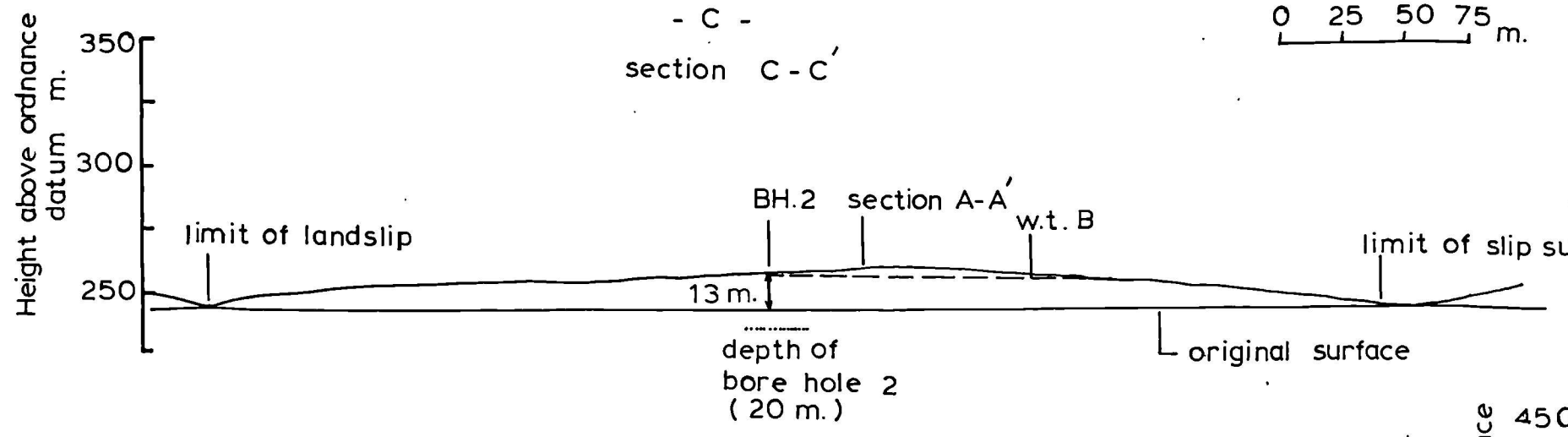
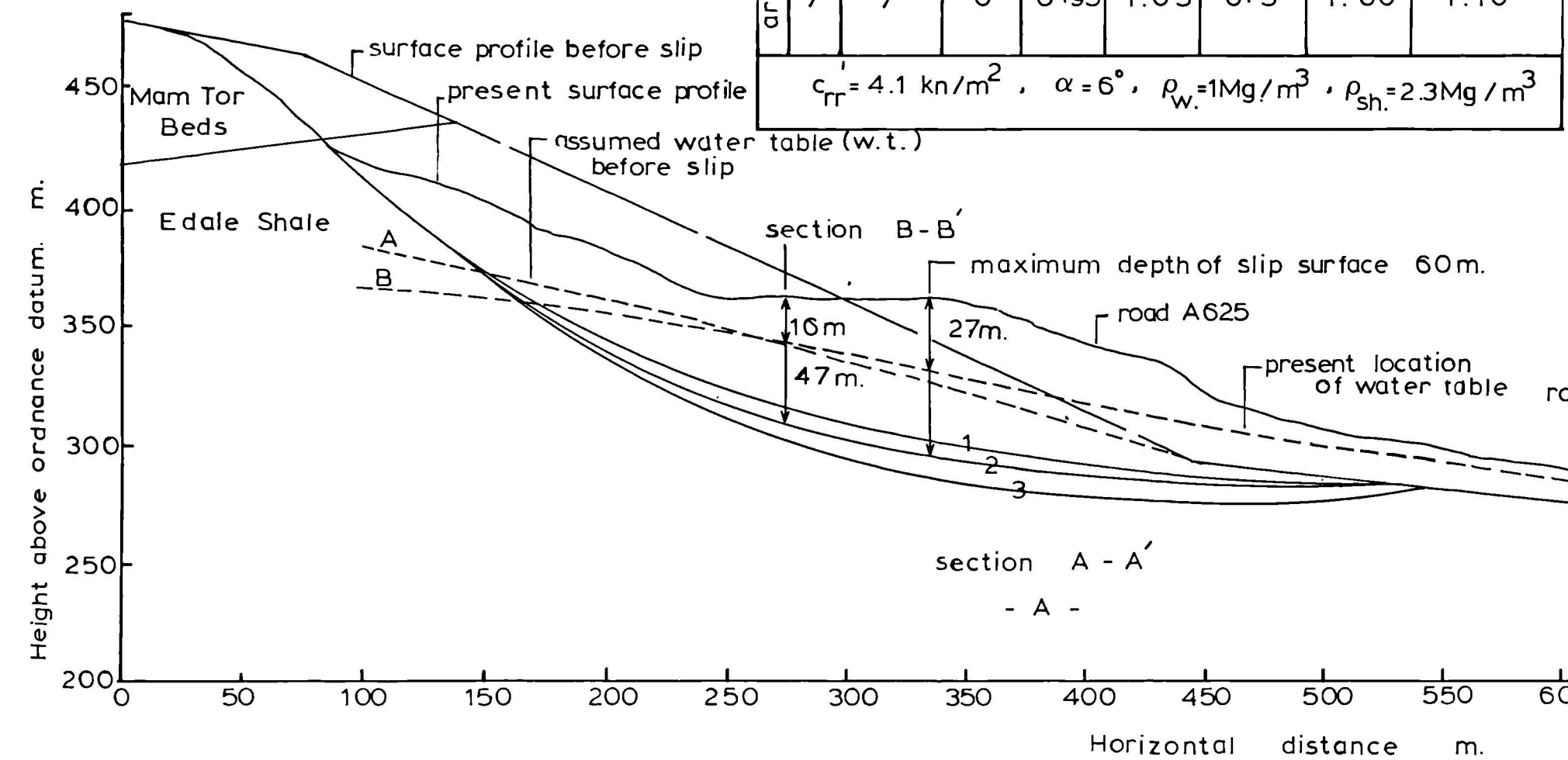
slip surface	factor of safety	ϕ_{rr} sh. deg.	c_{rr} sh. kn/m ²	ϕ'_{r} sst. deg.
2B	0.87	7.5	4.1	-
2B-3m.	0.90	7.5	4.1	-
2B	0.98	8.5	4.1	-
2B-3m.	1.02	8.5	4.1	-

Toe, Translational analysis

locations	depth to slip surface (z) m.	factor of safety		factor of safety (F.S.)		
		$\phi_{rr}=7.5$	$\phi_{rr}=8.5$	$\phi_{rr}=7.5$	$\phi_{rr}=8.5$	
		w.t. at surface		w.t. 1m. below surface		
area A	1	9	0.90	0.99	0.97	1.06
area A	2	8	0.92	1.02	0.99	1.09
area A	3	7	0.95	1.05	1.04	1.14

locations	depth to s.s. (z) m.	elevation of w.t. m.	F.S.		F.S.		F.S.	
			$\phi_{rr}=7.5$	$\phi_{rr}=8.5$	$\phi_{rr}=7.5$	$\phi_{rr}=8.5$	$\phi_{rr}=7.5$	$\phi_{rr}=8.5$
area B	4	10	2	0.99	1.10	2.5	1.02	1.13
area B	5	13	5	1.06	1.18	5.5	1.11	1.23
area B	6	11	2	0.97	1.08	2.5	0.99	1.10
area B	7	7	0	0.95	1.05	0.5	1.00	1.10

$c_{rr} = 4.1 \text{ kn/m}^2$, $\alpha = 6^\circ$, $\rho_w = 1 \text{ Mg/m}^3$, $\rho_{sh} = 2.3 \text{ Mg/m}^3$



slop	factor of safety	% change	
original	1	0.92	-
+5°	2	0.86	decrease 6.5
-5°	3	1.00	increase 8.5

FIG. 8.5 STABILITY ANALYSIS FOR MAM TOR LANDSLIP

safety factor increases to between 0.97 and 1.04. The relationship between the safety factor and the depth below ground surface of the slip plane (z) is indicated in Fig. 8.5D.

Observation of the water table in Borehole 2 indicate depth ranges from zero to 0.5m below the ground surface. Again by drawing a transverse cross section C - C' (See map Fig. 7.3) through this position in Fig. 8.5C indicates a depth to the original ground surface of about 13m.

In view of the uncertainty regarding the thickness of toe in Area B the instability was calculated for different slip surface depth with the water table (location 4, 5, 6 and 7) shown in Fig. 8.5 A. Hence the factor of safety ranges between 0.95 and 1.06. By lowering the water table by 0.5m the safety factor increases to between 0.99 and 1.11. Increasing the residual shear strength by one degree raises this figure by 0.09 to 0.12.

ii. Rushup Edge

a. Main unit (rotational part)

The most probable slip surface for first time sliding is shown in Fig. 8.6. Slip surface '2' gives a safety factor of 0.96 while slip surfaces '1' and '3' give figures of 0.99 and 1.06 respectively. Increasing the shear strength of sandstone from 35 to 37° increases the safety factor by only 0.04. Raising or lowering the water table shown in Fig. 8.6 by 5m. gives a safety factor of 0.93 and 0.99 which represents a change of 0.03. Increasing the original slope by 5° in Fig. 8.6A decreases the factor of safety from 0.96 to 0.93 and correspondingly increases it to 1.03 for a reduction in slope of the same amount.

The stability in the post initial condition gives a safety factor for slip surface '2' of 1.00 and 1.03 depending whether residual shear strength of sandstone 30 or 32° is used. An increase in safety factor by 0.09 to values of 1.09 and 1.12 results from an increase in residual shear strength of shale from 7.5° to 8.5° for residual shear strength of sandstone of 30° or 32°.

Main unit, Noncircular rotational analysis

slip surface	factor of safety (F.S.)	ϕ'_{rp} sh. deg.	c_{rp} sh. kn/m^2	ϕ'_{sst} deg.
1 A	0.99	13.5	16.6	35
1 A	1.03	13.5	16.6	37
2 A	0.96	13.5	16.6	35
2 A	1.00	13.5	16.6	37
3 A	1.06	13.5	16.6	35
3 A	1.10	13.5	16.6	37
2A+5m.	0.93	13.5	16.6	35
2A-5m.	0.99	13.5	16.6	35

slip surface	F.S.	ϕ'_{rr} sh. deg.	c_{rr} sh. kn/m^2	ϕ'_{r} sst. deg.
2 B	1.00	7.5	4.1	30
2 B	1.03	7.5	4.1	32
2 B	1.09	8.5	4.1	30
2 B	1.12	8.5	4.1	32

Toe, Translational analysis

location	depth to slip surface m.	elevat-ion of w.t. m.	factor of safety (F.S.)		
			$\phi'_{rr}=7.5^\circ$	$\phi'_{rr}=8.5^\circ$	
area A	1	4	0	1.05	1.14
	2	5	0	0.96	1.05
	3	7	3	1.10	1.21
	4	8	5	1.17	1.30
	5	5	3	1.28	1.40
	6	4	2	1.31	1.43

$\alpha = 6.5^\circ$

location	depth to slip surface m.	elevat-ion of w.t. m.	F.S.		
			$\phi'_{rr}=7.5^\circ$	$\phi'_{rr}=8.5^\circ$	
area B	7	13	13	1.11	1.24
	8	11	9	1.05	1.17
	9	8	5	1.01	1.12

$\alpha = 7.5^\circ$

$c_{sh.} = 4.1 \text{ kn/m}^2, \rho_w = 1 \text{ Mg/m}^3, \rho_{sh.} = 2.3 \text{ Mg/m}^3$

Height above ordnance datum m.	slope		F.S.	% change
	original	1		
original	1	0.96	-	
original +5	2	0.93	3	
original -5	3	1.03	7	

0 25 50 75 m.

0 50 m.

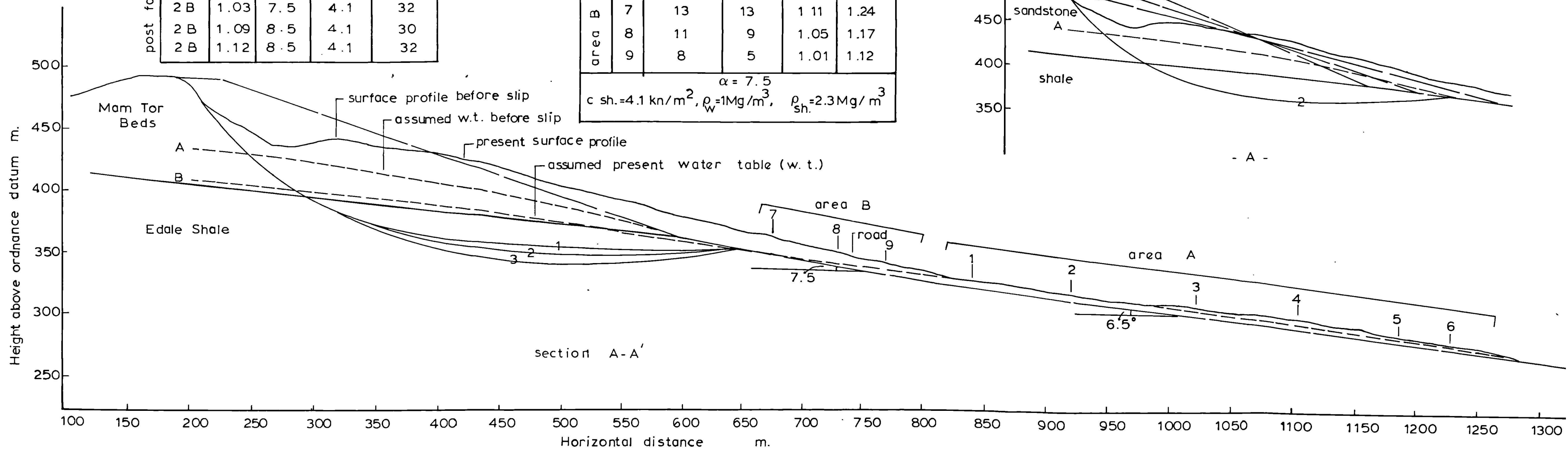


FIG. 8.6 STABILITY ANALYSIS FOR RUSHUP EDGE LANDSLIP

b. Toe (translational part)

The stability of the translational part is considered as two parts in Fig. 8.6. In area A, where the original ground surface slopes at an angle of 6.5° , the safety factors lies between 0.96 and 1.31 depending on the depth of the slip surface and elevation of water table. In area B, the ground slope is 7.5° and a safety factor between 1.01 and 1.11 is obtained. Increasing the residual shear strength by one degree increases the factor of safety in area A by 0.09 and 0.12, while the corresponding increases for area B is 0.11 and 0.13. Hence it would appear that the toe of the landslide is more stable than the main unit.

iii. Cold Side

a. Main unit (rotational)

Using the longitudinal profile of Fig. 8.7 for the most possible slip surface, a safety factor of 0.96 is obtained for slip surface '2' while slip surfaces '1' and '3' give values of 1.03 and 1.0 respectively. This factor is increased by only 0.04 if the shear strength of sandstone is increased from 35° to 37° , so it has little effect in position of the postulated slip surface. By lowering the water table shown in Fig. 8.7 by 5m., the factor of safety increases by only 0.02 from 0.96 to 0.98 while raising it by 5m reduces the factor from 0.96 to 0.94. As shown in Fig. 8.7A, the safety factor is reduced by only 0.006 if the original slope is increased by 5° , while reducing the original slope by 5° causes an increase in safety factor by 0.02.

The results for the stability of post-initial failure shown in Fig. 8.7 indicate factors of safety from 1.00 to 1.03 where the residual shear strength of the sandstone assumed is 30° and 32° respectively. An increase in safety factor by 0.08 results from an increase in residual strength of shale from 7.5° to 8.5° .

b. Toe

The stability of the toe of the landslide was calculated as a flow of landslide material. The results shown

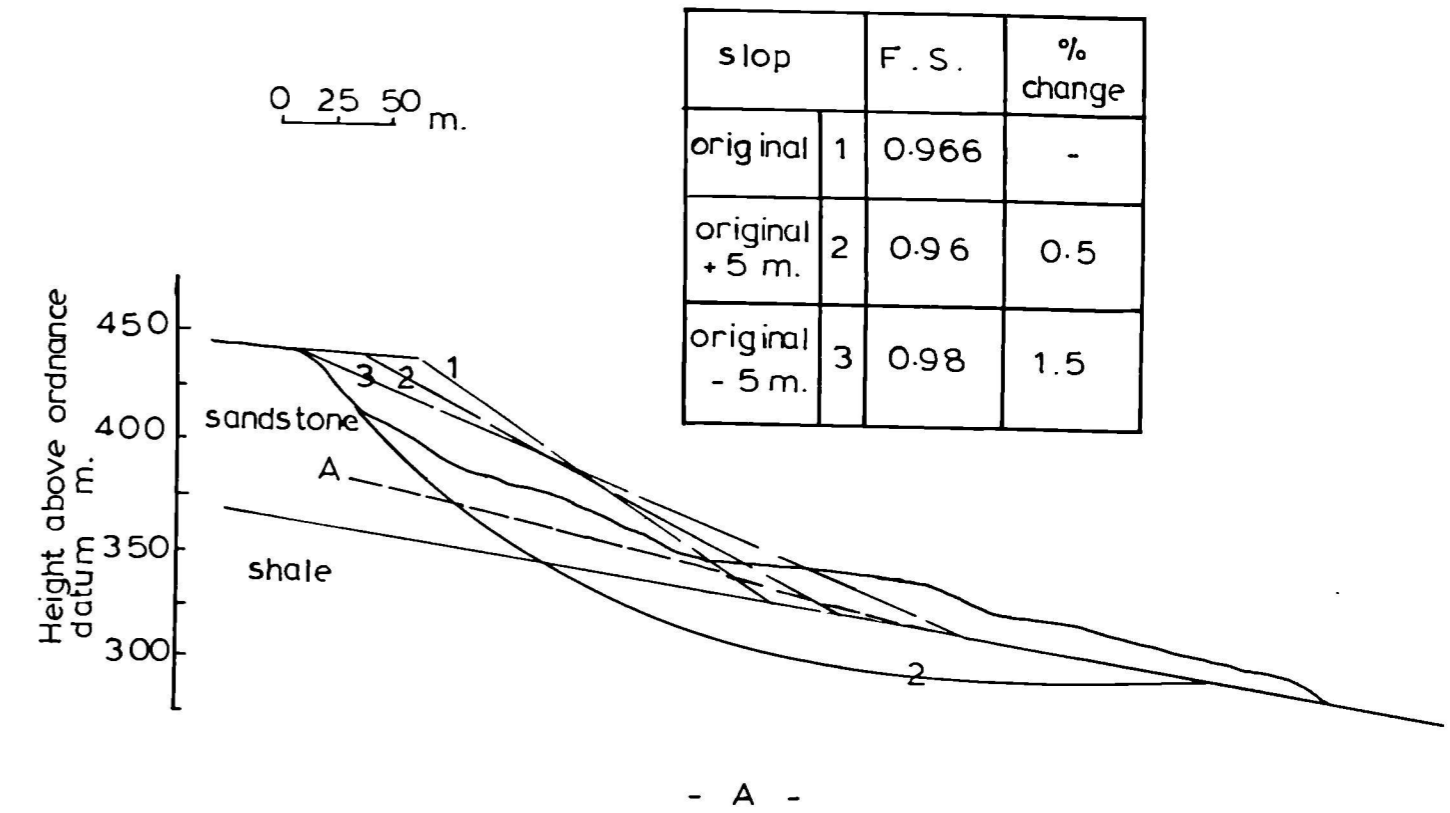
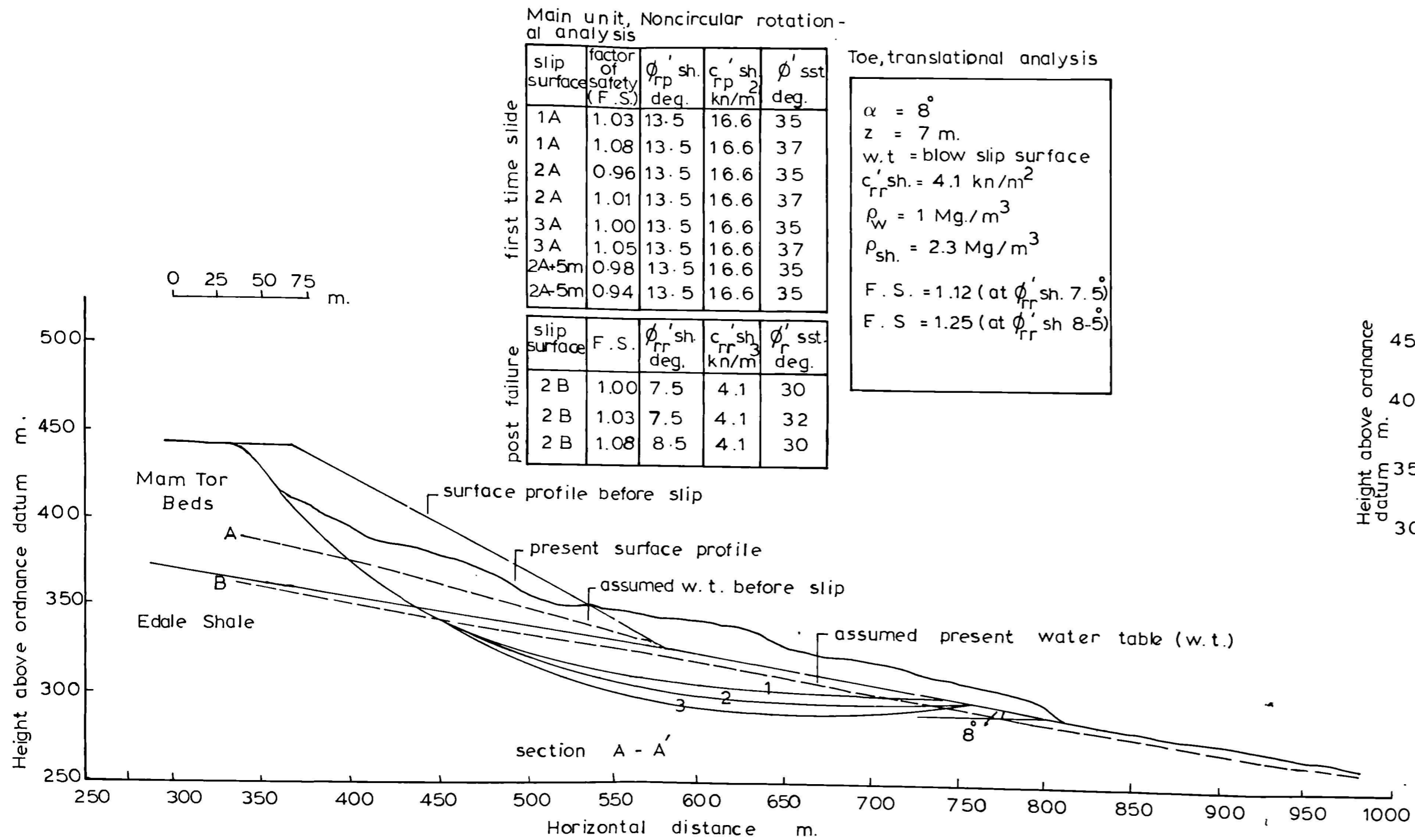


FIG. 8.7 STABILITY ANALYSIS FOR COLD SIDE LANDSLIP

in Fig. 8.7 give a safety factor of 1.12. By assuming a residual shear strength one degree higher than the laboratory measured one, the figure increases by 0.13 to 1.25.

iv. Back Tor

a. Main unit (rotational part)

The stability factors for the main unit at Back Tor landslip are shown in Fig. 8.8. Slip surface '2' gives a safety factor of 0.96 and corresponding values for slip surface '1' and '3' are 0.98 and 0.99 respectively. Increasing the shear strength of sandstone from 35 to 37° increases the factor of safety by 0.05. Thus the strength of this material has only a small effect on the factor of safety or postulated slip surface position. By raising the water table by 5m. there is a reduction in safety factor of only 0.01. Similarly, lowering the water table by 5m increases the safety factor by only 0.01.

The stability of post initial failure is also calculated and it was found to be 0.98 and 1.02 for a residual shear strength of sandstone of 30 and 32° respectively. Assuming the mobilized shear strength of shale is one degree higher than the laboratory one yields an increase in safety factor of 0.07.

b. Toe (translational)

The stability of the toe of the landslip is also calculated in Fig. 8.8. Again the stability has been calculated for different locations and for different depths to the slip surface and elevations of water table. The safety factor ranges between 1.19 and 1.33. By assuming a residual shear strength of shale one degree higher than the measured one, the figure increases by 0.12 to 0.15. Thus it would appear that the toe is more stable than the main unit. It is significant that no evidence of recent landslip activity was noticed in the field.

v. Burr Tor

a. Main unit (rotational)

The stability analyses of the Burr Tor landslip are

Main unit, Noncircular rotational analysis

slip surface	factor of safety (F.S.)	ϕ'_{rp} sh. deg.	c'_{rp} sh. kn/m ²	ϕ'_{sst} deg.
1 A	0.98	13.5	16.6	35
1 A	1.04	13.5	16.6	37
2 A	0.96	13.5	16.6	35
2 A	1.01	13.5	16.6	37
3 A	0.99	13.5	16.6	35
3 A	1.04	13.5	16.6	37
2A+5m.	0.95	13.5	16.6	35
2A-5m.	0.97	13.5	16.6	37

slip surface	F.S.	ϕ'_{rr} sh. deg.	c'_{rr} sh. kn/m ²	ϕ'_{rst} deg.
2 B	0.98	7.5	4.1	30
2 B	1.02	7.5	4.1	32
2 B	1.05	8.5	4.1	30

Toe, translational analysis

locations	depth to slip surface m.	elevation of w.t. m.	F.S.	
			ϕ'_{rr} sh. 7.5	ϕ'_{rr} sh. 8.5
1	9	7	1.33	1.48
2	7	4	1.28	1.42
3	5	2	1.28	1.40
4	7	3	1.20	1.33
5	8	4	1.20	1.34
6	6	2	1.19	1.31

$\alpha = 6^\circ$ c'_{rr} sh. = 4.1 kn/m²
 $\rho_w = 1 \text{ Mg/m}^3$ $\rho_{sh.} = 2.3 \text{ Mg/m}^3$

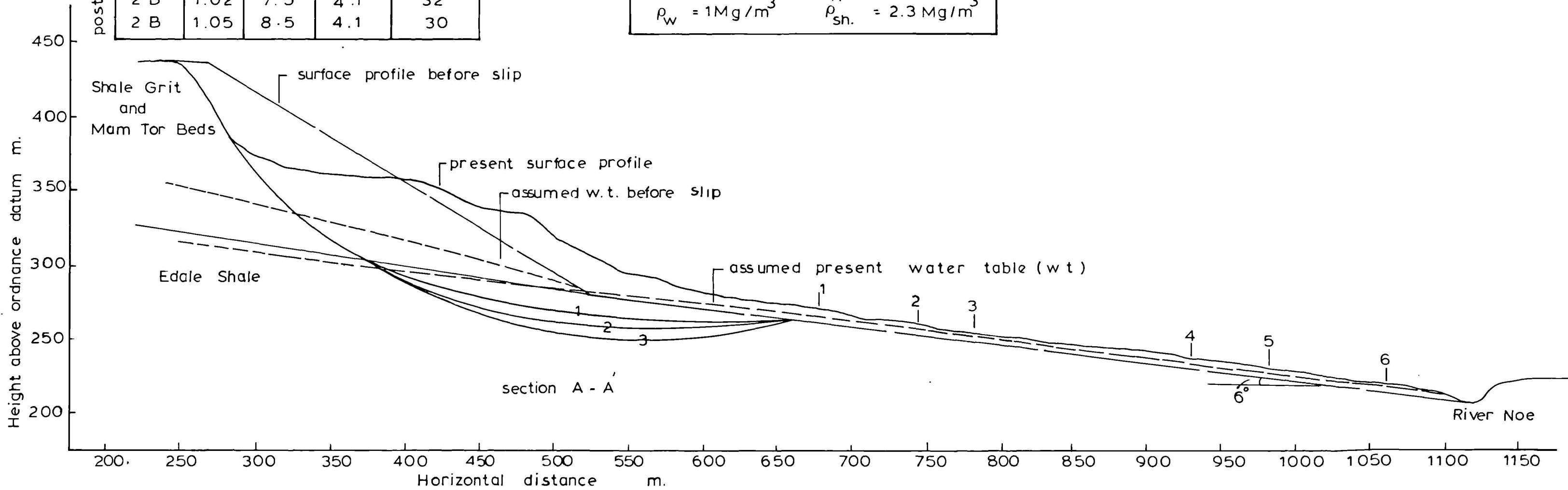
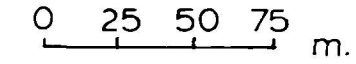


FIG. 8.8 STABILITY ANALYSIS FOR BACK TOR LANDSLIP

shown in Fig. 8.9. Slip surface '2' gives a safety factor of 0.97 while slip surface '1' and '3' give safety factors of 1.00 and 1.03 respectively. An increase in shear strength for sandstone from 35 to 37° increases the factor of safety by 0.02, so apparently it has little effect on the stability. By assuming water table 'A' shown in Fig. 8.9 is lowered by 5m increases the safety factor by 0.03, while raising it by the same amount reduces the value by 0.03.

The stability of the post-initial failure produces a factor of safety of 0.98. Assuming the residual shear strength of shale is one degree higher than that used in the analysis gives a safety factor of 1.07, an increase of 0.09. As mentioned in Chapter 7 there is no evidence of any recent activity of this landslide, so the first value appears a little low in view of the likely seasonal fluctuation of water table elevation.

b. Toe

The stability analysis of the toe of this landslide which consists of a small translational flow of landslide debris gives a safety factor of 1.72. By assuming the mobilized shear strength is one degree higher than the test one, gives a safety factor of 1.86 so it would appear that the toe is more stable than the main unit.

vi. Bretton Clough

a. Main unit (rotational)

The stability of the Bretton Clough landslide is analysed with respect to two cross-sections located on map Fig. 7.11. The stability analyses for first time slides using postulated slip surfaces are shown in Fig. 8.10.

For section A-A', slip surface '2' gives a factor of safety of 0.95, while slip surface '1' and '3' give safety factors of 0.97 and 1.0 respectively. Increasing the shear strength of sandstone from 35 to 37° increases the safety factor by only 0.02. By lowering or raising water table 'A' by 5m the figure respectively increases or decreases by 0.05. For section B-B', postulated slip surface '2' gives a safety factor of 0.96 while slip

Main unit, Noncircular rotational analysis

first time slide	slip surface	factor of safety (F.S.)	ϕ'_{rp} sh deg.	c'_{rp} sh. kn/m^2	ϕ'_{sst} deg.
	1 A	1.00	20	10.6	35
1 A	1.02	20	10.6	37	
2 A	0.97	20	10.6	35	
2 A	0.99	20	10.6	37	
3 A	1.03	20	10.6	35	
3 A	1.05	20	10.6	37	
2A+5m.	0.94	20	10.6	35	
2A-5m	1.00	20	10.6	35	

post failure	slip surface	F.S	ϕ'_{rr} sh. deg	c'_{rr} sh. kn/m^2	ϕ'_{r} sst deg
	2 B	0.98	9.5	7.6	-
2 B	1.07	10.5	7.6	-	

Toe, Translational analysis

$\alpha = 7^\circ$
 $z = 8$ m
 w.t. = below slip surface
 c'_{rr} sh = 7.6 kn/m^2
 $\rho_w = 1$ Mg/m^3
 $\rho_{sh} = 2.3$ Mg/m^3
 F.S. = 1.72 (at $\phi'_{rr} 9.5^\circ$)
 F.S. = 1.86 (at $\phi'_{rr} 10.5^\circ$)

0 25 50 75 m.

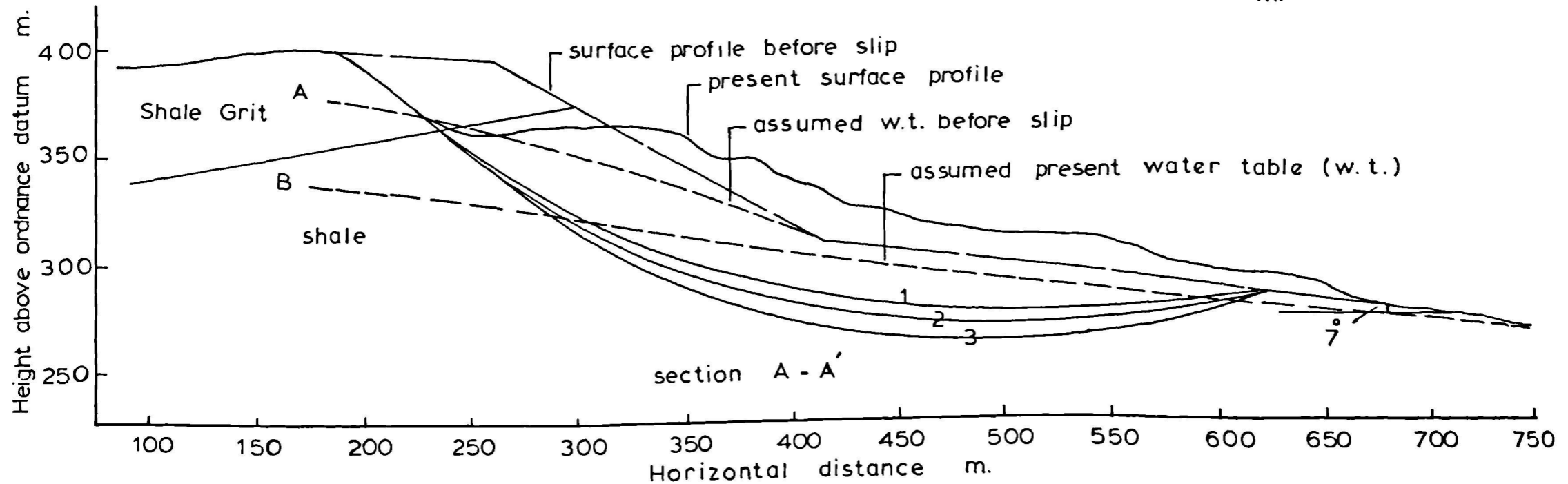


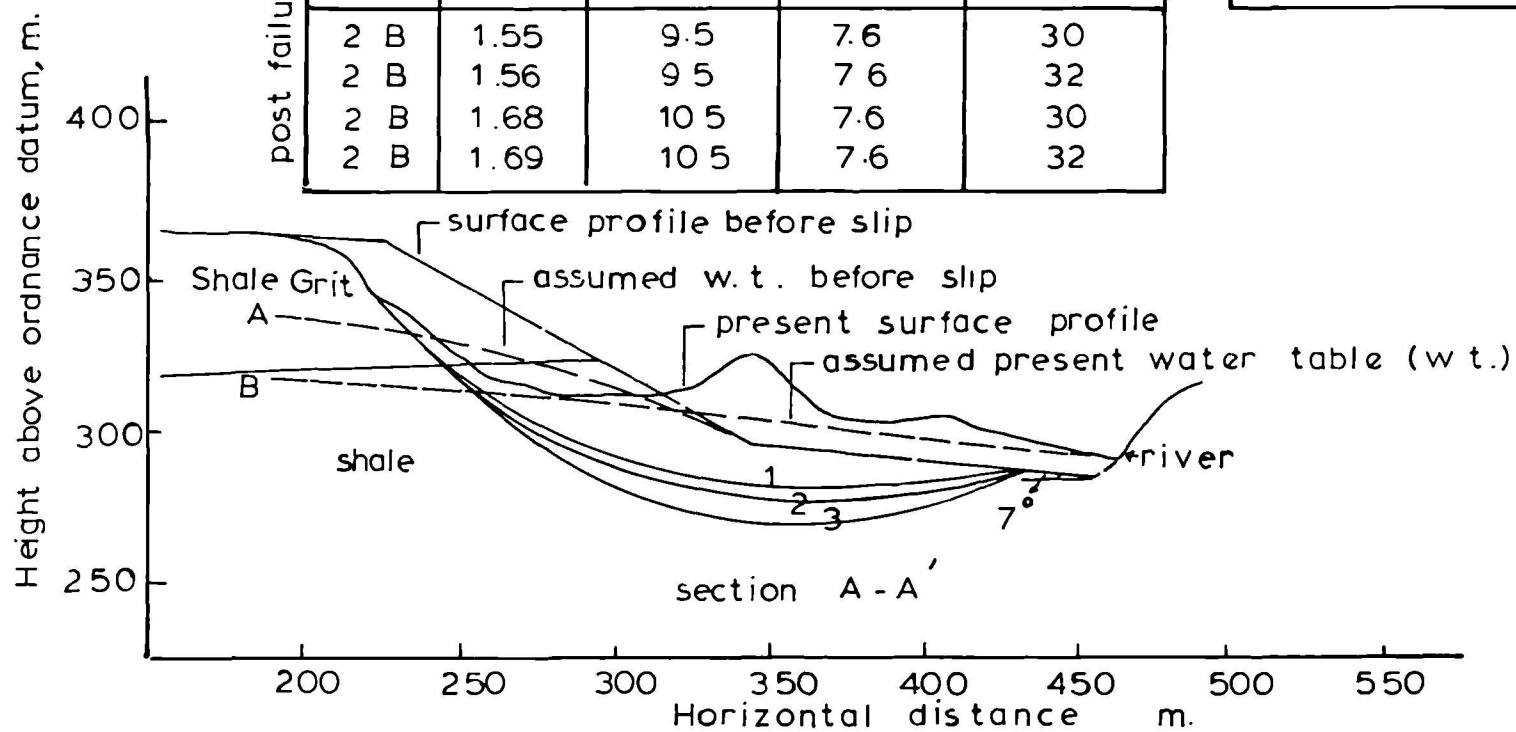
FIG. 8.9 STABILITY ANALYSIS FOR BURR TOR LANDSLIP

Main unit, Noncircular rotational analysis

slip surface	factor of safety (F. S.)	ϕ'_{rp} sh deg.	c'_{rp} sh. kn/m^2	ϕ'_{sst} deg.	post failure	slip surface	F. S.	ϕ'_{rr} sh deg.	c'_{rr} sh. kn/m^2	ϕ'_{rst} deg.
1 A	0.97	20	10.6	35	first time slide	2 B	1.55	9.5	7.6	30
1 A	0.99	20	10.6	37		2 B	1.56	9.5	7.6	32
2 A	0.95	20	10.6	35		2 B	1.68	10.5	7.6	30
2 A	0.97	20	10.6	37		2 B	1.69	10.5	7.6	32
3 A	1.00	20	10.6	35						
3 A	1.02	20	10.6	37						
2A+5m	0.90	20	10.6	35						
2A-5m	1.00	20	10.6	35						

Toe, translational analysis

$\alpha = 7^\circ$
 $z = 9m.$
 $w.t. = 2m.$
 $c_{rr} sh = 7.6 kn/m^2$
 $\rho_w = 1 Mg/m^3$
 $\rho_{sh} = 2.3 Mg/m^3$
 $F.S. = 1.21$ (at $\phi'_{rr} sh 9.5$)
 $E.S. = 1.31$ (at $\phi'_{rr} sh 10.5$)



Main unit, Noncircular rotational analysis

slip surface	factor of safety (F. S.)	ϕ'_{rp} sh. deg.	c'_{rp} sh. kn/m^2	ϕ'_{sst} deg.	first time slide	slip surface	F. S.	ϕ'_{rr} sh. deg.	c'_{rr} sh. kn/m^2	ϕ'_{rst} deg.
1 A	1.01	20	10.6	35	post failure	2 B	1.21	9.5	7.6	-
1 A	1.01	20	10.6	37		2 B	1.33	10.5	7.6	-
2 A	0.96	20	10.6	35						
2 A	0.96	20	10.6	37						
3 A	1.03	20	10.6	35						
3 A	1.03	20	10.6	37						
2A+5m	0.90	20	10.6	35						
2A-5m	1.02	20	10.6	35						

Toe, translational analysis

locat-ions	depth to slip surface (z) m.	elevat-ion of w. t. m.	F. S.	
			$\phi'_{rr} sh 9.5^\circ$	$\phi'_{rr} sh 10.5^\circ$
1	12	6	1.25	1.36
2	5	0	1.32	1.40

$\alpha = 8^\circ$
 $c_{rr} sh = 7.6 kn/m^2$
 $\rho_w = 1 Mg/m^3$
 $\rho_{sh} = 2.3 Mg/m^3$

0 25 50 75 m.

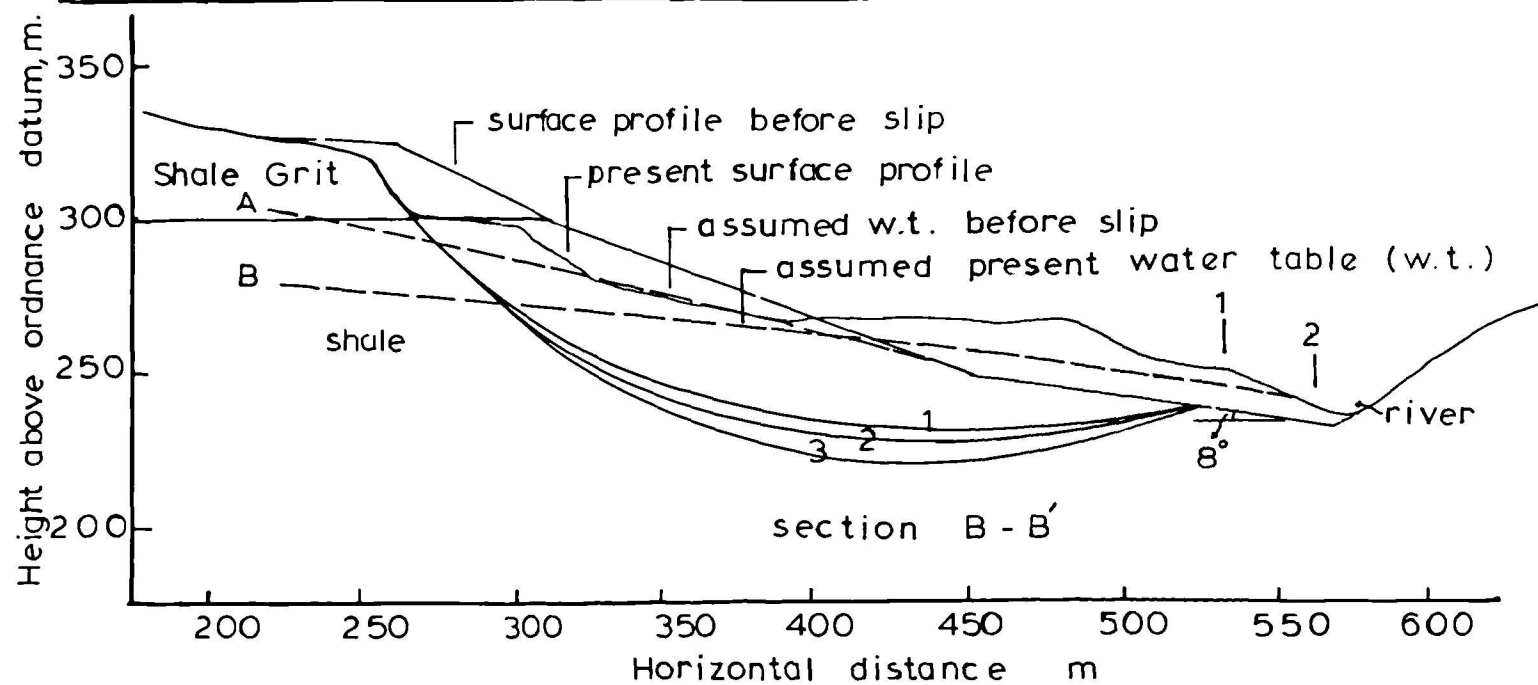


FIG. 8.10 STABILITY ANALYSIS FOR BRETTON CLOUGH LANDSLIP

surfaces '1' and '3' gives values of 1.01 and 1.03 respectively. Changing the shear strength of sandstone from 35° to 37° increases the safety factor by less than 0.005. A 5m reduction in the height of the water table 'A' gives a safety factor of 1.02 while raising it by the same amount produces a safety factor of 0.90, an increase or decrease of 0.06.

Analyses of the post-initial failure indicate in Section A-A' of Fig. 8.10 that the landslide has obtained a very stable condition since slip surface '2' gives safety factors of 1.55 and 1.56 for residual shear strength of sandstone of 30 and 32° respectively. By assuming a residual shear strength of shale one degree higher than the measured one, these figures increase by 0.13. The relatively stable condition attained by this landslide may be attributed to the restraint due to the accumulation of landslide debris in the valley. The post-initial failure analysis for section B-B' gives a safety factor of 1.21 for slip surface '2'. Assuming the residual shear strength of shale is one degree higher than the laboratory value, this increases the safety factor to 1.33. These values are less than the corresponding ones for section A-A' because the landslide material in this section appears to be shallower in the zone of depletion and deeper in the zone of accumulation.

b. Toe

The analyses of the toe of the landslide which forms a small translational slide yield factors of safety of 1.21 for section A-A' and 1.25 and 1.32 for section B-B'. These figures increase by 0.08 to 0.11 when the assumed residual shear strength of the shale is one degree higher than the laboratory value.

vii. Alport Castles

The stability analysis of Alport Castles landslide is represented by two cross sections located on map Fig. 7.12.

a. Main unit (rotational)

The stability analyses for first-time sliding for

several slip surfaces are shown in Fig. 8.11. Slip surface '2' in Section A-A' gives a safety factor of 0.95, while slip surfaces '1' and '3' both produce a value of 0.99. An increase in safety factor of only 0.04 occurs if the shear strength of sandstone is increased from 35 to 37°. By lowering or raising by 5m water table 'A' shown in fig. 8.11, section A-A', the safety factor is changed by 0.03. Section B-B' shows the location of two landslip surfaces. For the first of these the most probable slip surface is number '2' which gives a safety factor of 0.95 while slip surfaces '1' and '3' give values of 0.99 and 0.97 respectively. The factor of safety is increased by up to 0.05 if the shear strength of the sandstone is increased from 35 to 37°. An increase or decrease in safety factor by 0.03 occurs if water table 'A' is changed by 5m to give a safety factors of a 0.92 and 0.98 respectively. For the second landslip, slip surface '2' gives a safety factor of 0.98 while surfaces '1' and '3' give safety factor of 0.99 and 1.0 respectively. These figures are increased by 0.02 if the shear strength of sandstone is increased from 35 to 37°. Raising or lowering water table 'A' by 5m decreases or increases the safety factor by 0.02 respectively.

The post-initial failure analysis is also shown in Fig. 8.11 in which the safety factor for the most probable slip surface '2' in Section A-A' is 1.35. This value increases by 0.05 if the residual shear strength of sandstone is increased from 30 to 32°. If the residual shear strength of the shale is increased by one degree the factor of safety is increased by 0.11. This high factor of safety in this cross-section is attributed to large thickness of landslip material in the zone of accumulation. Analysis of Section B-B' yields lower safety factors in which for the first time landslip the safety factor is 0.98. This is increased by 0.05 if the residual shear strength of sandstone is raised from 30° to 32°. By assuming the residual shear strength of shale is one degree higher, the safety factor is increased by 0.05. In case of second landslip, slip

Main unit, Noncircular rotational analysis

slip surface	factor of safety (F. S.)	ϕ'_{rp} sh deg.	c'_{rp} sh. kn/m^2	ϕ'_{sst} deg.
1 A	0.99	17	9.8	35
1 A	1.03	17	9.8	37
2 A	0.95	17	9.8	35
2 A	0.99	17	9.8	37
3 A	0.99	17	9.8	35
3 A	1.03	17	9.8	37
2A+5m	0.92	17	9.8	35
2A-5m	0.98	17	9.8	35
post failure				
slip surface	F. S.	ϕ'_{rr} sh deg.	c'_{rr} sh. kn/m^2	ϕ'_{sst} deg.
2 B	1.35	7	6.5	30
2 B	1.40	7	6.5	32
2 B	1.46	8	6.5	30

Toe, Translational analysis

locations	depth to slip surface (z) m.	elevation of w. t. m.	F. S.	
			ϕ'_{m7°	ϕ'_{m8°
1	17	8	0.92	1.03
2	22	17	1.02	1.15
$\alpha = 7^\circ$ $c'_{sh} = 6.5 \text{ kn/m}^2$ $\rho_w = 1 \text{ Mg/m}^3$ $\rho_{sh} = 2.3 \text{ Mg/m}^3$				

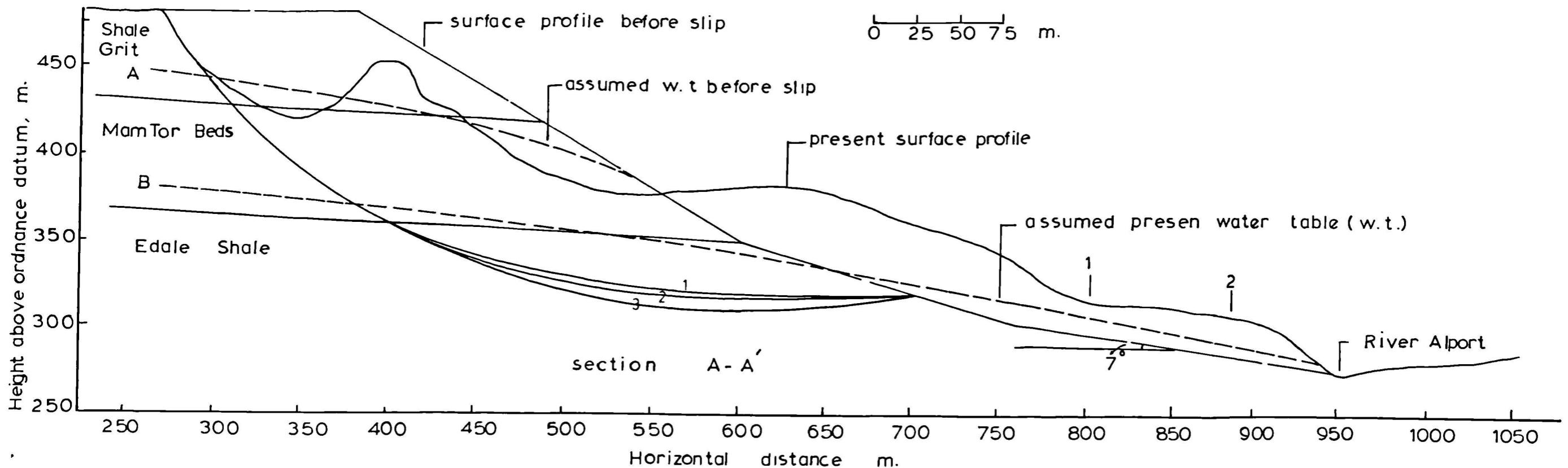


FIG. 8.11 STABILITY ANALYSIS FOR ALPORT CASTELS LANDSLIP

Main unit, Noncircular rotational analysis

		first slip		slop 1	
first time slide	slip surface	factor of safety (F.S.)	ϕ'_{rp} sh. deg.	c_{rp} sh. kn/m^2	ϕ' sst. deg.
		1 A'	0.99	17	9.8
	1 A'	1.05	17	9.8	37
	2 A'	0.95	17	9.8	35
	2 A'	1.00	17	9.8	37
	3 A'	0.97	17	9.8	35
	3 A'	1.01	17	9.8	37
	2A+5m.	0.92	17	9.8	35
	2A-5m	0.98	17	9.8	35
post failure	slip surface	F.S.	ϕ'_{rr} sh. deg.	c_{rr} sh. kn/m^2	ϕ'_r sst. deg.
	2 B	0.98	7.0	6.5	30
	2 B	1.03	7.0	6.5	32
	2 B	1.03	8.0	6.5	30

Main unit, Noncircular rotational analysis

		second slip		slop 2	
first time slide	slip surface	factor of safety (F.S.)	ϕ'_{rp} sh. deg.	c_{rp} sh. kn/m^2	ϕ' sst. deg.
		1 A	0.99	17	9.8
	1 A	1.01	17	9.8	37
	2 A	0.98	17	9.8	35
	2 A	1.00	17	9.8	37
	3 A	1.00	17	9.8	35
	3 A	1.02	17	9.8	37
	2A+5m	0.96	17	9.8	35
	2A-5m	1.00	17	9.8	35
post failure	slip surface	F.S.	ϕ'_{rr} sh. deg.	c_{rr} sh. kn/m^2	ϕ' sst. deg.
	2 B	1.00	7.0	6.5	30
	2 B	1.03	7.0	6.5	32
	2 B	1.08	8.0	6.5	30

Toe, Translational analysis

locations	depth to slip surface (z) m.	elevation of w. t. m.	F. S.	
			ϕ'_{rr} sh. 7.0	ϕ'_{rr} sh. 8.0
1	18	10	0.94	1.06
2	3	0	1.35	1.47
3	7	2	1.03	1.14
$\alpha = 7^\circ$		$c_{rr} = 6.5 \text{ kn/m}^2$		
$\rho_w = 1 \text{ Mg/m}^3$		$\rho_{sh} = 2.3 \text{ Mg/m}^3$		

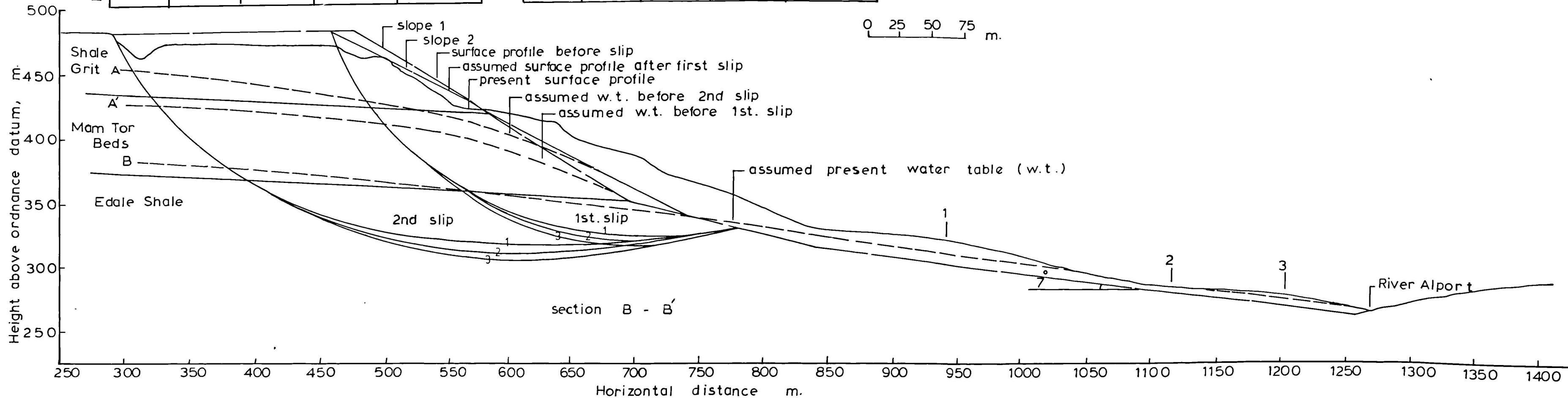


FIG. 8.11 STABILITY ANALYSIS FOR ALPORT CASTELS LANDSLIP

surface '2' gives a safety factor of 1.00. This increases by 0.03 if the residual shear strength of sandstone is increased by 2°. Assuming that the residual shear strength of the shale is higher by one degree than the residual shear strength determined in laboratory increases the safety factor by 0.08.

b. Toe (translational)

The stability analysis of the toe of the landslide is also calculated for both sections shown in Fig. 8.11. For Section A-A' the factor of safety ranges between 0.92 and 1.02. By assuming the residual shear strength of shale is one degree higher increases the safety factor to 1.03 and 1.15 respectively. In case of Section B-B', the factor ranges between 0.94 and 1.35 depending on the position of the slip surface and the water table. These values are increased by 0.12 if the residual shear strength of the shale is one degree higher.

viii. Rowlee Pasture

Stability analyses for first-time sliding are carried out for the two cross sections located on map Fig. 7.13.

a. Main unit (rotational)

Slip surface '2' shown in Section A-A' in Fig. 8.12 gives a safety factor of 0.95, while slip surfaces '1' and '3' gives respectively safety factors of 0.99 and 0.98. Increasing the shear strength of sandstone by 2° increases the factor of safety by up to 0.06 and altering the water table by 5m reduces or increases the value by 0.03. For Section B-B' the safety factor is 0.91 for slip surface '2' and 1.00 and 1.05 for slip surfaces '1' and '3' respectively. An increase in safety factor up to 0.04 is produced by increasing the shear strength of sandstone by 2°, while changing the water table by 5m produces a change in safety factor of 0.02.

Analysis of post initial failure stability for both Sections A-A' and B-B' yield a safety factor of 0.98. This value increases by 0.04 when the residual shear strength of sandstone is increased by 2°. The factor of safety is increased by 0.06 when the residual mobilized shear strength of the shale is one degree higher.

Main unit, Noncircular rotational analysis

slip surface	factor of safety (F. S.)	ϕ'_{rp} sh. deg.	c_{rp} sh. kn/m^2	$\phi'_{sst.}$ deg.
1 A	0.99	18	10.9	35
1 A	1.05	18	10.9	37
2 A	0.95	18	10.9	35
2 A	0.99	18	10.9	37
3 A	0.98	18	10.9	35
3 A	1.03	18	10.9	37
2A+5m.	0.92	18	10.9	35
2A-5m.	0.98	18	10.9	35

slip surface	F. S.	ϕ'_{rr} sh. deg.	c'_{rr} sh. kn/m^2	ϕ'_{r} sst. deg.
2 B	0.98	7.5	4.3	30
2 B	1.02	7.5	4.3	32
2 B	1.04	8.5	4.3	30

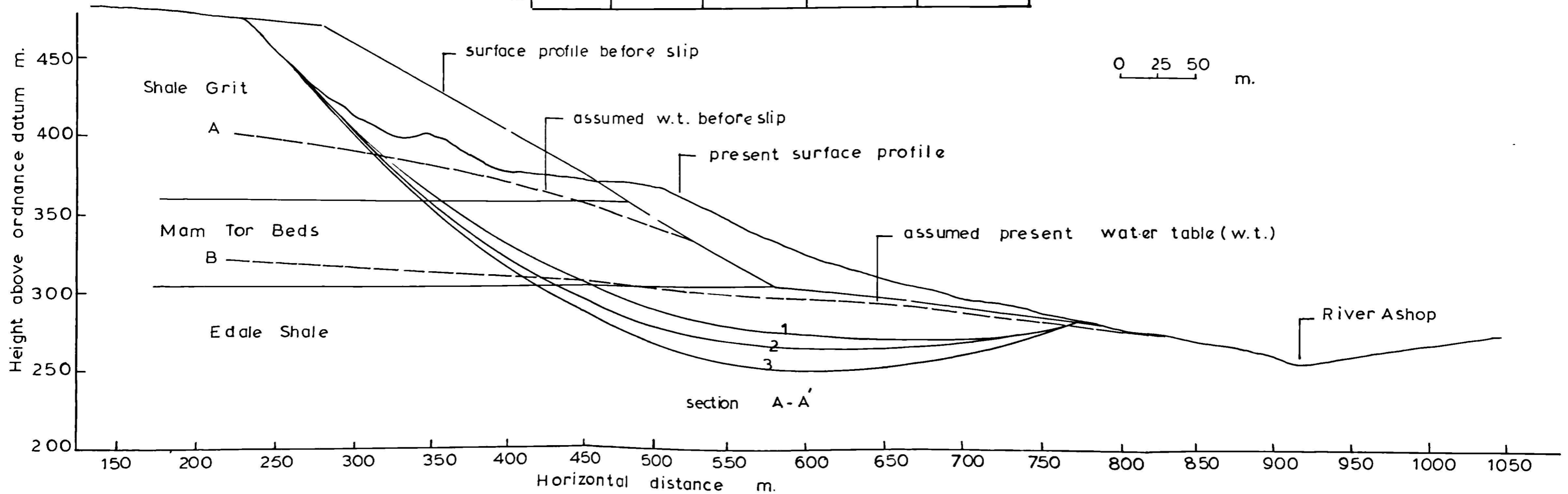


FIG. 8.12, STABILITY ANALYSIS FOR ROWLEE PASTURE LANDSLIP

Main unit, rotational noncircular analysis

slip surface	factor of safety (F.S.)	ϕ'_{rp} sh. deg.	c_{rp} sh. kn/m^2	ϕ'_{sst} deg.
1 A	1.00	18	10.9	35
1 A	1.04	18	10.9	37
2 A	0.91	18	10.9	35
2 A	0.94	18	10.9	37
3 A	1.05	18	10.9	35
3 A	1.08	18	10.9	37
2A+5m.	0.89	18	10.9	35
2A-5m.	0.93	18	10.9	35

slip surface	F.S.	ϕ'_{rr} sh. deg.	c_{rr} sh. kn/m^2	ϕ'_{sst} deg.
2 B	0.98	7.5	4.3	30
2 B	1.03	7.5	4.3	32
2 B	1.04	8.5	4.3	30

Toe, translational analysis

locations	depth to slip surface (z) m.	elevation of w.t. m.	factor of safety	
			ϕ'_{rr} sh. deg.	ϕ'_{sst} sh. deg.
1	9	3	0.88	0.97
2	4	0	0.94	1.01

$\alpha = 7.5^\circ$ $\rho_w = 1 Mg/m^3$
 $c_{rr} = 4.1 kn/m^2$ $\rho_{sh} = 2.3 Mg/m^3$

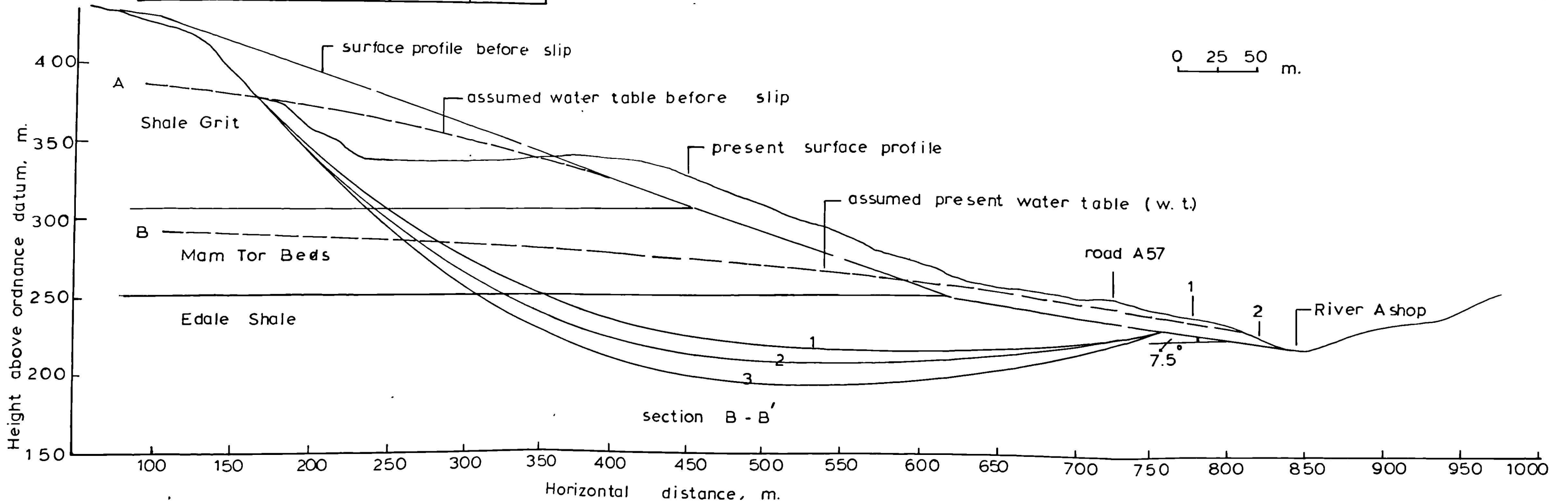


FIG. 8.12, STABILITY ANALYSIS FOR ROWLEE PASTURE LANDSLIP

b. Toe

In Section A-A' the toe is not developed and it has not been analysed. In Section B-B', the stability of the toe is calculated assuming a small translational flow of material from the main unit. This suggests a factor of safety of between 0.88 and 0.94 depending on the slip surface position and water table elevation. These values increase to 0.97 and 1.01 respectively by assuming the residual shear strength of the shale is one degree higher than the laboratory value. In fact, field observations (Chapter 7) indicate that the landslide Section A-A' has not been subject to recent activity. It is certainly more stable than section B-B' where the A57 road and river bank have been affected by minor movements.

ix. Cowms Moor

The stability analyses for first time sliding using postulated slip surfaces for the Cowms Moor landslide are represented in two cross sections located on map Fig. 7.14 and the analyses shown in Fig. 8.13. As mentioned in Chapter 7, it is convenient to divide the landslide into an upper and lower part.

a. Main unit (rotational)

The analysis for a first-time slide of the upper landslide shown in Section A-A' of Fig. 8.13 gives a safety factor which ranges between 0.96 and 0.98 for slip surface '2', while for slip surfaces '1' and '3' the figures range between 0.97 - 0.99 and 1.00 - 1.03 respectively. The increase in safety factor produced when the shear strength of sandstone is increased by 2° is 0.04 and 0.05 and raising or lowering by 5m water table 'A' causes changes the safety factor by 0.07. In section B-B' the upper landslide gives a safety factor that ranges between 0.92 and 0.95 for slip surface '2' while for slip surface '1' and '3' the safety factor is from 0.97 to 0.99 and 0.99 to 1.02 respectively. An increase of 0.04 to 0.05 in this figure is produced when the residual shear strength of sandstone increases from 35° to 37°. Lowering or raising

Main unit, noncircular rotational analysis

upper slip				
first time slide				
slip surface	factor of safety	$\phi_{rp}'_{sh}$ deg.	$c_{rp}'_{sh}$ kn/m ²	ϕ'_{sst} deg.
1 A	0.97	17	9.8	35
1 A	1.01	17	9.8	37
1 A	0.99	18	10.9	35
1 A	1.04	18	10.9	37
2 A	0.96	17	9.8	35
2 A	0.99	17	9.8	37
2 A	0.98	18	10.9	35
2 A	1.02	18	10.9	37
3 A	1.00	17	9.8	35
3 A	1.04	17	9.8	37
3 A	1.03	18	10.9	35
3 A	1.07	18	10.9	37
2A+5m	8.9	17	9.8	35
2A-5m	1.03	17	9.8	35
2A+5m	0.91	18	10.9	35
2A-5m	1.05	18	10.9	35

Main unit, noncircular rotational analysis

upper slip				
post failure				
slip surface	factor of safety	$\phi_{rr}'_{sh}$ deg.	$c_{rr}'_{sh}$ kn/m ²	ϕ'_{sst} deg.
2 B	1.36	7	6.5	30
2 B	1.45	7	6.5	32
2 B	1.38	7.5	4.3	30
2 B	1.46	7.5	4.3	32
2 B	1.41	8	6.5	30
2 B	1.43	8.5	4.3	30

Main unit, noncircular rotational analysis

lower slip				
first time slide				
slip surface	factor of safety	$\phi_{rp}'_{sh}$ deg.	$c_{rp}'_{sh}$ kn/m ²	ϕ'_{sst} deg.
1 A	0.96	17	9.8	35
1 A	0.98	17	9.8	37
1 A	0.99	18	10.9	35
1 A	1.02	18	10.9	37
2 A	0.94	17	9.8	35
2 A	0.96	17	9.8	37
2 A	0.98	18	10.9	35
2 A	1.00	18	10.9	37
3 A	0.97	17	9.8	35
3 A	0.99	17	9.8	37
3 A	1.01	18	10.9	35
3 A	1.03	18	10.9	37
2A+5m	0.90	17	9.8	35
2A-5m	0.98	17	9.8	35
2A+5m	0.94	18	10.9	35
2A-5m	1.02	18	10.9	35

Main unit, noncircular rotational analysis

lower slip				
post failure				
slip surface	factor of safety	$\phi_{rr}'_{sh}$ deg.	$c_{rr}'_{sh}$ kn/m ²	ϕ'_{sst} deg.
2 B	1.03	7	6.5	30
2 B	1.07	7	6.5	32
2 B	1.05	7.5	4.3	30
2 B	1.09	7.5	4.3	32
2 B	1.10	8	6.5	30
2 B	1.13	8.5	4.3	30

Toe, translational analysis

locations	depth to slip surface (z) m.	elevation of water table m.	factor of safety	
			$\phi_{r30}'_{sst}$	$\phi_{r32}'_{sst}$
1	13	3	2.90	2.14
2	8	0	2.49	2.69

$\alpha = 8^\circ$
 $c_r'_{sst} = 0$
 $\rho_w = 1 \text{ Mg/m}^3$
 $\rho_{sst} = 2.59 \text{ Mg/m}^3$

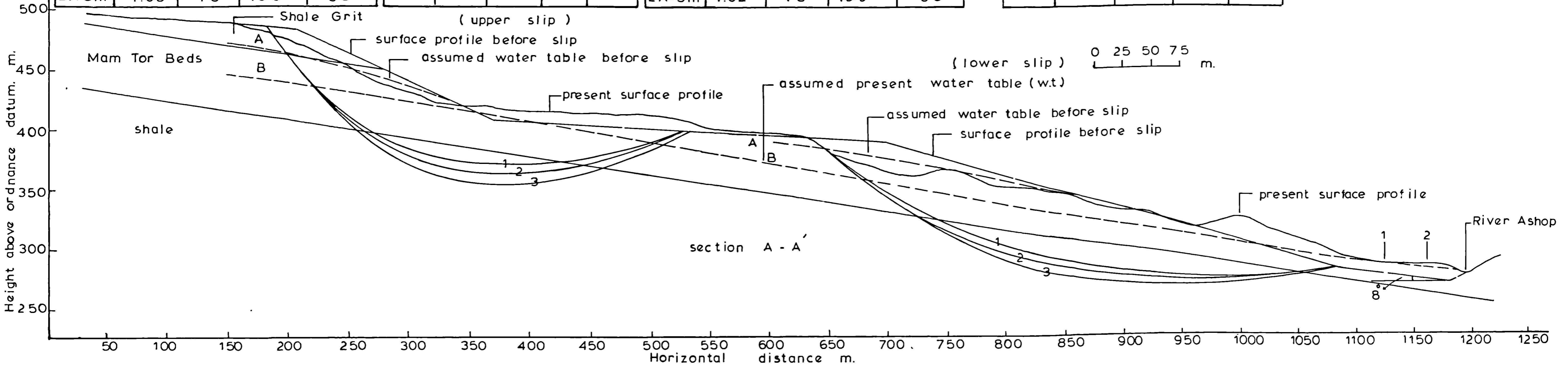


FIG 8.13 STABILITY ANALYSIS FOR COWMS MOOR LANDSLIP

Main unit, rotational noncircular analysis

upper slip				
first time slid				
slip surface	factor of safety	ϕ'_{rp} sh. deg.	c'_{rp} sh. kn/m ²	ϕ'_{sst} deg.
1 A	0.97	17	9.8	35
1 A	1.01	17	9.8	37
1 A	0.99	18	10.9	35
1 A	1.04	18	10.9	37
2 A	0.92	17	9.8	35
2 A	0.96	17	9.8	37
2 A	0.95	18	10.9	35
2 A	0.99	18	10.9	37
3 A	0.99	17	9.8	35
3 A	1.03	17	9.8	37
3 A	1.02	18	10.9	35
3 A	1.06	18	10.9	37
2A+5 m.	0.88	17	9.8	35
2A-5 m.	0.97	17	9.8	35
2A+5 m.	0.91	18	10.9	35
2A-5 m.	0.99	18	10.9	35

Main unit, rotational noncircular analysis

upper slip				
post failure				
slip surface	factor of safety	ϕ'_{rr} sh. deg.	c'_{rr} sh. kn/m ²	ϕ'_{rst} deg.
2 B	1.25	7.0	6.5	30
2 B	1.35	7.0	6.5	32
2 B	1.28	7.5	4.3	30
2 B	1.34	7.5	4.3	32
2 B	1.32	8.0	6.5	30
2 B	1.34	8.5	4.3	30

(upper slip)

Main unit, noncircular rotational analysis

lower slip				
first time slide				
slip surface	factor of safety	ϕ'_{rp} sh. deg.	c'_{rp} sh. kn/m ²	ϕ'_{sst} deg.
1 A	0.97	17	9.8	35
1 A	1.00	17	9.8	37
1 A	1.00	18	10.9	35
1 A	1.03	18	10.9	37
2 A	0.92	17	9.8	35
2 A	0.95	17	9.8	37
2 A	0.96	18	10.9	35
2 A	0.99	18	10.9	37
3 A	0.98	17	9.8	35
3 A	1.00	17	9.8	37
3 A	1.02	18	10.9	35
3 A	1.04	18	10.9	37
2A+5 m.	0.87	17	9.8	35
2A-5 m.	0.98	17	9.8	35
2A+5 m.	0.90	18	10.9	35
2A-5 m.	1.03	18	10.9	35

Main unit, rotational noncircular analysis

lower slip				
post failure				
slip surface	factor of safety	ϕ'_{rr} sh. deg.	c'_{rr} sh. kn/m ²	ϕ'_{rst} deg.
2 B	1.05	7.0	6.5	30
2 B	1.09	7.0	6.5	32
2 B	1.07	7.5	4.3	30
2 B	1.11	7.5	4.3	32
2 B	1.11	8.0	6.5	30
2 B	1.13	8.5	4.3	30

(lower slip)

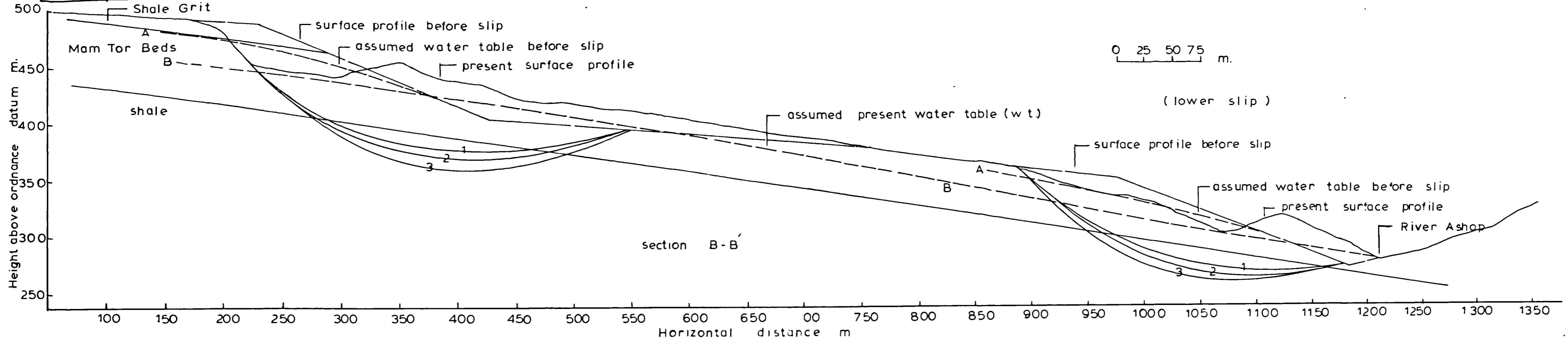


FIG 8.13 STABILITY ANALYSIS FOR COWMS MOOR LANDSLIP

the water table by 5m causes an increase or decrease in safety factor amounting to 0.04.

For the lower landslip the postulated slip surface in Section A-A' gives factors of safety for first-time sliding of 0.94 - 0.98 for slip surface '2' and between 0.96 to 0.99 and 0.97 to 1.01 for slip surfaces '1' and '3' respectively. The corresponding values for cross section B-B' are 0.92 to 0.95 for slip surface '2' and 0.97 to 1.00 and 0.98 to 1.02 for surfaces '1' and '3' respectively. An increase in safety factor of between 0.02 to 0.03 occurs when the shear strength of sandstone is increased from 35 to 37°, and changing the position of the water table by 5m causes a change in safety factor of 0.04 for Section A-A'. The corresponding values for Section B-B' are 0.04 to 0.06.

The post-initial failure stability for Section A-A' of slip surface '2' of the upper landslip is found to range 1.36 to 1.38 depending on the strength value adopted where as for Section B-B' the range is 1.25 - 1.28. An increase in safety factor of between 0.09 and 0.08 occurs when the residual shear strength of sandstone is increased from 30 to 32° for Section A-A' and the corresponding increase is only 0.06 for Section B-B'. By changing the residual shear strength of shale by one degree, the safety factor for Section A-A' increases by only 0.05 while for cross-section B-B' it is between 0.06 and 0.07. Slip surface '2' of the lower landslip of Section A-A' gives a safety factor which ranges between 1.03 and 1.05 while for Section B-B' slip surface '2' gives a value of 1.05 to 1.07. For both sections the factor of safety is increased by 0.04 by increasing the shear strength of sandstone from 30 to 32°. By increasing the residual shear strength of the shale by one degree, the factor of safety is increased by 0.07 to 0.08 in cross-section A-A' and by 0.06 in cross-section B-B' depending on the length of slip surface assumed to cut the shale beds.

b. Toe

The stability of the toe of the lower landslip shown in Section B-B' of Fig. 8.13 was calculated by assuming

a small translational slide. The factors of safety range between 2.49 and 2.90 depending on the thickness of the landslide material and elevation of water table. This high factor of safety is explained by the presence of sandstone beneath the slip. In the case of the toe of the upper landslide, since the original ground slope is less than 5° movement is most improbable on the sandstone present in the area.

x. Kinder Scout

Only two cross sections located on map Fig. 7.15 were chosen to represent the landslips in the Kinder Scout area.

a. Main unit (rotational)

The slip surfaces used in the stability analysis are shown in Fig. 8.14, Section A-A' and B-B'. Slip surface '2' of Section A-A' gives a first time safety factor of 0.95 while for Section B-B' the corresponding figure is 0.94. Slip surface '1' and '3' both give higher safety factors of 0.99 and 0.97 respectively. Lowering or raising the water table 'A' shown in both Sections A-A' and B-B' by 5m., gives an increase or decrease in the value of 0.06.

The post-initial failure analysis shown in Fig. 8.14 for Section A-A' gives a safety factor of 1.37 and 1.01 for Section B-B'. This higher value may be attributed to the large thickness of landslide material in the zone of accumulation. By assuming the mobilized shear strength in the field is higher by one degree than the residual shear strength obtained from ring shear tests, the factor of safety is increased by 0.11 for Section A-A' and 0.08 for Section B-B'.

b. Toe

The stability of the toe was calculated as a small translational slide of landslide material. The safety factors range between 0.97 and 1.08 for Section A-A' while for Section B-B' they are between 0.91 and 1.02. If the residual shear strength of the shale is one degree higher than the measured value then the safety factor is

Main unit non-circular rotational analysis				
Slip surface	Factor of safety	ϕ'_{rp} Sh Degrees	C'_{rp} Sh KN m^2	
First time slide				
1A	0.99	24	79	
2A	0.95	24	79	
3A	0.97	24	79	
2A+5 m	0.89	24	79	
2A-5 m	1.01	24	7.9	
Post failure				
Slip surface	Factor of safety	ϕ_{rr} Sh Degrees	C_{rr} Sh KN m^2	
F2B	1.37	13	4.9	
F2B	1.48	14	4.9	

Toe (Translation Analysis)				
Location	Depth to slip surface 2 (m)	Elevation of water table (m)	Factor of safety	
			ϕ_{rr} 13.0	ϕ_{rr} 14.0
1	19	Below original slope	0.97	1.05
2	13		0.99	1.07
3	6		1.08	1.15
$\alpha = 14^\circ$ $C'_{rr} = 4.9 \text{ kN m}^2$ $\rho_w = 1 \text{ Mg m}^3$				
$\rho_{sh} = 2.3 \text{ Mg m}^3$				

Main unit, non-circular rotational analysis			
Location	Factor of safety	ϕ'_{rp} sh Degrees	C'_{rp} sh kN/m^2
First time slide			
1A	0.99	24	79
2A	0.94	24	79
3A	0.97	24	79
2A+5m	0.88	24	79
2A+5m	1.00	24	79
Post failure			
Location	Factor of safety	ϕ_{rr} sh Degrees	C_{rr} sh kN/m^2
2B	1.01	13	4.9
2B	1.09	14	4.9

Toe (Translation analysis)				
Location	Depth to slip surface 2 (m)	Elevation of water table (m)	Factor of safety	
			13°	14°
1	7	Below original slope	0.91	0.97
2	3		1.02	1.08
$\alpha = 17^\circ$ $C'_{rr} = 4.9 \text{ kN/m}^2$ $\rho_w = 1 \text{ Mg/m}^3$				
$\rho_{sh} = 2.3 \text{ Mg/m}^3$				

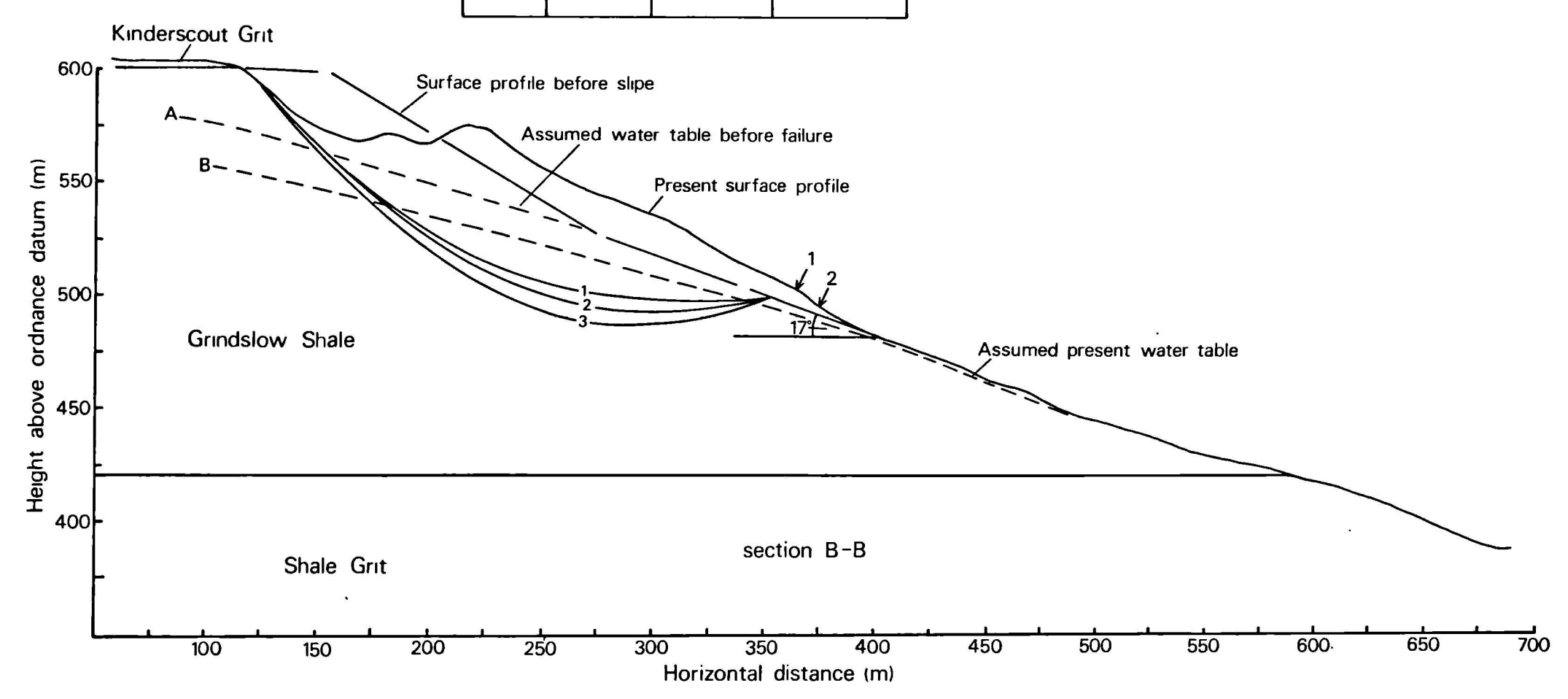
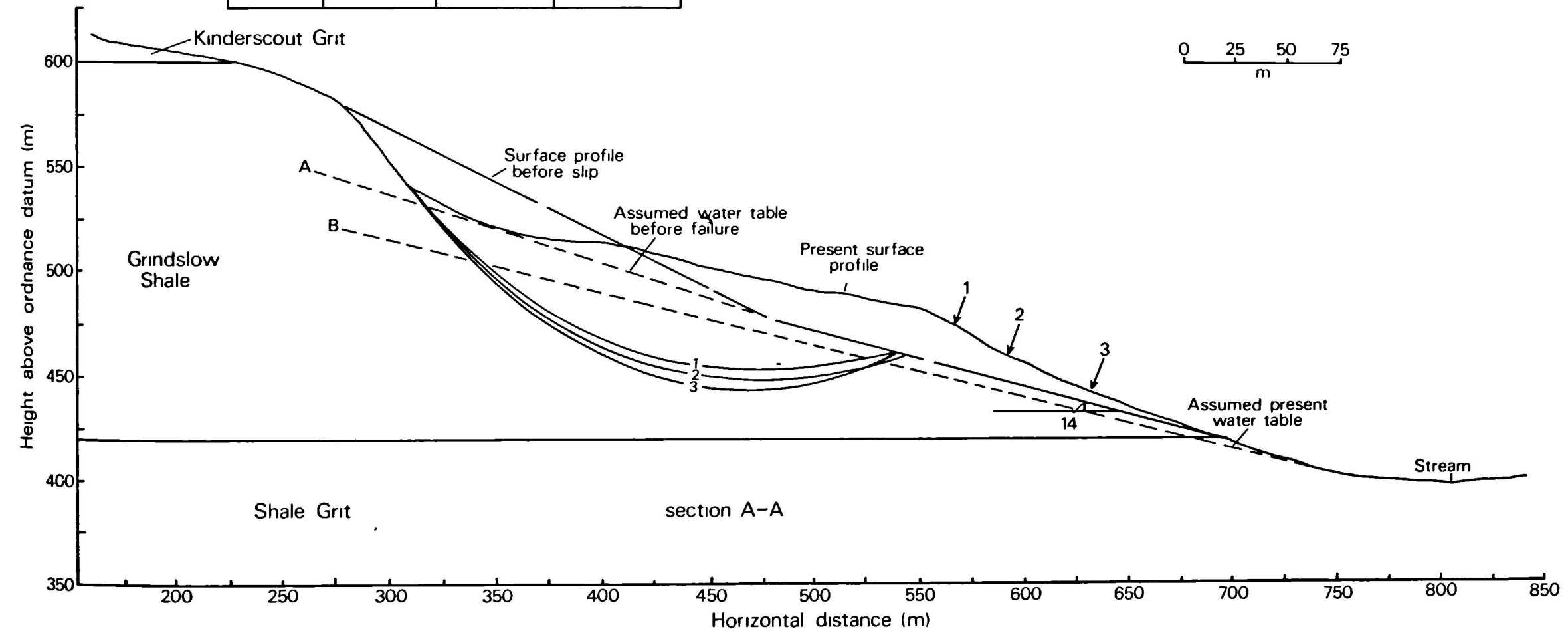


Fig. 8.14 STABILITY ANALYSIS FOR KINDER SCOUT LANDSLIP

increased by 0.06. No evidence of instability has been noted in Chapter 7, so it would appear that the laboratory remoulded ring residual shear strength is lower than the field value.

8.8 Summary and Discussion

The analysis of stability for first time sliding on the basis of remoulded peak strength has been used to determine the position of the most probable slip surface. The post failure stability condition has then been predicted by an analysis based on the most critical slip surface using the remoulded residual shear strength. Detailed mapping and observations described in Chapter 7 of the stability state of the landslips analysed may be compared with these predictions. It should be remembered that there exist a number of explanations for apparent divergence from the predicted stability condition of which the most important probably include a lack of knowledge regarding piezometric pressures, the position of the slip surface, the density of the sliding material, the ground surface profile prior the second movement and the shear resistance mobilized on the slip surface. Furthermore, there is uncertainty regarding the representativeness of the chosen cross-section and the accuracy of the analysis itself. While having the advantage of being convenient to apply, the analysis used does involve a number of simplifying assumptions. In particular it is assumed that interslice forces cancel out and that shear stress mobilized on shear surface is constant (See Section 8.3).

Increasing or decreasing the original slope modifies the factor of safety value. As shown in Fig. 8.5 E for Mam Tor increasing the slope by 5° causes a decrease in safety factor of up to 8.5% while decreasing the slope by the same amount increases the safety factor of up to 6.5%. Kinder Scout, Bretton Clough and Burr Tor have comparable geometry to this landslip and so the changes

will be of a similar magnitude. On the other hand, Cowms Moor, Rowlee Pasture (Section B-B') and Alport Castles are similar in terms of their geometry to the Rushup Edge landslip. Hence from Fig. 8.6A the change in factor of safety for these slips will be decrease about 3% or increase 7% for 5° change in slope. In the case of the Rowlee Pasture (Section A-A') and Cold Side landslips the changes are a decrease of 0.5% or an increase of 1.5% for the same geometrical change (See Fig. 8.7 A). Changes in safety factor due to the elevation of the water table depend on the geometry of the landslip but typically a 5m. increase or decrease alters the safety factor by up to 7%

All the landslips except for Mam Tor and part of Rowlee Pasture appear from field observations to have reached a stable or near stable condition. In the case of Mam Tor it is possible to compare the laboratory ring shear ϕ_{rr}' with the shear resistance mobilized on the post-initial failure slip surface owing to the greater certainty which exists regarding the location and depth of the slip surface. The depth of unweathered shale was measured in Borehole '1' and water table observations are available for both Borehole 1 and 2. However, as seen in Fig. 8.5 the post-initial failure analysis for the main unit gives a safety factor of 0.87. In fact as explained in Chapter 7 the survey at Mam Tor indicates that the movement is intermittent, so that it would appear to be stable during dry periods corresponding with a low water table. Rainfall data presented in Fig. 7.6 show that higher values in 1983 correspond with more rapid movements indicated in Tables 7.3 and 7.4. Section 7.2 discusses circumstantial correlation of instability with climate. In fact it would be necessary to lower the water table by about 10m. in order to achieve a stable condition. Reducing its height by 3m. giving a safety factor of 0.90 which is still rather low, but since from Fig. 8.4 A seasonal fluctuation of only 0.8m has been measured it would appear that the laboratory ϕ_{rr}' value under

estimates the field residual shear strength by about 1° . Increasing ϕ_{rr}' by 1° would produce a safety factor of 0.98, which seems reasonable in view of the observed stability condition. A similar argument may be applied in respect of the toe of the Mam Tor landslip. As shown in Fig. 8.4 B the maximum seasonal fluctuation in the height of water table is about 0.5m. Since the difference between the predicted factor of safety of 0.90 and unity corresponds to a lowering of the water table of one metre, it appears that, the mobilized residual shear strength is underestimated by about 1° in the ring shear tests on tumbled samples.

At Rushup Edge the landslip has a factor of safety approaching unity however, increasing ϕ_{rr}' of the shale by 1° would appear to simulate more closely the field condition since no evidence for activity was noted (Chapter 7).

Similar effects were also noted in case of Cold Side, Back Tor and Burr Tor landslips where the analyses show that the increasing of residual shear strength of shale by 1° raises the safety factor to a little more than unity which again corresponds with the apparently stable condition recorded in Chapter 7.

Apart from main unit Section $\beta-\beta'$ of Alport Castles and the toe of Rowlee Pasture, the landslips would appear from field observations to be stable. So for Mam Tor, Rushup Edge, Cold Side, Back Tor, Burr Tor and Kinder Scout toe, it would be necessary for the mobilized shear strength to be of at least one degree higher than that obtained in the laboratory test (Ring shear, tumbled samples). Instability of the toe of Rowlee Pasture landslip would still occur even if the residual shear strength was raised by this amount.

In case of Bretton Clough landslip, using the ϕ_{rr}' of shale obtained by the ring shear apparatus gives a high safety factor which appears to agree with the stable condition of the landslip. This high factor of safety is attributed to restraint due to the accumulation of landslip debris in the valley.

The analysis of the upper Cowms Moor landslip is inconclusive since although a stable condition may be predicted by assuming that the mobilized residual shear strength is one degree higher than the laboratory value, due to the sensitivity of this analysis to the proportion of sandstone and shale, increasing the shear strength of the sandstone by 2° would have a similar effect. In the case of the lower Cowms Moor and the main unit of Kinder Scout landslips the laboratory values may be approximately equal to that mobilized on the slip surface.

As shown in Table 5.11 the difference between the standard crushed-remoulded and tumbled-remoulded ring shear, ϕ_{rr} , ranges between 1.5 - 6.5°. Since a one degree change in residual shear strength causes an increase in factor of safety by up to 12.5% (See Table 8.6), use of the value of ϕ_{rr} for the standard crushed-tumbled sample would appear to overestimate the factor of safety by a considerable amount. The cohesion intercept has only a small effect on the factor of safety but, as shown in Table 5.11, the crushed-remoulded sample gives a higher cohesion intercept which would enhance the calculated factor of safety further. Since shear box residual strengths are more than ring shear ones it would appear that a considerable over-estimate of the factor of safety would have occurred had standard shear box test results been used in the analysis.

The magnitude of the inaccuracies in the boundary condition assumptions discussed in Section 8.7 indicates that in a typical analysis the value of factor of safety is most sensitive to the value of residual shear strength of the shale. Table 8.6 shows the percentage change in safety factor of each slip due to the changes in this parameter and also the shear strength of sandstone. The variation in these percentages depends on the length of the slip surface assumed to cut the shale and the sandstone beds and also on the area of sandstone and shale affected by the movement. Thus a change in ϕ_{rr} of only 1° will increase or decrease the factor of safety by up

Table 8.6 The effect of water table, the shear strength of shale and sandstone used in the stability analysis.

LANDSLIP	D/L ratio	FACTOR OF SAFETY			
		water table +5m % for first time slide	shale +1° % ϕ_{rr}'	sandstone	
				+2 °% ϕ_r'	+2 °% ϕ'
Mam Tor	0.10	4.0	12.5	-	1.0
Rushup Edge	0.11	3.0	9.0	3.0	4.0
Cold Side	0.08	2.0	8.0	3.0	5.0
Back Tor	0.12	1.0	7.0	4.0	5.0
Burr Tor	0.09	3.0	9.0	-	2.0
Bretton Clough					
A - A'	0.09	5.0	8.0	0.05	2.0
B - B'	0.10	6.0	10.0	-	<0.5
Alport Castles					
B - B' first slip	0.17	3.0	5.0	5.0	5.0
A - A' second slip	0.16	2.0	8.0	3.0	2.0
A - A'	0.16	3.0	8.0	3.5	4.0
Rowlee Pasture					
A - A'	0.13	2.0	6.0	4.0	4.0
B - B'	0.12	3.0	6.0	5.0	3.0
Cowms Moor					
A - A' upper slip	0.11	7.0	3.5	6.5	4.0
lower slip	0.10	4.0	7.5	4.0	2.0
B - B' upper slip	0.15	4.5	5.5	5.0	4.5
lower slip	0.13	5.5	5.5	4.0	3.0
Kinder Scout					
A - A'	0.15	6.5	8.0	-	-
B - B'	0.16	6.0	8.0	-	-

to 12.5% compared with up to 6.5% due changes in the shear strength of sandstone of 2°.

8.9 Conclusion

It is difficult to determine the amount of error which may arise in any particular parameter which forms part of the calculations. However changes in the parameters other than residual shear strength of the shale are large in comparison with the apparent uncertainty in these values. On the other hand, a 1° change in ϕ_{rr} which produces a large change in the factor of safety determined, is a small change in comparison with the value of other parameters such as water table. Hence it would appear that the factor of safety obtained in the calculation is most sensitive to the residual shear strength value adopted and less sensitive to the other boundary conditions. It then follows that in view of the relatively large changes in factor of safety required to bring the field observations into agreement with the stability predictions, the mobilized field shear strength may be at least one degree higher than the value obtained by ring shear tests on thoroughly disaggregated material.

It would appear that the effects of over consolidation and cementation (See Section 5.5.5) are not completely removed in the case of crushed-remoulded samples since the samples are not disaggregated during preparation. A high percentage of clay grain aggregates remain intact even when sheared to residual. Either these are not broken down during testing, or they are lost from the shear plane before full disaggregation occurs. The remoulded tumbled sample overcomes this difficulty since most of the grains are disaggregated during preparation. It may also be concluded that incomplete disaggregation occurs on actual shear planes although irregularity of the slip surface may also be responsible for this effect.

An additional important conclusion which may be drawn from these results relates to the use of a remoulded

peak value of shear strength for the analysis of first-time sliding. It is argued (See Section 8.2) that first-time sliding depends on the establishment of a continuous shear surface on which the critical strength is mobilized. Furthermore the remoulded peak strength is little lower than this parameter. The fact that in the analyses for first-time sliding, the most critical slip surfaces yielded factors of safety in the range 0.91 to 1.02 (See Fig. 8.5 to 8.14) suggests that the remoulded peak value is near to the mobilized strength of material since it is not expected that the slopes would have existed in a condition in which the factor of safety was much less than unity. It should be borne in mind that, as was the case with residual strength, the value used was determined by ring shear tests on thoroughly disaggregated material, Standard shear box tests yielded higher values than these.

CHAPTER 9

CONCLUSION

9.1 General Conclusions

This chapter includes the general conclusions for this study. In reading these, reference should be made to the concluding remarks written at the ends of individual relevant chapters.

The stability of the landslips studied in North Derbyshire have been studied in the context of the interaction of geometry of the slopes, shear strength of relevant rocks and the hydrological conditions. Hence factors of safety against failure for the landslips have been found by the limit equilibrium method from comparisons of factor of safeties for individual landslips, it is possible to deduce values of residual shear strength mobilized on the shear surfaces. These field, residual shear strength are compared with laboratory ones. In addition by plotting the average shear strength stress against the effective normal stresses in Fig. 9.1 for each landslip the overall average residual shear strength is equal to $c' = 0$ $\phi_r = 11.2^\circ$. Mention is made later of the testing conditions but briefly the remoulded residual ring shear strength of thoroughly disaggregated shale would appear to be about 1° less than that mobilized in the field.

Of the ten landslips studied, present day instability appears to be confined to the one at Mam Tor where the movements have been monitored. Part of the toe at Rowlee Pasture landslip also displays instability and slight instability related to river erosion affects the toes of the Bretton Clough, Alport Castles and Cowms Moor landslips but it would appear that these slips have achieved stability so far as mass movement is concerned.

The movement of the Mam Tor landslip has been shown to be intermittent. It is probably controlled by changes of groundwater level in response to seasonal variation in the amount of rain fall.

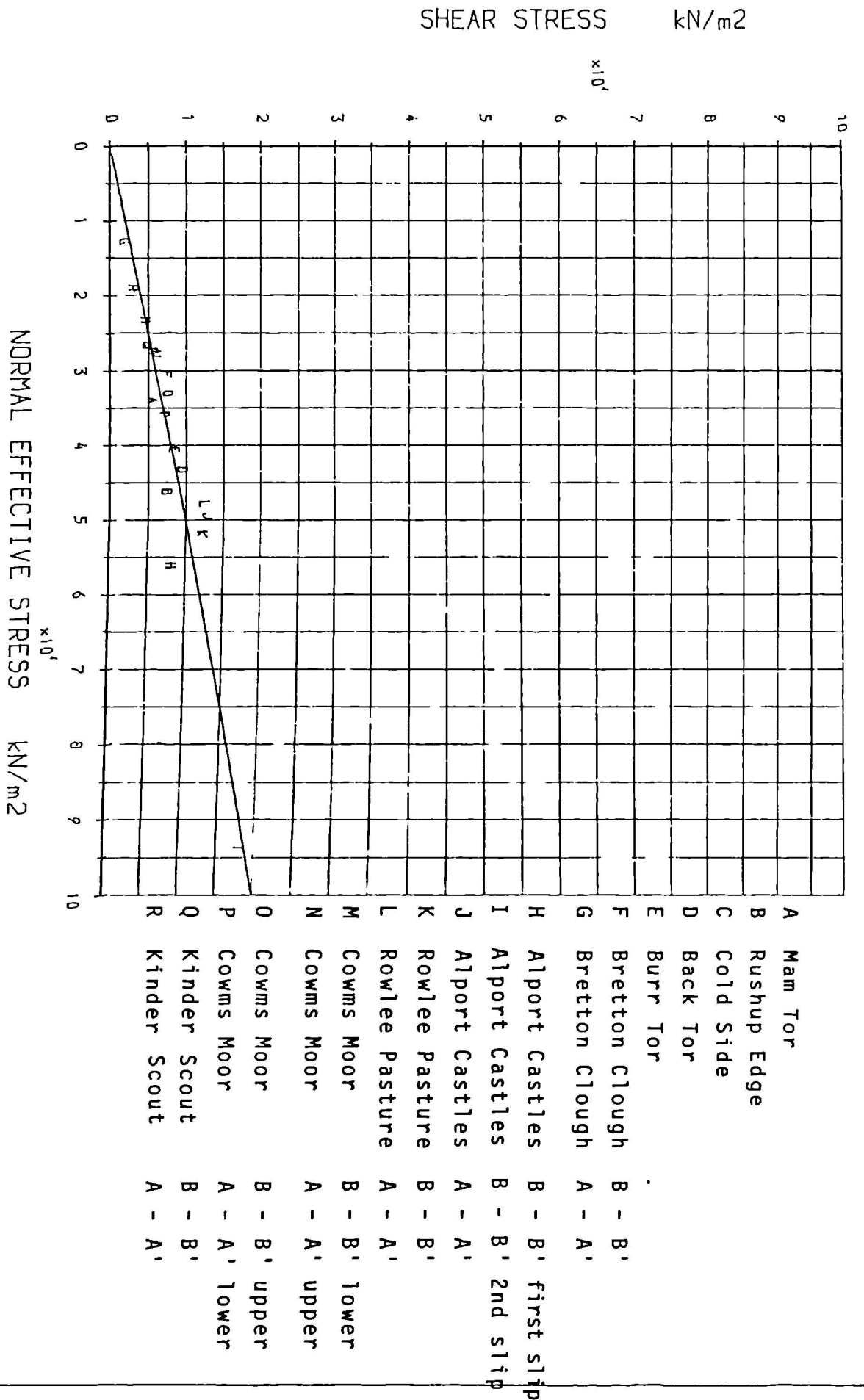


Fig. 9.1 Field residual shear strength

Following a consideration of a number of classification systems for land instability in Chapter 6 it was concluded that the one proposed by Skempton and Hutchinson (1969) is the most useful one to use for this study. Although mixing mechanism and material, it is simple to use and relates to appropriate methods of analysis. In terms of this classification, most of the landslips studied are rotational non-circular types. Those at Mam Tor and Rushup edge show well developed toes which form translational slides of landslip debris. The inhomogeneity of the underlying bedrock material would appear to be the main reason for the non-circular nature of the slip surfaces. Besides changes of lithology due to the presence of sandstone or ironstone beds, bedding in the shale and weathering may also have contributed to this inhomogeneity.

Although simplifying assumptions are necessary a limit equilibrium method of slices has been used in this study. This method can be adapted for any shape of slip surface and it is easy to change the boundary conditions to carry out parametric studies where many of the conclusions are based on comparisons. It has been necessary either to determine or assume values of various parameters. Some of the boundary conditions have been established by geomorphological mapping and laboratory shear strength determinations have also been used. The stability of the slopes has been analysed in respect of both first time failure and subsequent instability. It is argued in Chapter 5 that the appropriate shear strength parameters are respectively the remoulded peak and remoulded residual values.

The value of factor of safety is shown to be very sensitive to shear strength value and furthermore the value for shale has much greater influence than that of the sandstone. The actual amount depends on the situation but an increase of up to 12.5% in safety factor corresponds with a one degree increase in ϕ_{rr}' of shale, while for sandstone the figure is up to 6.5% for a ϕ_{rr}' increase of 2°. The position of the water table has also

been investigated for each landslip. The actual effect depends on the geometry of the slip, but since a change of 5 m. in water table height is necessary to bring about a change up to 7% in the value of factor of safety it would appear that the comments made with regard to the mobilized shear strength are valid.

A very important aspect of this study has comprised applying techniques of geomorphological mapping and measurement of actual movement to the investigation of stability. These have been used to indicate the stability condition of slopes and also to establish the geometry of failures. Clearly inaccuracies may occur in the assessment of the geometry but these can be considered in terms of their effect on the factor of safety.

As would be anticipated, increases of the steepness of the original slope decreases the safety factor. In fact the change is not linear so that reducing steepness has smaller relative effect. Again a comparatively large change of 5° in original slope angle is required to decrease the safety factor by up to 8.5% increase by as much as 5.5%.

As mentioned earlier various testing techniques were used to determine the residual shear strength. Clearly, besides testing a number of different samples, since in landslip studies rarely it is possible to test undisturbed shear plane material, methods of testing and sample preparation have been investigated. Basically these comprise ring shear and shear box tests on material disaggregated either by tumbling in water or crushing. The effect of sample grain size has also been studied by sieving the material.

The tests indicate that the ring shear value of remoulded residual shear strength (ϕ_{rr}) is on average about 2° lower than the corresponding shear box value. These differences have been subjected to a statistical analysis which indicates that the variation in the residual shear strength is probably engendered by the test method. Hence it is a function of the equipment

rather than the samples. In fact this analysis casts doubt on the *accuracy* of the shear box test.

The degree of roughness of the slip surface may have an important effect on the comparison since it is more likely to be more significant in case of the shear box tests.

It could be argued that in well disaggregated material a flatter surface is produced in the ring shear where the shear relief is severely restrained compared with the natural situation. It is envisaged that natural rock mass inhomogenieties and existing discontinuities would be significant in the latter case.

Tumbled remoulded ring shear samples always produce a lower residual shear strength than crushed remoulded material. The difference in ϕ'_{rr} angle ranges between 1.5-6.5°, and the remoulded crushed samples show a higher cohesion intercept. The effect of over-consolidation and cementation appear not to be completely removed in case of crushed remoulded sample, where the samples are not disaggregated during preparation. It also appears that the clay grain aggregates remain intact even when sheared. Since from the previous discussion regarding observed stability condition it was concluded that the mobilized residual shear on the slip surfaces is about 1° higher than the ring shear tumbled value, clearly crushed samples yield rather high results. It is implied from this that incomplete breakdown of aggregates occurs due to both natural and test shearing

A further conclusion which arises from the study is that the remoulded peak value of shear strength is quite near to the mobilized shear strength for first time failure. In the analyses to determine the most critical slip surface for the first time sliding, a factors of safety not much less than unity were obtained.

During the study, the opportunity has been taken to investigate other causes of variation in the residual shear strength value. Thus, changes in the normal effective stress (σ'_n) produce effects compatible with

those found by other authors in that ϕ_{rr}' decreases with increasing σ_n' value. The stress envelope has been found to be linear with a positive cohesion intercept value over the σ_n' range used even for a stress value as low as 24.5 KN/m².

Providing the condition for full drainage is not violated the rate of displacement appears to have very little effect on residual shear strength over several orders of magnitude. Apart from the observation that the first normal stress value produces an anomalously high shear stress value, apparently the loading sequence has no effect on the residual shear strength result.

A good correlation exists between ϕ_{rr}' and the moisture content at the end of a test. Also as would be expected ϕ_{rr}' increases with decreased clay fraction, increased amount of quartz, decreased proportion of mixed layer clay and decreased liquid limit and plasticity index. The value of c_{rr}' decreases with increasing clay fraction and clay quartz ratio or *decreasing* quartz content and proportion of silt size clay aggregates. No correlation could be found to exist between c_{rr}' and the liquid limit, plasticity index or amount of organic carbon present.

Finally, it should be noted that the residual shear strength of remoulded tumbled samples obtained by ring shear tests are lower than those obtained from other methods of preparation and testing. Stability calculations suggest that this value is a little lower than the mobilized strength in the field. Hence in calculating the stability of existing failures a factor of safety a little on the "safe" side would be produced. However, calculations based on shear box data for samples prepared in the normal way would yield erroneously high factors of safety.

9.2 Suggested Further Research

An insufficiency of time has prevented further work

from being carried out in connection with this research. Clearly the practicality of field based studies in which the weather exerts significant control must also be considered. It has been necessary to make various assumptions which could form the basis of more research, and some important gaps in (published) knowledge have been revealed.

The analysis of the stability of various landslips has included the use of a number of unknown factors some of which have been determined by detailed geomorphological mapping. However, a more rigorous comparison between back analysed shear strength and laboratory determined values would be possible if some of the boundary conditions were known with more precision. Furthermore, it would be possible to prove the geomorphological conclusions. As mentioned in Chapter 6, standard methods of locating slip surface include trial pitting, the drilling of holes and the installation of slip detectors. Geophysical methods may possibly also be applied since a density contrast would probably exist between landslip debris and underlying bedrock. Obviously, more information regarding piezometric pressures would be of great value. It would be necessary to fully instrument each slope with (preferably) hydraulic piezometers. Again geophysical methods may also prove useful. Of particular interest would be the response of pore water pressures to rainfall and individual rainfall events. Hence continuous measurements of rainfall, run-off and infiltration would be required.

Variation in shear strength value have been discussed and the effects of preparation and testing method investigated. Clearly with regard to the measurement of residual shear strength of indurated shales, much depends on the methods adopted. A clearer understanding of the mechanism of breakdown of mudrocks on shear surfaces would be of immense value. It is therefore suggested that investigations involving the effect of method of breakdown such as freeze and thaw, wetting and drying, chemical weathering and breakdown by grinding should be undertaken. Similar work on younger, less indurated mudrocks with

both similar and contrasting composition would probably lead to a clearer understanding of mudrock behaviour.

APPENDIX A

A.1 Calibration of Proving Rings

The proving rings for the ring shear and shear box apparatus were calibrated by - Wykeham Farrance Engineering Limited - Table A.1 shows the calibration factors derived from Figures A.1, A.2 for these rings.

Table A.1 Calibration factors for proving rings used in the ring shear and shear box apparatus.

Apparatus	Ring Shear		Shear Box	
	Proving ring number	9379 A	9379 B	9808
Date of calibration	17-10-1979		Tension	Compression
Calibration certificate number	25860		14162	
Calibration (div= 0.002mm)	0.195 N/div	0.196 N/div	3.567x10 ⁻³ KN/div	3.367x10 ⁻³ KN/div

A.2 Calculation of Shear Stress

i. Ring shear apparatus

The average shearing stress (τ) mobilized on the annular shear surface is calculated on the assumption that the normal effective stress and the shearing stress are uniformly distributed across the width of the failure surface in the horizontal plane. Following Bromhead (1979), a uniform stress distribution yields.

$$\text{Shear stress } \tau = \frac{3(F_1+F_2)L}{4\pi (R_2^3-R_1^3)} \dots\dots\dots(A.1)$$

where R_1 and R_2 are respectively the inner and outer sample radii (35mm and 50mm)

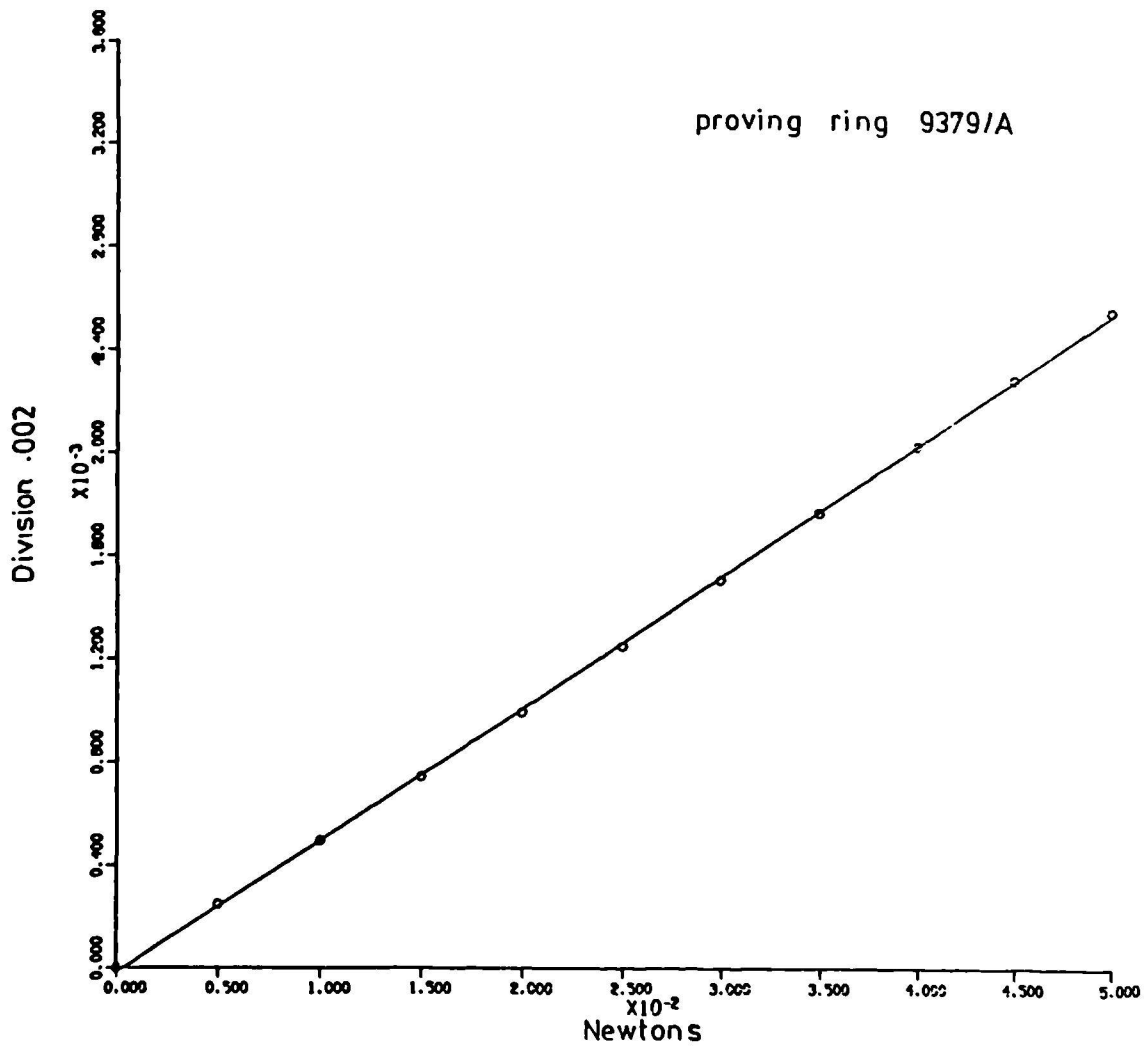
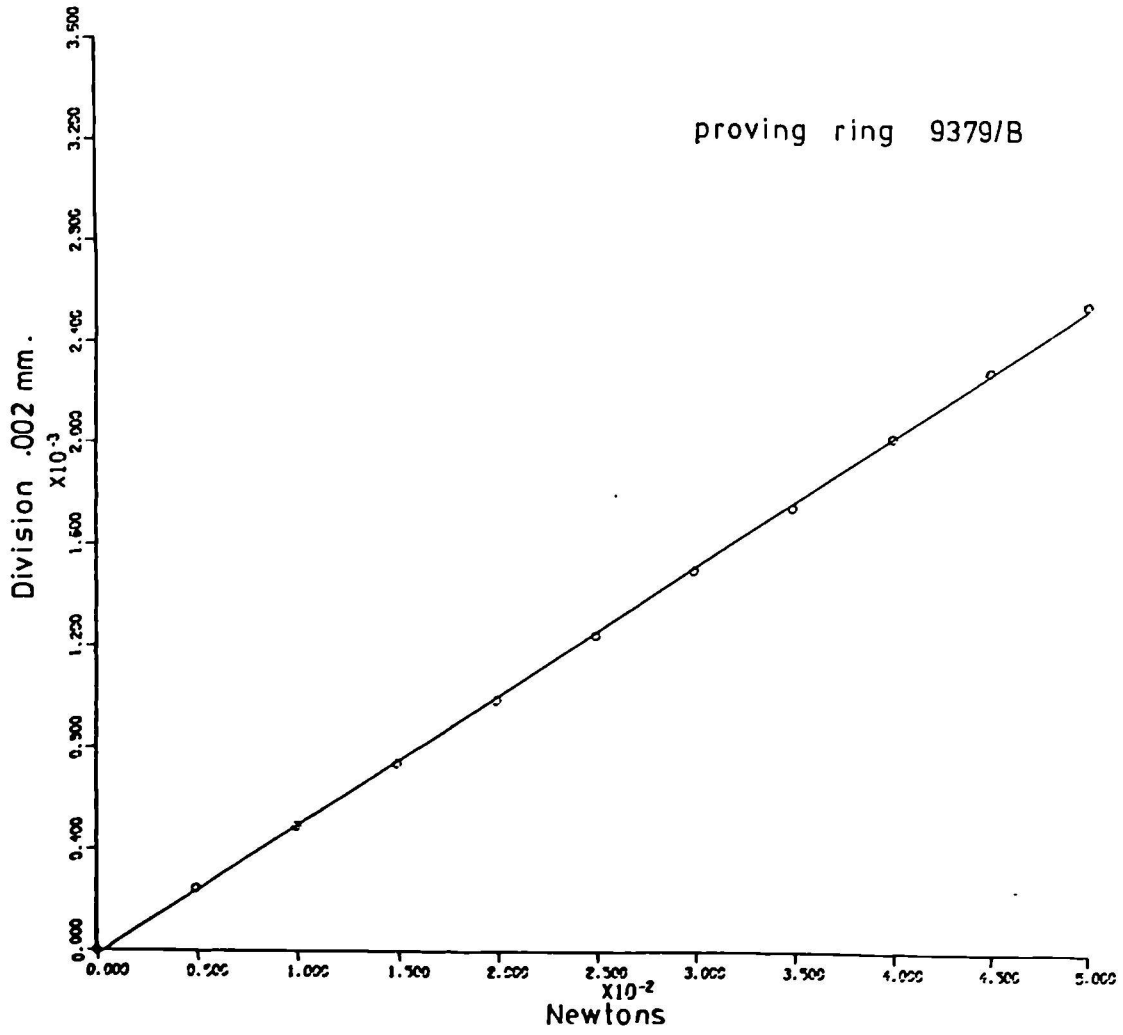


Fig. A.1 Calibration curve of proving rings for ring shear apparatus.

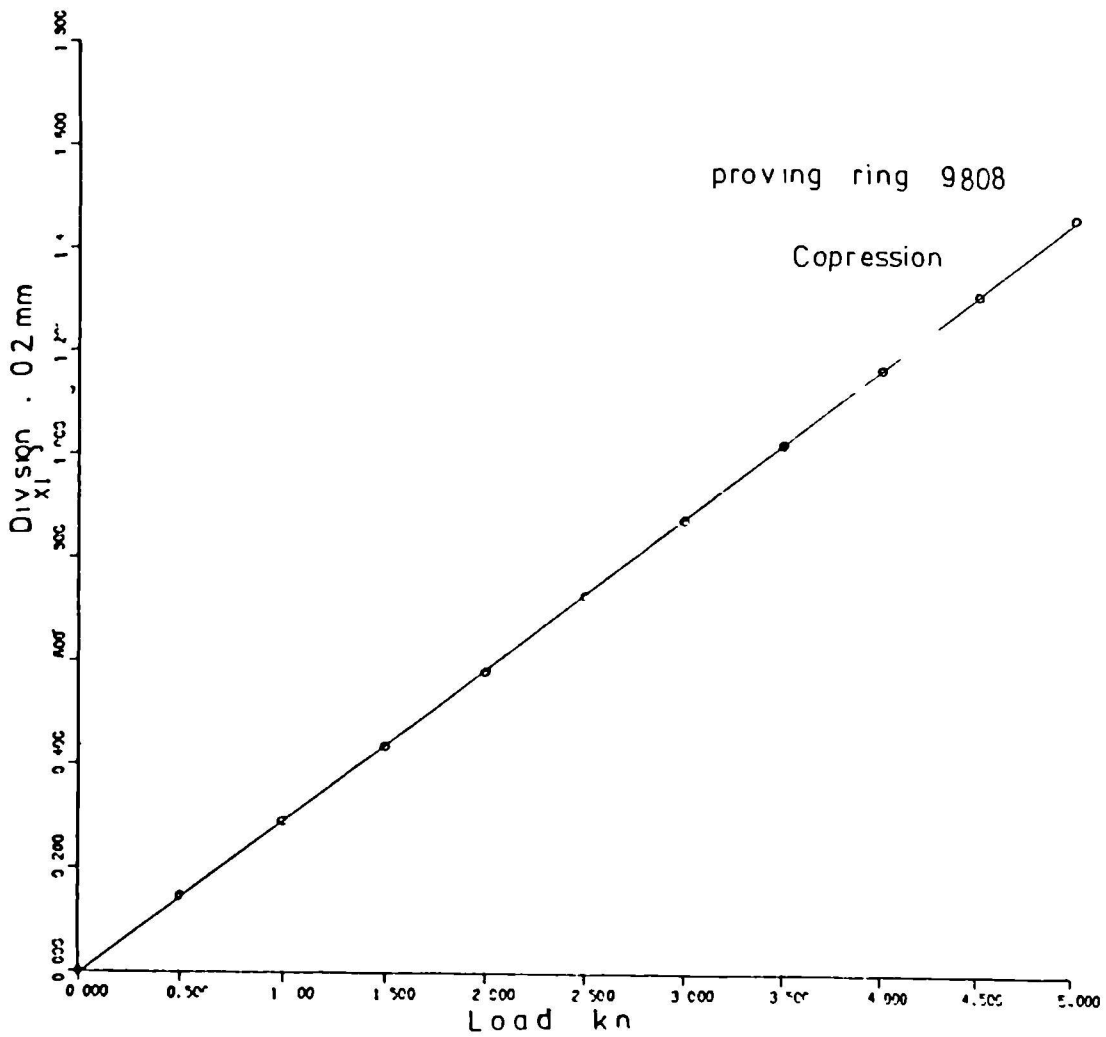
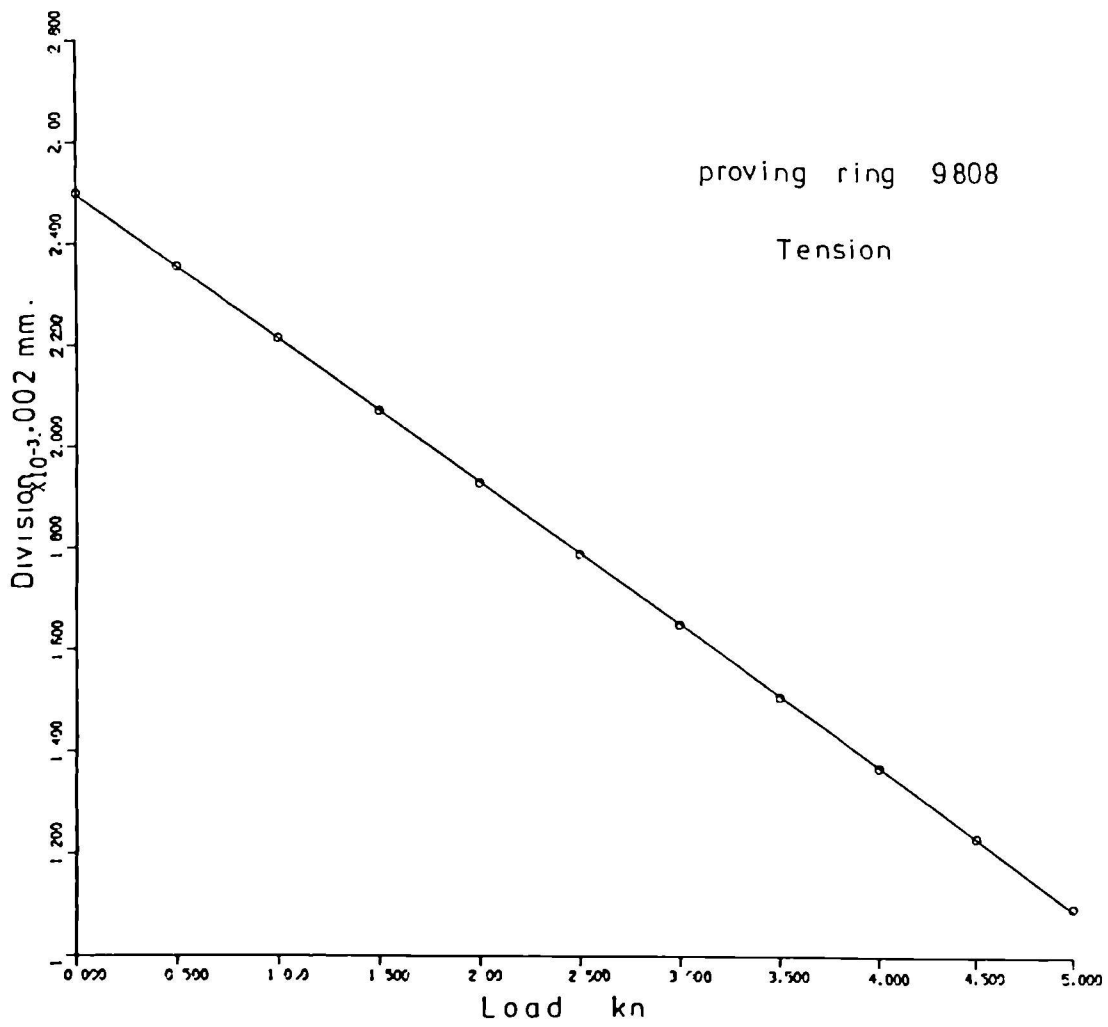


Fig. A.2 Calibration curve of proving ring for shear box apparatus.

F_1 and F_2 are the forces applied by the proving ring
L is the distance between the two proving ring
 $F = PRC (S_1 - S_0)$

where

PRC = proving ring constant

S_0 = original proving ring gauge reading

S_1 = gauge reading

The normal effective stress is given by

$$\sigma_n = \frac{P}{\pi(R_2^3 - R_1^3)} \dots\dots\dots(A.2)$$

where p is the total vertical load.

The annular displacement in degree is converted to an average linear displacement in mm. by multiplying by 0.742.

ii. Shear box

The shear stress mobilized on the shear surface is given by:

$$\tau = \frac{PRC \times (S_1 - S_0)}{\text{Area} - (D_1 - D_0) \times 0.002 \times L} \dots\dots\dots(A.3)$$

where

PRC = proving ring constant

S_1 = proving ring dial gauge reading

S_0 = initial proving ring dial gauge reading

Area= initial area

D_1 = shear displacement dial gauge reading

D_0 = initial displacement dial gauge reading

L = length of side of box

The shear strain is given by

$$\frac{(D_1 - D_0) 0.002}{L}$$

A.3 Calculation of Shearing Rate

In case of a drained testing, complete dissipation of pore water during shear is necessary. In practice it is assumed that 95% drainage is achieved by allowing a long enough time to failure. The coefficient of consolidation value c_v (See Bishop and Henkel 1957) at t_{100} is found from the straight line portion of a plot of height change of specimen against the square root of time for consolidation. The value of c_v is calculated from the expression

$$c_v = \frac{\pi}{4} \cdot \frac{H^2}{t_{100}} \dots\dots\dots(A.4)$$

where H is the half specimen thickness

The time to failure for 95% dissipation of pore water pressure is

$$t_f = \frac{10H^2}{c_v} \dots\dots\dots(A.5)$$

To calculate the shearing rate, a strain to failure must be assumed and this is judged by experience.

$$\text{The rate of strain} = \frac{\sum fd}{\sum t_f} \dots\dots\dots(A.6)$$

where $\sum fd$ = strain at failure under fully drained conditions (taken as 5mm in these tests).

The calculation yielded values of 0.120 deg/min. for the ring shear test and 0.036 mm/min. for the shear box.

A.4 Calculation of the Load Used in Apparatus

In order to find the appropriate normal effective stress to be used in the laboratory the following assumptions were made.

The depth of the shear surface in field, d 20m

The height of watertable, hw, 14m.

The density of the shale, $\rho_s = 2.3 \text{ Mg/m}^3$

The density of water, $\rho_w = 1 \text{ Mg/m}^3$

$$\begin{aligned} \sigma_n' &= (\rho_s \times d) - (\rho_w \times hw) \dots\dots\dots(A.7) \\ &= (2.3 \times 20) - (1 \times 14) \text{ Mg/m}^2 \end{aligned}$$

So $\sigma_n' = 313.92 \text{ KN/m}^2$

The load applied to sample.

$$\text{Load (kg)} = \frac{\sigma_n' \times \text{surface area}}{9.81} \dots\dots\dots(A.8)$$

i. Ring shear

The surface area is equal to $40.05 \times 10^{-4} \text{ m}^2$

the load used = 128.16 kg.

$$= 130 \text{ kgm}$$

for a ratio 10:1 lever loading system

The load used is 13kg.

ii. Shear box

Surface are = $36 \times 10^{-4} \text{ m}^2$

The load is = 11.5 kg.

APPENDIX B

COMPUTER PROGRAM FOR CALCULATING AND
PLOTTING RING SHEAR TEST RESULTS

The calculation and plotting of the ring shear test results were processed by 1906 computer.

The program calculates the shear stress, linear displacement and shear stress to normal effective stress ratio and plots graphs of shear displacement versus shear stress and change in vertical thickness. The program also tabulates these data. Fig. B1 is a listing of the program.

Fig. B.1 Computer program for calculating and plotting ring shear test results.

```

LIBRARY(GHOST)
LIBRARY(GHOST)
PROGRAM(AECD)
INPUT 1=CRO
OUTPUT 2=LPO
TRACE 2
END

MASTER THANDON
CALL GPINFO('PEN NUMBER 7L-3 IN HOLDER NUMBER 2;BLACK INK',44)
DIMENSION IDATE(100,10),TIME(100,10),VDIAL(100,10),TOOS(100,10)
1,STRA(100,10),STRB(100,10),ROTAT(100,10),TOO(100,10),ROTATL(100
1,10),N(10),S(10),ROST(10)
READ(1,100)NUMB
100 FORMAT(I3)
READ(1,85)(S(I),N(I),I=1,10)
85 FORMAT(5(F0.0,I0))
DO 5 J=1,NUMB
READ(1,83)ROST(J)
83 FORMAT(F0.0)
NREAD=N(J)

READ(1,101)(IDATE(I,J),TIME(I,J),VDIAL(I,J),STRA(I,J),STRB(I,J),
1ROTAT(I,J),I=1,NREAD)
101 FORMAT(I0,5F0.0)
5 CONTINUE
DO 10 J=1,NUMB
NREAD=N(J)
WRITE(2,84)ROST(J)

84 FORMAT(20X,'RATE OF STRANS',F7.3,/)
WRITE(2,80)N(J),S(J)
80 FORMAT(/,' NO OF READINGS',20X,'SIGMA',/,3X,I3,29X,F6.2,/)
WRITE(2,81)
81 FORMAT(6X,'DATE',13X,'TIME',12X,'V.DIAL',12X,
*'STR.A',13X,'STR.B',13X,'ROTATION',/)
DO 10 I=1,NREAD
WRITE(2,99) IDATE(I,J),TIME(I,J),VDIAL(I,J),
*'STRA(I,J),STRB(I,J),ROTAT(I,J)
99 FORMAT(5X,I6,5(10X,F7.2),/)
10 CONTINUE
WRITE(2,98)
98 FORMAT(5(/))
DO 1 J=1,NUMB
STRA1=STRA(1,J)
STRB1=STRB(1,J)
ROT=ROTAT(1,J)
NREAD=N(J)
DO 1 I=1,NREAD
VDIAL(I,J)=VDIAL(I,J)*0.002
STRA(I,J)=(STRA(I,J)-STRA1)*0.195
STRB(I,J)=(STRB(I,J)-STRB1)*0.196
ROTAT(I,J)=(ROTAT(I,J)-ROT)*0.742
TOO(I,J)=(STRA(I,J)+STRB(I,J))*0.436
ROTATL(I,J)=ALOG10(ROTAT(I,J)+0.00001)
TOOS(I,J)=TOO(I,J)/S(J)
1 CONTINUE
DO 86 J=1,NUMB

```

```

NREAD=N(J)
WRITE(2,82)
82 FORMAT(1X,'CHANGE IN THIC.',8X,'SHEAR ST.',
*3X,'SH. STR./N. STR.',6X,'DISPL.',8X,'LOG DISPL.',/)
WRITE(2,102)(VDIAL(I,J),T00(I,J),T00S(I,J),ROTAT(I,J),ROTATL(I,J),
1I=1,NREAD)

102 FORMAT(5X,F6.4,10X,F5.1,10X,F7.3,10X,F7.2,10X,F7.4,/)
WRITE(2,87)
87 FORMAT(//,50X,20('*'),//)
86 CONTINUE
CALL PAPER(1)
CALL PSPACE(0.2;0.7,0.5,0.8)

CALL CSPACE(0.0,1.0,0.0,1.0)
CALL CTRSET(1)
CALL CTRMAG(8)
CALL PLOTCS(0.4,0.45,'DISPLACEMENT MM',15)
CALL PLOTCS(0.4,0.05,'DISPLACEMENT MM',15)
CALL CTRORI(1.0)
CALL PLOTCS(0.15,0.15,'CHANGE IN THICKNESS',19)
CALL PLOTCS(0.15,0.6,'SHEAR STRESS KN/M2',18)
CALL CTRORI(0.0)
CALL MAP(0.0,170.0,0.0,150.0)
CALL SCALSI(20.0,20.0)
CALL BORDER
CALL PSPACE(0.2,0.7,0.1,0.4)
CALL BORDER
CALL MAP(0.0,170.0,0.0,3.5)
CALL SCALSI(20.0,0.2)
CALL CTRSET(4)
CALL CTRMAG(5)
DO 4 J=1,NUMB
CALL POSITN(0.0,0.0)
CALL PSPACE(0.2,0.7,0.5,0.8)
CALL MAP(0.0,170.0,0.0,150.0)
NREAD=N(J)
IF(J.EQ.1)I37=37

IF(J.EQ.2)I37=43
IF(J.EQ.3)I37=45
IF(J.EQ.4)I37=50
IF(J.EQ.5)I37=51
IF(J.EQ.6)I37=52
IF(J.EQ.7)I37=53
IF(J.EQ.8)I37=54
IF(J.EQ.9)I37=56
IF(J.EQ.10)I37=59
DO 2 I=1,NREAD

CALL JOIN(ROTAT(I,J),T00(I,J))
CALL TYPENC(I37)
CALL POSITN(ROTAT(I,J),T00(I,J))
2 CONTINUE
CALL PSPACE(0.2,0.7,0.1,0.4)
CALL MAP(0.0,170.0,0.0,3.5)
CALL POSITN(0.0,0.0)
DO 4 I=1,NREAD

CALL JOIN(ROTAT(I,J),VDIAL(I,J))
CALL TYPENC(I37)
CALL POSITN(ROTAT(I,J),VDIAL(I,J))
4 CONTINUE
CALL GREND
STOP
END

```

APPENDIX C

C.1 Introduction

The samples of shale were subjected to analysis by X-ray diffraction techniques. Using this method, the type of minerals present in samples can be established and it is also possible to estimate the relative abundances of certain minerals. The X-ray reflection takes place from lattice plane with indices (hkl) according to the Bragg Law.

$$n\lambda = 2d(hkl) \sin \theta \dots\dots\dots(C.1)$$

Where

$d(hkl)$ is the true lattice spacing for plane hkl.

λ = the wave length of the radiation

θ = the glancing angle of reflection

n = the order of reflection

The quantity which can be measured experimentally from X-ray is

$$d(hkl)/n = \lambda/2 \sin \theta$$

and this is ordinarily called the lattice spacing for nth order reflection and is the quantity given in any tabulation of spacing deduced from the data. With clay minerals the most useful atomic spacings are those perpendicular to the crystallographic c axis, that is the 001 atomic planes.

The criteria for the clay identification were obtained from Brown (1961). Carrol (1970) and Brindley and Brown (1980). Basal reflection from the common clay minerals produce the most intense diffraction peaks for 2 θ angles in the range 4° to about 30°. Unfortunately each peak is not at a distinct position on the trace since various peaks overlap with each other.

For example the (002) chlorite peak and 001 kaolinite peak both occur at about $2\theta = 12.4^\circ$ (7.1 \AA d - spacing). Other chlorite peak often occur at about $2\theta = 8.9^\circ$ (10 \AA) and $2\theta = 6.3^\circ$ (14 \AA).

A Phillips X-ray diffractometer was used with operating conditions as follows:

Tube type	Cu broad focus
	pw 2253/20
Voltage and current	35 kV, 40 mA
Filter	Ni
Goniometer	Vertical w/1050/70
X-ray Generator	pw 1130/90
Channel control	pw 1390
Range	1×10^4 c.p.s.
Time constant	1 second
Chart speed	2 cm. per min.

C.1.1 Mineral identification technique

The various techniques will be described under the following titles: whole rock mineral identification. Identification and semi-quantitative estimation of clay minerals.

i. Whole rock sample mineral identification

The smear technique of Gibbs (1965) was employed. For this about 10 gm of tumbled sample was left overnight in a loosely covered container to air dry. The sample was then ground to fine powder in an agate mortar, water was added and after further grinding the paste was transferred on to glass slide ensuring a uniform smear. This was dried by leaving it overnight and mounted in the goniometer. The identification of the minerals was carried out from the intensity 2θ scan using the data of Chao (1969).

ii. Identification and semi-quantitative estimation of clay minerals.

The best method of preparing clay mineral samples

for analysis is by X-ray diffraction is the subject of considerable debate in the literature. Most authors agree that the use of $< 2 \mu\text{m}$ (or smaller) size fraction gives the best result. The preparation method used was smear mounting on glass plate as described by Gibbs (1965). The separation of $< 2 \mu\text{m}$ clay fraction was carried out in an MSE centrifuge (Super Minor Centrifuge)

About 10 gm. of tumbled sample was air dried and ground in an agate mortar. The resulting powder was placed in a centrifuge tube with a 1.5 g/l concentration sodium hexametaphosphate (calgon) deflocculant solution. After a few minutes of mechanical shaking, it was centrifuged for about 15 minutes. The calgon was poured off the top of the sedimented material and the centrifuging repeated with new calgon. This operation was carried out 5 or 6 times until the clay fraction was completely deflocculated. The sample was then washed in distilled water 5 or 6 times in order to remove all traces of calgon. The suspend material was then separated in to its constituent grain size by using different settling velocities as quantified by Stoke's Law. Stoke's Law has been modified by Jackson (1973) to take into account the effect of centrifugation. As viscosity varies significantly with temperature, calibration curves of Fig. C.1 were used to give convenient spin time ranges for different particles sizes.

The $< 2 \mu\text{m}$ size fraction was separated from the suspension by centrifuge. The suspension was transferred to centrifuge tubes and the levels adjusted to balance the centrifuge. The temperature of the suspension was measured and the centrifuging time adjusted accordingly. The $< 2 \mu\text{m}$ fraction is removed by centrifuging at 1000 rpm at a given temperature (Fig. C.1). The suspension above the sediment which contains the $< 2 \mu\text{m}$ fraction was transferred to clear tubes, sedimented by centrifuging at 3000 rpm for about one hour. This fraction was placed

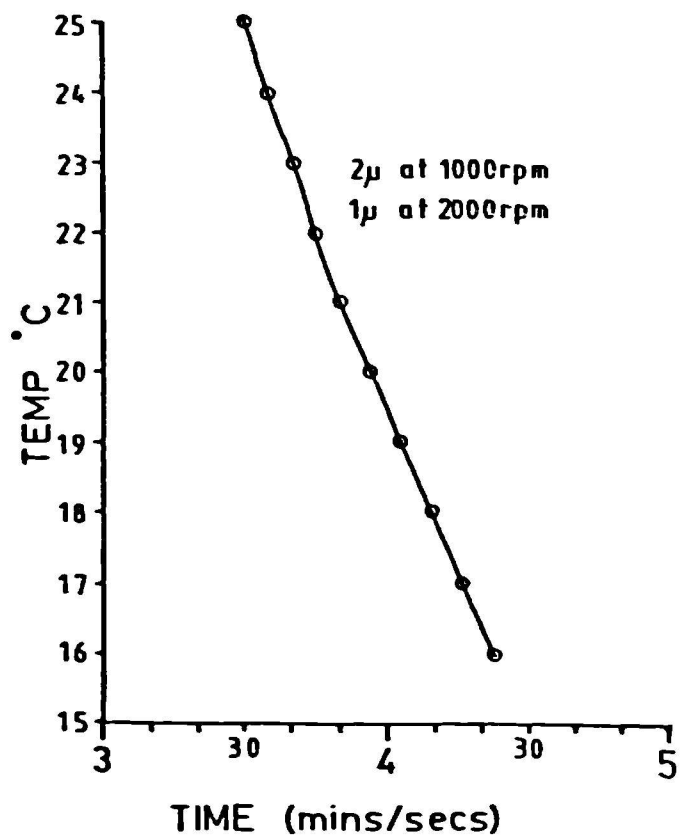


Fig. C.1 Centrifuging time for particle size separation at various temperatures.

on a clean glass and air dried slide as described by Gibbs (1965) for XRD smear mount.

Each sample was X-rayed as follows:

- a. Air-dried (as prepared)
- b. Treated with ethylene Glycol by placing the smear in a dessicator, containing ethylene glycol at 60° C for about 30 minutes.
- c. Heated at 300°C for one hour
- d. Heated at 550° C for one hour.

C.2 XRD Results

C.2.1 Whole rock samples

Fig. C.2 for sample CW1 is reproduced here as an example to demonstrate the interpretation of the data. The following discussion concerns the whole rock smear mount of all 13 samples analysed.

Quartz was found to be the dominant mineral present in all samples with the main quartz peak at 3.35 Å with smaller peaks at 4.21 Å, 2.46 Å and 2.29 Å .

Kaolinite and illite are perhaps the two most abundant minerals after quartz. The main peaks of these clay minerals occur about 7.15 Å (001) and 3.57° (002) for kaolinite and at 10 Å, 5 Å, 4.48 Å and 3.3 Å for illite. The 3.3 Å peak coincides with the main quartz peak in some traces and may produce a bump on the side of this peak.

Another clay mineral detected is chlorite with peaks at 14 Å and 4.7 Å. The expandable clay minerals from a particular borehole sample (MTBH) and elsewhere in the Mam Tor area (MT5 and MT6) show a broad peak at 11 Å which may be indicative of a relative abundance. Pyrite was detected in some samples (CW1, CW2 and CW3) by a very small peak at 2.7 Å. Pyrite was not detected in the XRD in MTBH sample even though it was observed to be present in the core. (See Section 3.2.2) It would appear that

it occurs in localized patches unless it is too poorly crystallized to be detected. Veer (1981) does not report pyrite in various boreholes samples although his samples were from shallower depths than those of the present work.

Trace amounts of gypsum at 8.26 \AA were detected in samples from Hope Valley Cement Works quarry (CW1, CW2, CW3), and trace amount of feldspar 3.17 \AA was present in all 13 samples tested.

C.2.2 < 2 μm clay fraction

The various clay mineral types were recognised from the traces as follows:

Kaolinite was defined by its characteristic well-defined basal reflection at 7.17 \AA (001), ($2\theta = 12.33$) and 3.57 \AA (002), ($2\theta = 24.9$). It is not affected by glycolation or heating to 300°C , while heating to 550°C removes the basal reflection as shown in Fig. C.3.

Illite was identified by its characteristic well defined basal reflection at $10\text{-}10.07 \text{ \AA}$ (001) ($2\theta = 8.8\text{-}8.7$) and 5 \AA (002), ($2\theta = 17.75$). The (003) illite reflection overlaps with 001 quartz peak and could not identified on the whole rock XRD diffractometer trace.

Mixed layer clay was characterised by a broad basal X-ray diffraction peak between 14 \AA and 10 \AA ($2\theta = 6.5$ and 8.8°), Nearness to 10 \AA indicate that illite is more abundant constituent of the mixed layering.

The illite peak and expandable clay reflections with basal d - spacings between 10 and 12 \AA (See Fig. C.3) were distinguished by glycolation and heating. When treated with ethylene glycol the d-spacing of the expandable clay increases to about $12 - 14 \text{ \AA}$. Heating the glycolated sample causes dehydration and collapse back to about 10 \AA . Therefore the difference in area between the glycolated 10 \AA peak and the one obtained after heating is usually taken as a quantitative measure of the proportion of expandable clay relative to illite.

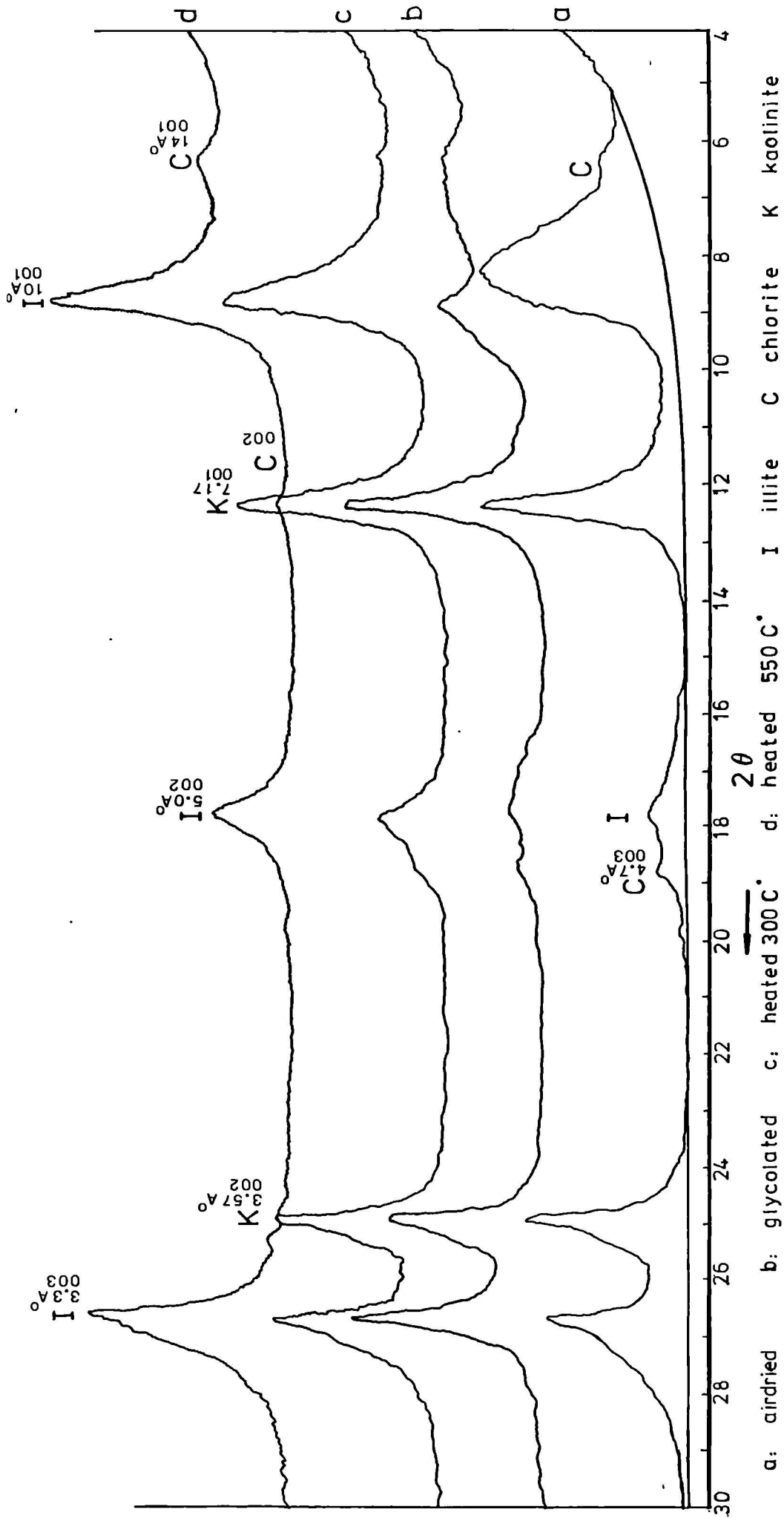


Fig. C.3 X-ray diffraction of orientated smear mounts of the $\leq 2 \mu\text{m}$ clay fraction after different treatments.

The 002 and 003 illite peaks remain when the heating is increased to 550°C.

Chlorite when present was identified by its basal reflection at 14 Å (001) ($2\theta = 6.3^\circ$), and 4.7 Å (003) ($2\theta = 18.8^\circ$). The 002 chlorite reflection is overlapped by the kaolinite (001) but the loss of kaolinite peak due to heating to 550°C with only a slight decrease in d - spacing for chlorite enables its presence to be detected.

C.3 Semi-quantitative Estimation of Clay Minerals

Estimating the amount of clay minerals, poses many problems since as explained by Brindley and Brown (1980) and Pierce and Siegal (1969), many factors including the variation in the degree of crystallinity of individual clays, the effects of various treatments, compositional variation within clay minerals orientation effects, preparation method and machine condition render estimation by XRD difficult. The presence of impurities such as iron oxide and organic matter also causes problems which usually results in the development of high background radiation levels on the diffractograms. In fact Brewster (1980) described how increases in background radiation may increase the likelihood of identifying the mineralogical composition of mixed-layer clay. It is also possible that the concentration and crystallinity of some expandable minerals increase and hence the reliability of the estimation is reduced. Cubitt (1975) demonstrated statistically that peak area measurements produce superior results compared with peak height measurements.

For distinguishing between samples in this study the peak area produced by smear mounts were determined. A constant base line to represent background was drawn as in trace Fig. C.3 using French curves. The area was then measured by planimeter. These area measurements require appropriate corrections which depends on the

various intensity factors for each clay mineral. In this study Schultz's (1960) method was adopted. Briefly, for this the proportion of kaolinite is measured by the area of 7.17 A° peak and for chlorite (when present) by the 14° peak on the air dried trace, the proportion of illite by the area of the 10 A° peak on the glycolated trace. The difference between the measurement of the 10 A° illite peak on the glycolated trace and the 300°C heated trace was taken to be the proportion of mixed-layer clay present.

Schultz (1960) found that poorly crystallised fire-clay type kaolinite gave 7 A° peak area about equal to the area of the 10 A° peak on an equal amount of illite or mixed layer clay, where as well crystallised kaolinite generally gave 7 A° peaks of twice of this area. Hence by calculating the degree of crystallinity, the amount of kaolinite may be determined. Schultz (1960) defined crystallinity of kaolinite as the ratio of 7 A° area to 7 A° height.

The degree of crystallinity found by Schultz (1960) for various type of kaolinite ranges between 1.1 - 2 where 1.1 - 1.3 would be well crystallised kaolinite, 1.3 - 1.7 intermediate, $\gt 1.7$ is poorly crystallised. The crystallinity values of the kaolinite present in the shales analysed vary between 1.00 and 1.39 as shown in Table C.1. Values between 1.0 and 1.1 are regarded as very well crystallised kaolinite and the correction factor of 0.5 was applied to the kaolinite peak areas. Intermediate crystallinity kaolinite had values between 1.1 - 1.2 and a correction factor of 0.75 was used. While the lower limit of poorly crystalline kaolinite taken to be 1.4 and a factor of 1.0 was applied. The relative abundances of clay minerals, corrected for kaolinite crystallinity value, for $\lt 2 \mu\text{m}$ clay fraction are shown in Table 5.4.

Sample	Schultz "kaolinite crystallinity"
MTBH	1.32
CW1	1.24
CW3	1.02
CW4	1.06
MT5	1.19
MT6	1.08
CM	1.12
BUT	1.21
AC	1.39
RP	1.24
CS	1.07
BCL	1.00
KS	1.31

Table (C.1) Schultz (1960) "Kaolinite crystallinity" for < 2 micron clay fraction.

APPENDIX D

STATISTICAL ANALYSIS

D.1 Introduction

A statistical analysis was carried out on the results of ring shear and shear box tests to determine whether differences between the results obtained for each apparatus are significant.

The analysis has been carried out for:

- i. Values of ϕ_{rr} obtained from the ring shear and shear box.
- ii. Values of c_{rr} obtained from the ring shear and shear box.
- iii. Results for the tumbled shear box samples for c_{rr} and ϕ_{rr} .
- iv. Results for the tumbling ring shear samples for ϕ_{rr} and c_{rr} .
 - a. Using all 13 samples
 - b. Using only 7 samples tested in both the shear box and ring shear apparatus.

D.1.1 Test procedure

A randomized block design was used to test the results of the ring shear and shear box. The experimental data (measurements made by the same operator) were arranged in blocks where with rows for different treatments. If an equal number of measurements were made for each treatment in each block and if the order of tests within a block is randomized, then the experiment is called a randomized block. The data are classified according to two characteristics in a two-way table, a procedure described by Chatfield (1970) as two-way analysis of variance. The proposed mathematical model is:

$$X_{ij} = \mu + bi + tj + \epsilon_{ij} \quad (i = 1 \text{ to } r, j = 1 \text{ to } c)$$

where

r = rows, c = columns

- X_{ij} = Observation on treatment j in block i
- μ = Over-all average of the response variable
- b_i = Effect of i th block
- t_j = Effect of j th treatment
- ϵ_{ij} = Random error.

Since μ is the over-all mean, the treatment and the block effects must be such that

$$\sum_{i=1}^r b_i = \sum_{j=1}^c t_j = 0$$

The best point that estimates of unknown parameter is

$$\hat{\mu} = \bar{x}$$

$$\hat{b}_i = \bar{x}_{i.} - \bar{x} \quad (i = 1 \text{ to } r)$$

$$\hat{t}_j = \bar{x}_{.j} - \bar{x} \quad (j = 1 \text{ to } c)$$

where, $\bar{x} = \frac{\text{the sum of all the data}}{\text{No. of data}}$

$\hat{\mu}$, \hat{b}_i , \hat{t}_j are the estimated value ie experimental value.

μ , b_i , t_j are the mathematical model ie real value.

The total corrected sum of squares given by

$\sum_{i,j} (X_{ij} - \bar{x})^2$ can be split in three component to become

$$\sum_{i,j} (X_{ij} - \bar{x})^2 = c \sum_{i=1}^r (x_{i.} - \bar{x})^2 + r \sum_{j=1}^c (x_{.j} - \bar{x})^2 +$$

$$\sum_{i,j} (x_{ij} - \bar{x}_{i.} - \bar{x}_{.j} + \bar{x})^2$$

The component on the right handside of this equation measures the block variation, the second component measures the treatment variation and the third component measures the residual variation.

The corresponding degrees of freedom are as follows:

	<u>d.F.</u>
Blocks (rows)	r-1
Treatment (columns)	c-1
Residual	(r-1) (c-1)
<hr/>	
Total	rc - 1

Each sum of squares is divided by the appropriate number of degrees of freedom to give the corresponding mean square. Neither the treatment mean square nor the residual mean square is affected by whether or not there is a significant variation between blocks. Thus, the ratio

$$F = \frac{\text{treatment mean square}}{\text{residual mean square}}$$

will follow an F - distribution with (c-1) and (r-1) (c-1) degrees of freedom if a null hypothesis is true. (This assumes that there is no bias estimate in work and $\epsilon_{ij} = 0$ can be found for all i and j). The observed F-ratio can then be compared with the chosen upper percentage point of this F-distribution by reference to a standard table.

To illustrate the main point of the analysis a step by step explanation of the calculation will be followed using ϕ_{rr} test results of the ring shear and shear box.

Table D.1 a Statistical analysis of residual shear strength values for ring shear and shear box.

Sample	Remoulded residual Shear strength, ϕ_{rr}		Sum (x.j) of sample
	Ring shear	Shear box	
MTBH	7.5	9	16.5
CM	8.5	9	17.5
RP	7.5	9	16.5
CW1	7.5	11.5	19.0
KS	13.0	12.5	25.5
MT5	6.5	8.5	15.0
AC	7.0	13.5	20.5
Sum for apparatus (Xi.)	57.5	73	130.5

The sum for sample (x.j) and the sum for apparatus (Xi) should be the same which in this example (Xij) = 130.5. Now the source of variation - should be calculated according to the table D.1b:

Table D.1 b Two-way ANOVA analysis

Source of Variation S.V.	Degree of Freedom d.f.	Sum of Squares S.S.	Mean sum of square S.S/d.f	F-ratio row & column mean square <u>Residual</u>
Between samples (rows)	$(r - 1) = 6$	$c \sum_{j=1}^r (\bar{X}_j - \bar{X})^2 = 37.179$	6.196	2.258
Between apparatus (columns)	$(c - 1) = 1$	$r \sum_{i=1}^c (X_{ij} - X)^2 = 17.161$	17.161	6.254
Residual	$(r-1)(c-1) = 6$	$\sum_{i,j} (X_{ij} - \bar{X}_{i.} - \bar{X}_{.j} + \bar{X})^2 = 16.464$	2.744	
Total	$(rc - 1) = 13$	$\sum_{i,j} (X_{i.j} - X)^2 = 70.804$		

The residual sum squares can be calculated from Residual s.s = Total s.s - (s.s. of rows + s.s of columns).

The mean sum of squares is calculated by dividing s.s/degrees of freedom, and the F-ratio is calculated by dividing the mean sum squares of rows and then columns by the residual. The results are shown in Table D.1 b.

The F-ratio results are compared with F-distribution tables of a certain significance level. It seems reasonable to choose a 5% level which allows an error of up to 5%. The calculated F-ratio for the samples (rows) = 2.238 was compared with the tabulated F - distribution = 4.28 at 5% level of significance under (6,6) d.f., while the F-ratio corresponding to the apparatus (columns) = 6.254 was compared with the tabulated F = 5.99 under (1,6) d.f. at 5% level.

These values can be compared with the F-ratios obtained in the tests. If the F-ratio obtained from the analysis is higher than that obtained from the table then the analysis shows the results are statistically significant at the chosen level, but lower values indicate non-significant results. So in the above example the analysis shows a non-significant difference between the samples (rows) such that tabulated $F_{0.05} (6,6) = 4.28$ while a significant difference appears for different apparatus (columns) with $F_{0.05} (1,6) = 5.99$.

The analysis of the other four tests are shown in Tables D.2, D.3, D.4. and D.5.

Test (1) ϕ_{rr}' results obtained from the ring shear and shear box. - as shown in the example Section D. 1.1 (Table D.1, a and b).

Test (2) c_{rr}' results obtained from ring shear and shear box.

Table D.2 a Statistical analysis of cohesion intercept values for ring shear and shear box.

Samples	Remoulded cohesion strength c_{rr}		Sum for sample
	Ring shear	Shear box	
MTBH	4.1	10.5	14.6
CM	6.8	17.8	24.6
RP	4.3	9.5	13.8
CW1	2.5	8.2	10.7
KS	4.9	27.0	31.9
MT5	4.9	14.5	19.4
AC	6.5	14.3	20.8
Sum from apparatus	34	101.8	135.8

Table D.2 b Two-way ANOVA analysis

S.V	d.F.	s.s	s.s./d.F	F-ratio mean sum of Sq/res.
Between samples (rows)	$(r-1) = 6$	157.67	26.278	1.529
Between App. (column)	$(c-1) = 1$	328.34	328.34	19.106
Residual	$(r-1)(c-1) = 6$	103.11	17.185	
Total	$(rc-1) 13$	598.12		

Using different apparatus ring shear and shear box, for c_{rr} results, the analysis shows that there are no significant differences between the samples (rows) such that tabulated $F_{0.05} (6,6) = 4.28$, while significant

differences appear when different apparatus (columns) are used where the tabulated $F_{0.05 (1,6)} = 5.99$.

Test 3 Shear box ϕ'_{rr} and c'_{rr} results.

Table D.3 a Statistical analysis of residual shear strength values for shear box.

Samples	Remoulded residual strength Parameters of shear box.		Sum for sample
	ϕ'_{rr}	c'_{rr}	
MTBH	9.0	10.5	19.5
CM	9.0	17.8	26.8
RP	9.0	9.5	18.5
CW1	11.5	8.2	19.7
KS	12.5	27.0	39.5
MT5	8.5	14.5	23.0
AC	13.5	14.3	27.8
Sum of ϕ'_{rr} & c'_{rr}	73.0	101.8	174.8

Table D.3 b Two-way ANOVA analysis

S.V.	d. F.	S. S.	S.S./d.f.	F. ratio
Between samples (rows)	6	162.92	27.15	1.48
Between ϕ'_{rr} & c'_{rr} (Columns)	1	59.24	59.24	3.34
Residual	6	109.66	18.27	
Total	13	331.82		

The results show no significant differences between samples such that tabulated $F_{0.05 (6,6)} = 4.28$ and also no significant differences between ϕ_{rr} and c_{rr} using the shear apparatus since tabulated $F_{0.05 (1,6)} = 5.99$.

Test 4. a 13 samples tested in the ring shear apparatus:

Table D.4 a Statistical analysis of residual shear strength values for ring shear.

Samples	Remoulded residual shear strength parameters for ring shear.		Sum for samples
	ϕ_{rr}	c_{rr}	
MTBH	7.5	4.1	11.6
CW1	7.5	2.5	10.0
CW2	10.5	2.4	12.9
CW3	12.5	3.8	16.3
MT5	6.5	4.9	11.4
MT6	8.0	3.8	11.8
CM	8.5	6.8	15.3
BUT	9.5	7.6	17.1
AC	7.0	6.5	13.5
RP	7.5	4.3	11.8
CS	8.5	3.1	11.6
BCL	12.0	8.9	20.9
KS	13.0	4.9	17.9
Sum of ϕ_{rr} & c_{rr}	118.5	63.6	182.1

Table D.4 b Two-way ANOVA analysis

S.V.	d.F.	S.S.	S.S./d.F.	F-ratio
Bet. samples (rows)	12	62.415	5.701	1.425
Bet. ϕ'_{rr} & c'_{rr} .(Columns)	1	115.923	115.923	31.768
Residual	12	43.793	3.649	
Total	25	222.13		

The results show no significant differences between samples such that tabulated. $F_{0.005 (12,12)} = 2.69$. However a very significant difference occurs between ϕ'_{rr} and c'_{rr} using the ring shear apparatus such that tabulated $F_{0.05 (1,12)} = 4.75$.

b: 7 samples tested in both the shear box and ring shear apparatus.

Table D.5 a Statistical analysis of residual shear strength values for ring shear.

Samples	Remoulded residual shear strength. Parameters for ring shear.		Sum for sample
	ϕ'_{rr}	c'_{rr}	
MTBH	7.5	4.1	11.6
CM	8.5	6.8	15.3
RP	7.5	4.3	11.8
CW1	7.5	2.5	10.0
KS	13.0	4.9	17.9
MT5	6.5	4.9	11.4
AC	7.0	6.5	13.5
Sum of ϕ'_{rr} & c'_{rr}	57.5	34	91.5

Table D.5 b Two-way ANOVA analysis

S.V.	d.F.	S.S.	S.S/d.F.	F-ratio
Between sam- ples. (rows)	6	22.238	3.706	1.134
Bet. ϕ_{rr} & c_{rr} .(Columns)	1	39.447	39.447	12.070
Residual	6	19.608	3.268	
Total	13	81.293		

The analysis shows no significant differences between samples such that tabulated $F_{0.05} (6,6) = 4.28$ but a significant difference exists for ϕ_{rr} and c_{rr} using the apparatus, such that tabulated $F_{0.05} (1,6) = 5.99$.

APPENDIX E

DETERMINATION OF THE HEIGHTS OF BACK
SCARP FROM AERIAL PHOTOGRAPHS.

The heights of the back scarps of the landslips were determined from aerial photographs by use of a Watts SB190 mirror stereoscope. The following procedure was employed.

The principal point, that is the central point of the photographs drawn by the intersection of the four crosses at the corners was determined and carefully marked. Then each overlapping pair of photographs were base-lined where the base line is defined as the line between the principal points, the base line is also called X-axis.

The scale of each photograph was found by taking corresponding distances off the photograph and the Ordnance Survey sheet. Care was taken to choose precise image points of approximately the same height that would be recognized on both the photograph and the control map. The flying height is given by:

$$\text{Scale} = \frac{f}{H} \dots\dots\dots(E.1)$$

where f = focal length of the lens (normally 152.4mm).

H = flying height

The photographs were then orientated correctly in the Watts Stereoscope. In this instrument two light spots are introduced into the viewing system and can be fused to form a floating mark in relation to the stereoscopic model formed from the pair of photographs. The floating mark can be brought to ground level by the adjustment of micrometer reading heads. The difference in reading being the difference in parallax.

These differences are then placed into the difference in parallax formula, equation E.2. The lower of the two points is referenced to a datum.

First the parallax adjustment necessary to bring the spot to ground level at a control point or the lower point of measurement is determined (point E) and then the spot is moved to the upper point of measurement (point A) and the difference in parallax between A and E is calculated ($\Delta P_{EA} = P_A - P_E$). The actual difference in height between point A and E is then given by equation E.2

$$\Delta h_{EA} = H - h_E \frac{P_{EA}}{P_A} \dots\dots\dots(E.2)$$

where

- E = Bottom point, taken as zero
- A = top point
- Δh_{EA} = The difference in the height between the two points A and E.
- H = Flying height
- h_E = The height of E.
- ΔP_{EA} = The difference in parallax between A and E.
- P_A = Parallax at A.

REFERENCES

- AGARWAL, K.B. (1967), The influence of size and orientation of sample on the undrained strength of London Clay. unpublished, Ph.D. thesis, University of London.
- AKROYD, T.N.W. (1964), Laboratory testing in soil engineering. Geotechnical Monograph No.1, Soil Mechanics Limited, 233 pp.
- ALLEN, J.R.L. (1960), The Mam Tor Sandstones: A "turbidite" Facies of the Namurian deltas of Derbyshire, England. Jour. Sed. pet. Vol. 30 No.2, 193-208
- AMIN, M.A. (1979), Geochemistry and mineralogy of Namurian sediment in Pennine basin, England., Unpublished Ph.D. thesis, University of Sheffield.
- ANDERSSON, J.G. (1906), Solifluction a component of sub-aerial denudation. Jour. of Geol., Vol. 14, 91-112.
In: Chandler, R.J. (1972), Periglacial mudslides in Vestspitsbergen and their bearing on origin fossil 'solifluction' shears in low angled clay slopes. Q.J.E.G. Vol.5, 223-241.
- ATTERBERG, A. (1911), Über die physikalische Bodenuntersuchung und über die plastizität der tone. Internationale Mitteilungen für Bodenkunde, Vol.1.
In: Akroyd, T.N.W. (1964), Laboratory testing in Soil Engineering. Geotechnical Monograph No.1, Soil Mechanics Ltd., 23 pp.
- ATTEWELL, P.B. and FARMER, I.W. (1975), Principle of Engineering Geology. London, Chapman and Hall, 1045 pp.
- ATTEWELL, P.B. and TAYLOR, R.K. (1973), Clay shale and discontinuous rock mass studies. Final report to

European Research Office; U.S. Army, Contract No., ERO-591-72 G005.

In: Cripps, J.C. and Taylor, R.K. (1981), The engineering properties of mudrocks. Q.J.E.G. Vol.14, 375-346.

BARTON, N. (1973), Review of a new shear strength criterion for rock joints. Eng. Geol., Vol.7, 287-332.

BASS, M.A. (1954), Study the characteristics and origin of some major area of landsliding in the Eastern Pennines and Isle of Wight., Unpublished M.Sc. thesis, Dept. of Geography, University of Sheffield.

BELL, F.G. (1981), Engineering properties of soil and rocks, Butterworths, 149pp.

BISHOP, A.W. (1955), The use of the slip circle in the stability analysis of slopes., Geotech. Vol.5, 7-17.

BISHOP, A.W. (1967), Progressive failure, with special reference to the mechanism causing it., Proc. Geotech. Conf., Oslo, Vol.2, 142-150.

BISHOP, A.W. and BJERRUM, L. (1960), The relevance of the triaxial test to the solution of stability problems.

Proc. research conference on shear strength of cohesive soils., Boulder, American Society of Civil Engineers., New York, 437-501.

BISHOP, A.W. and HENKEL, D.J. (1957), The measurement of soil properties in the triaxial test., London, Edward Arnold (publishers) Ltd., 190pp.

BISHOP, A.W. and LITTLE, A.L. (1967), The influence of the size and orientation of the sample on the apparent strength of London Clay at Maldon Essex., Proc. Geotech. Conf. Oslo., Vol.1, 89-96.

- BISHOP, A.W. and MORGESTERN, N.R. (1960), Stability coefficients for earth slopes. *Geotech.*, Vol. 10, No.4, 129-150.
- BJERRUM, L. (1967), Progressive failure in slopes of over-consolidated plastic clay and clay shales. The third Terzaghi lecture., *J. Soil Mech. Found. Engng. Div.*, Proc. ASCE Vol.93, SM5, 1-49.
- BLACK, R.F. (1966), Comments on periglacial terminology *Biul. peryglacialny*, Vol.15, 329-353.
In: Higginbottom, I.E. and Fookes, P.G. (1971), Engineering aspects of periglacial features in Britain. *Q.J.E.G.* Vol.3, 85-117.
- BREWSTER, G.R. (1980), *Effect of chemical pretreatment on X-ray powder diffraction characteristics of clay minerals derived from volcanic ash.*, *Clay and Clay Minerals*, Vol.28, 303-310.
- BRINDLEY, G.W. and BROWN, G. (1980), *Crystal structures of clay minerals and their X-ray identification.*, Mineralogical Society, London., 495pp.
- BRITISH STANDARD (B.S. 1377), (1975), *Method of testing soil for Civil Engineering purposes.*, British standard institution.
- BROMHEAD, E.N. (1979), *A simple ring shear apparatus.*, *Ground Engineering*, Vol.12, 40-44.
- BROMHEAD, E.N. (1984), *Slopes and embankments.*,
In: Attewell, P.B. and Taylor, R.K. (1984) (Ed.), *Ground movements and their effects on structures.*, Surrey University Press., 441pp.
- BROMHEAD, C.E.N., EDWARD, W. and WRAY D.A. (1933), *The geology of the country around Holmfirth and Glossop.*,

Geol. Survey, England and Wales., Mem., H.M.S.O. London., 209. In: The Mam Tor Sandstones: A turbidite Facies of Namurian delta of Derbyshire, England., Jour. Sed. Pet., Vol.30, No.2, 193-208.

BROWN, G. (1961), The X-ray identification and crystal structures of clay minerals., Mineralogy Society London., 544pp.

BROWN, R.D. (1977), Excursion itineraries for the 6th British Polish Seminar. Sheffield 1977, Sheffield University, Geography Dept..

BUCHER, F. (1975), Die Restscherfestigkeit natürlicher Böden, ihre Ernflussgrößen und Beziehungen als Eragebnis experimenteller Untersuchungen., Report No.103, Zürich: Institutes für Grundbau und Bodenmechanik Eidgenössische Technische Hochschule.
In: Lupini, F. Skinner, A.E. and Vaughan, P.R. (1981) Geotech. Vol.31, No.2, 181-213.

CAPPER. P.L. and CASSIE, W.F. (1969), The Mechanics of Engineering Soils., Fifth Ed. Spon's Civil Engineering Series.

CARROL, D. (1970), Clay Minerals: a guide to their X-ray identification., Geol. Soc. Am. spec. paper, 126pp.

CASAGRANDE, A. (1936), Characteristics of cohesionless soil affecting the stability of slopes and earth fills., Jour: of the Boston Society of Civil Engineers., Vol.23, No.1, 13-22.,
In: Lagatta, D.P. (1970), Residual strength of clays and clay shales by rotational shear tests., Harvard soil Mechanics Series., No.86, Cambridge, Massachusetts,

CASAGRANDE, A. (1949), Discussion of a paper by Bindiger, W.V. and Thompson, T.F., Excavation slopes in the Panama Canal., ASCE Transaction, Vol.114, 870-874.

In: Lagatta, D.P. (1970), Residual strength of clays and clay shales by rotational shear test., Harvard Soil Mechanics Series No.86, Cambridge, Massachusetts.

CARSON, M.A. and PETLEY, J.D. (1970), The existence of threshold hillslopes in the denudation of the landscape., Trans. Inst. Brit. Geog. Vol.49, 71-96.

CHANDLER, R.J. (1966), Measurement of residual strength in triaxial compression., Geotech. Vol.16, 181-186.

CHANDLER, R.J. (1970), A shallow slab slide in the Lias Clay near Uppingham, Rutland., Geotech. Vol.20, No.3, 253-260.

CHANDLER, R.J. (1972), Preglacial mudslides in Vestspitsbergen and their bearing on origin fossil "Solifluction" shears in low angled clay slopes., Q.J.E.G. Vol.5, 223-241.

CHAO, G.Y. (1969), 20 (cu) table for common minerals Carleton Univ. Dept. of Geol. Geological paper 69-2, Ottawa, Canada.

CHATFIELD, C. (1970), Statistics for technology studies in applied statistics., Penguin Books, 359pp.

CHATTOPADHYAY, K.P. (1972), Residual shear strength of some pure clay minerals, Unpublished Ph.D. thesis., University of Alberta.

CHOWDHURY, R.N., BERTOLDI, C. GRAD., I.E. (1977), Residual shear tests on soil from two natural slopes., Australian Geomechanics Jour. G7, 1-9.

COLLIN, A. (1846), Recherches experimentales sur les glissements spontane's des terrains, argileux.,

- Carilian - Goeury and Dalmont., Paris (Translation by W.R. Schriever Univ. of Toronto, Press (1966)., In: Lagatta, D.P. (1970), Residual strength of clay and clay shales by rotational shear test., Harvard Soil Mechanics Series No.86 Cambridge, Massachusetts.
- COLLINSON, J.D. and WALKER, R.G. (1967), Namurian sedimentation in the high peak., In: Neves, R. and Downie, C. (Eds.) Univ. of Sheffield., 80-88.
- CAPPER, P.L. and CASSIE, W.F. (1969), The Mechanics of Engineering Soils., Fifth Ed., E. and F.N. Spon. London.
- COULSON, J.H. (1972), Shear strength of flat surface in rock., Stability of rock slope., In: Cording E.J. (Ed.) proc. symp. rock Mech. 13th Urbana Illinois (1971) Am. soc. Civ. Engng. New York, 77-105.
In: Barton, N. (1973), Review of a new shear strength criterion for rock joints., Eng. Geol. Vol.7, 287-332
- CRAIG, R.F. (1983), Soil Mechanics., Van Nostrand Reinhold U.K. 3rd. Ed., 328pp.
- CRIPPS, J.C. and TAYLOR, R.K. (1981), The engineering properties of mudrocks Q.J.E.G. Vol.14, 346-375.
- CUBITT, J.M. (1975), A regression technique for the analysis of shale by X-ray diffraction., J. sed. pet. vol.45, 546-553.
- DAVIDSON, D.T. and SHEELER, J.B. (1952), Clay fraction in engineering soil., III: influence of amount on properties., Proc. High. Res. Board, Washington., 558-563.

DE BEER, E. (1967), Shear strength characteristics of the Boom clay., Proceedings of the Geotechnical conference, Oslo, Vol.1, 38-88.

DE, P.K. and FURDAR, SIR WILLIAM HALCROW and PARTNERS, ABERAMAN, ABERDARE, GLAMORGAN (1973), Discussion of Voight (1973), Correlation between Atterberg plasticity limits and residual shear strength of natural soil. Geotechnique vol. 23, 600-601.

DEERE , D.V. and PATTON, F.D. (1971), Slope stability in residual soil., Proc. ASCE 4th Pan American conf. Soil Mech. Found. Engng., San Juan R.P., 87-170.

DERBYSHIRE COUNTY COUNCIL (1966), Derbyshire County Council, Catalogues, unpublished., Event at Mam Tor landslide from 1909-1966.

DUNCAN, J.M. and WRIGHT, S.G. (1980), The accuracy of equilibrium methods of slope stability analysis., Engng-Geol., Vol. 16, 5-17.

EARLY, K.R. and SKEMPTON, A.W. (1972), Investigation of landslide at Walton's Wood, Staffordshire., Q.J.E.G. Vol.5, 19-41.

EDEN, R.A., STEVENSON, I.P. and EDWARDS, W. (1957), The Geology of the Country around Sheffield., Geol. Surv. England and Wales Mem. H.M.S.O. London., 238pp.

ELLIOTT, R.E. and STRAUSS, P.G. (1970), A classification of coal measures rock based on quartz content., Comptes Rendu de Congres. Int. Strat. Geol. Carbonif, Sheffield (1967), Vol.2, 715-724.

ENGINEERING GROUP WORKING PARTY (1972), Report by the Geological Society Engineering group working party., The preparation of maps and plans in term of Engineering Geology., Q.J.E.G., Vol.5, 295-382.

- FARMER, I.W. (1968), Engineering properties of rock., London., E. and F.N. Spon. Ltd.
- FEARSIDES, W.G., BISAT, W.S., EDWARDS, W., and WILCOCKSON, W.H. (1932), The geology of the eastern part of the Peak District., Geol. Assoc. London., Proc. Vol.43, 152-191.,
In: Allen, J.R.L. (1960), The Mam Tor Sandstones: A "turbidite" Facies of the Namurian delta of Derbyshire, England., Jour. Sed. Pet. Vol.30, No.2, 193-208.
- FELLENIOUS, W. (1927), Erdstatische Berechnungen mit Reibung und, Kohäsion und unter Annahme Kreiszyklindrischer Gleifflächen, Ernst. and Sohn, Berlin., 40pp.
In: Suklje, L. (1969), Rheological Aspects of Soil Mechanics., Wiley-interscience., 577 pp.
- FELLENIOUS, W. (1936), Calculation of the stability of earthdams., Trans. 2nd Congress on large dams. Washington, Vol.4, 445-459.,
In: Attwell, P.B., and Farmer, I,W. (1975), Principle of Engineering Geology, London, Champman and Hall., 1045pp.
- FERRIANS, O.J., KACHADOORIAN, R. and GREENE, G.W. (1969), Permafrost and related engineering problems in Alaska. U.S. Geol. Surv. Prof.paper No. 678, 1-37.,
In: Higginbottom, J.E. and Fookes, P.G. (1971), Engineering aspects of periglacial features in Britain Q.J.E.G. Vol.3, 85-117.
- FLEISCHER, S. (1972), Scherbruch - und Schergleitfestigkeit, von Bindigen Erdstoffen. Neue Bergbautechnik Vol.2, 98-99, Freiburg: Mining Academy.,
In: Lupini, F. Skinner, A.E. and Vaughan P.R. (1981), Geotech. Vol.31, No.2, 181-213.

FRANKS, J.W. and JOHNSON R.H. (1964), Pollen analytical dating of Derbyshire landslip: The Cown edge landslides, Charlesworth., New phytal vol.63, 209-216.

GARGA V.K. (1970), Residual shear strength under large strains and the effect of sample size on the consolidation of fissured clay., Unpublished., Ph.D. thesis, University of London.

GARRELS, R.M. and CHRIST, C.L. (1965), Solutions Minerals and Equilibria., Harper and Row New York 45 pp.
In Vear, A. (1981), The geochemistry of pyritic shale weathering within an active landslips., Unpublish,c., Ph.D. thesis University of Sheffield.

GEOLOGICAL SURVEY (1969), Sheet SK18 and part of SK17 Edale and Castleton scale: 1:25000, Classical Areas of British Geology., Institute of Geological Sciences.

GIBBS, R.J. (1965), Error due to segregation in quantitative clay mineral X-ray diffraction mounting techniques., Am. min., vol.50, 741-751.

HAEFELI, R. (1938), Mechanische Egenschaften von lockergesteinen, Schweizerische Bauzeitung, Vol.3, 321-325.

In Lagatta, D.P. (1970), Residual strength of clays and clay shales by rotational shear test., Harvard Soil Mechanics Series No. 86, Cambridge, Massachusetts.

HAEFELI, R. (1948), The stability of slopes acted upon by parallel seepages., Proc. 2nd int. conf. on Soil Mechanic, Rotterdam, Vol.1,57-62.

In: Attwell, P.B. and Farmer, I. W., Principle of Engineering Geology, Champman and Hall, 1045 pp.

- HELEY W. and MacIVER B.N. (1971), Engineering properties of clay shales., Report-1- Developments of classifications indexes of clay shales., Technical report 5-71-6, U.S. Army Engineer Waterways Experiment Station Vicksburg, Mississippi.
- HERMANN, H.G. and WOLFSKILL, L.A. (1966), Residual shear strength of weak clay., Technical report No.3, 699., Engineering properties of nuclear craters, Report 5, Cambridge, Massachusetts, Massachusetts Institute of Technology.
- HETTNER, A., (1972), The surface feature of land-problems and method of geomorphology., MacMillan, 193 pp.
- HIGGINBOTTOM, I.E. and FOOKES, P.G. (1971), Engineering aspects of periglacial features in Britain., Q.J.E.G. Vol.3,85-117.
- HILL, H.P. (1949), The Ladybower reservoir., Jour. Instn. Wat. Engrs. London, Vol. 3, 414 pp.
In: Walters, R.G.S. (1962), Dam Geology., Butterworths, London. 335 pp.
- HORN, H.M. and DEERE, D.V. (1962), Frictional characteristics of minerals., Geotech. Vol. 12, No.4, 319-335.
- HUDSON, R.G.S and COTTON, G. (1945), The carboniferous rocks of the Edale anticline, Derbyshire., Geological Soc. London Quart. Jour., Vol. 101, 1-35.
In: Allen, J.R.L. (1960), The Mam Tor Sandstones: A 'turbidite' Facies of the Namurian Delta of Derbyshire, England., Jour. Sed. Pet., Vol. 30, No.2, 193-208.
- HULTIN, S. (1916), Grusfyllningar, för Kajbyggnadar (Gravel fillings for quay constructions, in Swedish) Teiknisk, Tidskrift, Vol. 46, 292 pp.
In: Suklje, L. (1969), Rheological Aspects of Soil Mechanics. Wiley-intercience, 571 pp.

- HUNT, R.E. (1984), Geotechnical Engineering Investigation Manual., McGraw - Hill Book Company, 983 pp.
- HUTCHINSON, J.N. (1968), Mass Movement.,
In: Fairbridge, R.W. (Ed.) Encyclopaedia of Geomorphology, New York, 688-695.
- HUTCHINSON, J.N. (1982), Methods of locating slip surfaces in landslides., British Geomorphological research group, Technical Bulletin, No.30, 30 pp.
- HUTCHINSON, J.N., SOMERVILLE, S.H. and PETLEY, D.J. (1973), A landslide in periglacially disturbed Etruria Marl at Bury Hill, Staffordshire., Q.J.E.G., Vol. 6, 377-404.
- HVORSLEV, M.J. (1936), A ring shearing apparatus for determination of shearing resistance and plastic flow of soil., Proc. ICSMFE, Vol.2, 125-129.,
In: Lagatta, D.P. (1970), Residual strength of clay and clay shales by rotational shear test. Harvard Soil Mechanics Series No.86, Cambridge, Massachusetts.
- HVORSLEV, M.J. (1960), Physical components of the shear strength of saturated clays., A.S.C.E. Research Conference on shear strength of cohesive soils., Boulder, Colorado, 615-641.,
In: Lagatta D.P. (1970), Residual strength of clay and clay-shales by rotational shear test. Harvard Soil Mechanics Series No.86, Cambridge, Massachusetts.
- JACKSON, J.O. and FOOKES, P.G. (1974), The relationship of the estimated former burial depth of the lower Oxford Clay to some soil properties., Q.J.E.G., London, Vol.7, 137-79.
- JACKSON, J.W. (1923), On the correlation of Yoredales and Pendlesides, Naturalist, Hull, No.801, 337-338.
In: Stevenson, I.P. and Gaunt, G.D. (1971), Geology of Country around Chapel-en-le-Frith., Memoirs of

the Geological Survey of Great Britain., Natural Environment Research Council Inst. of Geol. Sci.

JACKSON, J.W. (1927), The succession below the Kinderscout Grit in North Derbyshire., Manchester Geological Soc. Jour. Vol.1, 15-32.

In: Allen, J.R.L. (1960), The Mam Tor Sandstones: A 'turbidite' Facies of the Namurian delta of Derbyshire, England., Jour. Sed. Pet. Vol.30, No.2, 193-208.

JACKSON, M.L. (1973), Soil chemical analysis, advanced course by M.L. Jackson, Madison 894.,

In: Ireland, B.J. (1982), Transmission electron microscopy of authigenic clay minerals., Unpublished, Ph.D. thesis, University of Sheffield.

JEFFERY, P.G. (1970), Chemical methods of rock analysis, International series of monographs in analytical chemistry, Vol.36, 489 pp.

JUMIKIS, A.R. (1965), Soil Mechanics., D. Van Nostrand Company INC., 791 pp.

KANJI, M.A. (1974), The relationship between drained friction angles and Atterberg limits of natural soils., Geotech., Vol. 24, No.4, 671-674.

KENNEY, T.C. (1967), The influence of mineral composition on the residual strength of natural soil., Proc. Geotech. Conf. Oslo, Vol.1, 123-130.

KENNEY, T.C. (1977), Residual Strength of mineral mixture, Proc. 9th inter. conf. Soil Mech. Vol.1, 155-160.

KRSMANOVIC, D. (1967), Initial and residual shear strength of hardrocks., Geotech. Vol.17, 145-160.,

In: Barton, N. (1973), Review of a new shear strength criterion for rock joints., Eng. Geol., Vol.7, 287-332.

- LAGATTA, D.P. (1970), Residual-strength of clays and clay-shales by rotational shear tests., Harvard Soil Mechanics Series, No.86, Cambridge, Massachusetts.
- LAPWORTH, H. (1911), Geology of dam trenches. Trans. Instn. Wat. Engr. London Vol.16, 25 pp.
In: Walters, R.G.S. (1962), Dam Geology, Butterworths London., 335 pp.
- LUNDEGARD, P.D. and SAMUELS, N.P. (1980), Fields classification of fine-grained sedimentary rocks., J. of sed. pet., Vol. 50, No.3, 781-786.
- LUPINI, J.E., SKINNER, A.E. and VAUGHAN P.R. (1981), The drained residual strength of cohesive soil. Geotech. Vol.31, No.2., 181-213.
- MAUGERI, M. (1976), L'apparecchio anulare di taglio nella determinazione della resistenza residua di terreni scottoposti a ridotte tensioni normali. Rivista Italiani di Geotecnica, No. 2, 114-124.
- MITCHELL, J.K. (1976), Fundamentals of soil behaviour, Series in soil engineering., John Wiles and Sons, New York.
- MORGENSTERN, N.R. and SANGREY D.A. (1978), Methods of stability analysis.,
In: Landslides Analysis and Control., Special report 176, 155-169, National Academy of Sciences, Washington D.C.
- MORGENSTERN N.R. and TCHALENKO J.S. (1967a), Microstructural observation on shear zones from slips in natural clays., Proc. of Geotech. conf. Oslo 1967, Vol. 1, 147-152.
- MORGENSTERN, N.R. and TCHALENKO, J.S. (1967b), Microscopic structure in kaolin subjected to direct shear., Geotech., Vol. 17, No.4, 309-328.
- NAGARAJ, T.S. and NARASIMHA RAO, S. (1974), The influence of clay composition and system chemistry on residual strength of saturated remoulded clay., Indian Geotech., J. 4, No.2, 161-173.

- NEMCOK, A. PASEK, J. and RYBAR (1972), Classification of landslides and other mass movement., Rock Mechanics, Vol.4, 71-78.
- PARCHER, J.N. and MEANS, R.E. (1968), Soil Mechanics and foundation., Charles E. Merrill publishing company., 573 pp.
- PARRY, R.H.G. (1972), Some properties of heavily over-consolidated Oxford Clay at a site near Bedford., Geotech., Vol.22, No.3, 485-507.
- PATTON, F.D. (1966), Multiple modes of shear failure in rock and related material., Thesis University of Illinois, 282 pp.,
In: Barton, N. (1973), Review of a new shear strength criterion for rock joints., Eng. Geol. Vol.7, 287-332.
- PECK, R.B. (1967), Stability of Natural Slopes., Jour. Soil Mech. found. Engng. Div. proc. ASCE, Vol.93, SM4, 403-417.
- PETERSON, K.E. (1916), Kajraset, i Goteborg des 5te mars. (Collapse of a quay wall at Gothenburg 5th March 1916 in Swedish), Teknisk Tidskrift, Vol.46, 289.,
In: Suklje, L. (1969), Rheological Aspects of Soil Mechanics., Wiley interscience., 571 pp.
- PETLEY, D.J. (1966), The shear strength of soil at large strain., Unpublished, Ph.D. thesis Univ. of London.
- PETLEY, D.J. (1984), Ground investigation sampling and testing for studies of slope instability.,
In: Brynsden, D. and Prior, D.B. (Eds.), Slope instability, John Wiley and Sons Ltd.
- PIERCE, J.W. and SIEGEL, F.K. (1969), Quantification in clay minerals studies and sedimentary rocks., J. sed. pet. Vol.39, 187-193.

- PITEAU, D.R. (1970), Geological factors significant to the stability of slopes cut in rock.,
In: Van Rensburg, P.W.J. (Ed.), planning open pit, Mines S. Africa Inst. Min. Met.,
In: Vear, A. (1981), The geochemistry of pyritic shale weathering within an active landslide., Unpublish, Ph.D. thesis, Univ. of Sheffield.
- POLISH CODE (1959), Polish Code PN-59/B - 03020.,
In: Witun, Z. and Starzewski, K. (1975), Soil Mechanics in Foundation Engineering, Vol.1, Properties of soil and site investigation, 2nd. Ed. 252 pp., Surrey Univ. Press.
- POTTER, P.E., MAYNARD, J.B. and PRYOR, W.A (1980), Sedimentology of shale study guide and reference source., Springer-Verlag, New York., Heidelberg Berlin,306 pp.
- RAMIAH, B.K., DAYALU, N.K. and PURUSHOTHAMARAJ, P. (1970), Influence of chemicals on residual strength of silty clay., Soils and foundations, Vol.10, 25-36.
- RIPLEY, C.F. and LEE, K.L. (1962), Sliding friction tests on sedimentary rock specimens., Trans. Int. Congr. Large dams, 7th Rome, Vol.4, 657-671.
In: Barton, N. (1973), Review of a new shear strength criterion for rock joints., Eng. Geol. Vol.7, 287-332.
- ROSCOE, K.H., SCHOFIELD, A.N. and WROTH, C.P. (1958), On the yielding of soils. Geotech., Vol.8, No.1, 22-53.
- SANDEMAN, E. (1920), The Derwent Valley Waterworks., Min. Proc., Instn. Civ. Engrs. Vol.206 152.,
In: Walters, R.C.S. (1962), Dam Geology, R.C.S., Butterworths, London, 335 pp.

- SAVIGEAR, R.A.G (1965), A technique of morphological mapping., *Annals. Assoc. Amer. Geogr.*, Vol.55, 514-538.
- SCHOFIELD, A.N. and WROTH, C.P. (1968), *Critical state soil mechanics*, London, McGraw-Hill.,
In: Skempton, A.W. 1970, *First time slides in over consolidated clays.*, *Technical notes: Geotech.* Vol. 20, 320-324.
- SCHULTZ, L.G. (1960), *Quantitative X-ray determination of some aluminous clay minerals in rocks.*, *Clay and Clay Minerals.*, *proc.*, 7th Nat. Conf. 216-224.
- SCOTT, C.R. (1969), *An introduction to soil mechanics and foundations.* , Maclaren and Sons, London., First ed., 316 pp.
- SCOTT, C.R. (1974), *An introduction to soil mechanics and foundations.*, Maclaren and Sons, London, 2nd ed.
- SCOTT, C.R. (1980), *An introduction to soil mechanics and foundations.*, Maclaren and Sons, London, 3rd ed., 406 pp. . .
- SEYCEK, J. (1978), *Residual strength of soils.*, *Bull. Int. Ass. Engng Geol.*, Vol.17, 73-75.
In: Lúpini, F., Skinner, A.E. and Vaughan, P.R. (1981). *The drained residual strength of cohesive soil*, *Geotech.* Vol.31, No.2, 181-213.
- SHARP, C.F,S. (1938), *Landslides and related phenomena-* Columbia Univ. Press., 133 pp., New York.
In: Zaruba, Q. and Menci, V. (1982), *Landslide and their control.*, *Development in Geotechnical Engineering*, Vol. 31, Second completely revised edition., Elsevier Scientific publishing company.

- SHARP, C.F.S. (1960), Landslides and Related Phenomena., Pageant, New York, 137 pp.,
In: Year, A. (1981), The Geochemistry of pyritic shale weathering within an active landslide., Unpublish, Ph.D. thesis, Univ. of Sheffield.
- SIMON, N.S. and MENZIES, B.K. (1978), The long-term stability of cuttings and natural clay slopes. ,
In: Scott, C.R. (1978) (Ed.), Development in soil mechanics - 1, Applied Science publishers Ltd., London, 441 pp.
- SIMPSON, I.M. (1982), The Peak District rock and fossils, 3, London, 120 pp.
- SKEMPTON, A.W. (1953a), Soil mechanics in relation to geology., proc. Yorks Geol. Soc., Vol.29, 33-62.,
In: Skempton A.W. and Hutchinson, J.N. (1969), Stability of natural slopes and embankment founda- foundations., 7th Int. Con. Soil Mech. and Found. Engng., State of art report, Mexico, 291-340.
- SKEMPTON, A.W. (1953b), Discussion on soil stability problems in road engineering., Proc. Inst. Civ. Eng., Vol. 2, 265-268.,
In: Skempton, A.W. and Hutchinson, J.N. (1969), Stability of natural slopes and embankment foun- dations., 7th Int. Conf. Soil Mech. and Found. Engng. State of the art report, Mexico, 291-340.
- SKEMPTON, A.W. (1953c), The Colloidal 'Activity' of clays, Proc. of the third international conference on soil Mech. found. Eng. Vol.1, 57-61, Switzerland.
- SKEMPTON, A.W. (1964), Long-term stability of clay slopes, Geotech., Vol.14, 77-101.
- SKEMPTON, A.W. (1965), Earth and Rock Dams, slopes and Open Excavations., Proc., 6th Int. Conf. Soil Mech Found. Engng., Montreal, Vol.3, 551-552.

- SKEMPTON, A.W. (1966), Some observation on tectonic shear zones., Proc. 1st Int. Conf. Rock Mech., Lisbon 1966, Vol.1, 318-335.
- SKEMPTON, A.W. (1970), First time slides in over-consolidated clays. Technical notes., Geotech. Vol. 20, 320-324.
- SKEMPTON, A.W. (1977), Slope stability of cutting in brown London Clay., 9th Inter. Conf. Soil Mech. Found. Engng., Japan, 261-269.
- SKEMPTON, A.W. and DELORY, F.A. (1957), Stability of natural slope in London Clay., Proc. 4th Int. Conf. Soil Mech. Found. Engng., London, Vol. 2, 378-381.
- SKEMPTON, A.W. and HUTCHINSON, J.N. (1969), Stability of natural slopes and embankment foundation., Proc. 7th Int. Conf. Soil Mech. Found. Engng., Mexico, State of Art., 291-340.
- SKEMPTON, A.W. and LA ROCHELLE, P. (1965), The Bradwell slip: a short term in London Clay., Geotech. Vol. 15, 221-242.
- SKEMPTON, A.W. and PETELY, D.J. (1967), The strength along structural discontinuities in stiff clays., Proc. Geotech. Conf., Oslo, Vol.2, 29-46.
- SKEMPTON, A.W. SCHUSTER, R.L. and PETLEY, D.J. (1969), Joints and fissures in London clay at Warysbury and Edgware., Geotech. Vol.19, 205-217.
- SMITH, E.G., RHYS, G.H. and EDEN, R.A. (1967), The geology of the country around Chesterfield, Matlock and Mansfield., Mem. Geol. Surv., Gt. Brit.; England and Wales, London.
- SMITH, G.N. (1982), Elements of Soil Mechanics for Civil and Mining Engineers., 5th ed., 424 pp.

- SPEARS, D.A. (1980), Towards a classifications of shales., J. Geol. Soc. London, Vol.137, 125-129.
- SPEARS, D.A. and TAYLOR, R.K. (1972), Influence of weathering on the composition and engineering properties of in situ, Coal Measures rocks., Int. J. Rock Mech. Min., Sci. Vol. 9, 729-756.
- STEVENSON, I.P. and GAUNT, G.D. (1971), Geology of Country around Chapel-en-le-Frith Memoirs of the Geological Survey of Gt. Britain., Natural Environment Research Council., Institute of Geological Sciences., 444 pp.
- STEWART, H.E. (1984), Links between Geotechnical and Engineering properties in weathered pyritic shales., Unpublished, Ph.D. thesis, Univ. of Sheffield.
- STEWART, H.E. and CRIPPS, J.C. (1983), Some engineering implications of chemical weathering of shale., Q. J.E.G., Vol.16, 281-289.
- SUKLJE, L. (1969), Rheological Aspects of Soil Mechanics., Wiley - Inter. Science., 571 pp.
- TAYLOR, D.W. (1948), Fundamentals of Soil Mechanics., John Wiley and Sons Inc., New York, 700 pp.
- TAYLOR, R.K. AND SPEARS, D.A. (1981), Laboratory investigation of mudrocks., Q.J.E.G., VOL.4, 291-309.
- TERZAGHI, K. (1936), Stability of slopes of natural clay., Proc. 1st Int. Conf. Soil Mech., Harvard, Vol.1, 161-165 pp. ,
In: Atterwell P.B. and Farmer I.W. (1975) principles of Engineering Geology, London, Chapman and Hall, 1405 pp.
- TERZAGHI, K. (1950), Mechanism of landslides.,
In: Application of Geology to Engineering Practice., Berkey Volume, Geol. Soc. Am., 83-125.

- TERZAGHI, K. and PECK, R.B. (1948), Soil Mechanics in Engineering Practice., John Wiley and Sons Inc., New York, 729 pp.
- TIEDEMANN, B. (1937), Über die schubfestigkeit bindiger Böden., Bautechnik 15, Nos. 30 and 33, 400-403, 433-435.,
In: Lagatta, D.P. (1970), Residual strength of clays and clay shales by rotational shear test., Harvard Soil Mechanics Series No.86, Cambridge, Massachusetts.
- TILL, R. and SPEARS, D.A. (1969), The determination of quartz in sedimentary rocks using an X-ray diffraction method., Clay and Clay Minerals, Vol.17, 323-327.
- TOWNSEND, F.C. and GILBERT, P.A. (1976), Effects of specimen type on the residual strength of clays and clay shales: Soil specimen preparation for laboratory test., ASTM-STP 599 American Society of Testing Material., 43-65.
- VARNES, D.J. (1958), Landslides types and processes.,
In: Eckel, E.B. (ed.), Landslides and Engineering Practice, HRB, Special report 29, 20-47.,
In: Varnes, D.J. (1978), Slope Movement Types and Process.,
In: Landslide Analysis and Control, Special report 176, 12-33., National Academy of Sciences, Washington, D.C.
- VARNES, D.J. (1978), Slope movement types and processes.,
In: Landslides Analysis and Control, Special report 176, 12-33., National Academy of Sciences, Washington, D.C.
- VAUGHAN, P.R., HIGHT, D.W., SODHA, V.G. and WALBANCKE, H.J. (1978), Factors controlling the stability of

- clay fill in Britain., Clay Fills, 203-217, London: Institution of Civil Engineering.,
In: Lupini, F., Skinner, A.E. and Vaughan, P.R. (1981)., The drained residual strength of cohesive soil, Geotech., Vol.2, 181-213.
- VEAR A. (1981), The Geochemistry of pyritic shale weathering within an active landslide., unpublished, Ph.D. thesis Univ. of Sheffield.
- VEAR, A. and CURTIS, C.D. (1981), A quantitative evaluation of pyrite weathering., Earth surface processes and landsforms, Vol.6, 191-198.
- VICKERS, B. (1978), Laboratory work in Civil Engineering Soil Mechanics., Granada Publishing, 148 pp.
- VOIGHT, B. (1973), Technical note: Correlation between Atterberg plasticity limits and residual shear strength of natural soils., Geotech., Vol.23, No.2, 265-267.
- WALKER, R.G. (1966), Shale Grit and Grindslow Shales: Transition from turbidite to shallow water sediments in the Upper Carboniferous of Northern England., Jour. Sedimen. Petrol. Vol.36, 90-114.,
In: Collinson, J.D. and Walker R.G. (1967) Namurian Sedimentation in the high peak.,
In: Neves, R. and Downie, C. (Ed.) Geological Excursion the the Sheffield Region, Univ. of Sheffield., 80-88.
- WALTERS, R.G.S (1962), Dam Geology., Butterworths, London, 335 pp.
- WEEKS, A.G. (1969), The stability of natural slopes in south-east England as affected by periglacial activity., Q.J.E.G., Vol.2, 47-61.

- WENTWORTH, C.K. (1972), A scale of grade and class terms for clastic sediments., J. Geol., Vol.30, 377-392.
- WILUN, Z. and STARZEWSKI, K. (1975), Soil Mechanics in Foundation Engineering, Vol.1, Properties of soils and site investigation, 2nd. Ed., 252 pp., Surrey Univ. Press.
- ZARUBA, Q. and MENCL, V. (1969), Landslides and their control., Elsevier, Amsterdam, Academia, Prague, 205 pp.
- ZARUBA, Q. and MENCL, V. (1982), Landslides and their control., Development in Geotechnical Engineering 31, Second completely revised edition., Elsevier Scientific publishing company, 324 pp.
- BISHOP, A.W., GREEN, G.E. GARGA, V.K. ANDRESEN A. and BROWN, J.D. (1971)
A new ring-shear apparatus and its application to measurement of residual strength.
Geotech., Vol. 21, 273-378.
- MYSLIVEC, A. (1976), About the calculation of stability of slopes., Proc. 6th European conf. Soil Mech. found. Eng. Vienna, Austria., Vol. 11,75-80.